BEHAVIOR AND EFFECT OF NANOCELLULOSE ON MUCUS AND MUCOSAL LAYER IN THE GASTROINTESTINAL TRACT

by

YU-JU LIN

(Under the Direction of FANBIN KONG)

ABSTRACT

Nanocellulose defines cellulosic compounds smaller than 100 nm in at least one dimension. As a relatively new material, the applications of nanocellulose are expending and there are emerging interests in using nanocellulose as food additives. The mucus layer in the gastrointestinal tract serves as the first defensive barrier to react with foreign objects that enter through the oral route. The interaction between the nanocellulose and mucus gel layer would greatly determine the fate of nanocellulose and reflect the gut health. The goal of the current study was to investigate the behavior of nanocellulose in the GI tract and the health effects, especially the impact on mucus and mucosal layer. Three types of nanocellulose, cellulose nanofiber (CNF), 2,2,6,6-tetramethylpiperidine-1-oxyl radical-oxidized CNF (TEMPO-CNF), and cellulose nanocrystals (CNC), were studied. In the first project, porcine mucosal membrane and mucins were used to investigate mucoadhesion properties of three types of nanocellulose and the mechanisms *ex vivo* and *in vitro*. Results showed all nanocellulose possessed mucoadhesive properties in the stomach and the small intestine. In the second part, mice were fed with a Western diet and 30 mg/kg body weight of three types of nanocellulose daily for six weeks. Different nanocellulose did not show a harmful effect on basic physiological parameters. The effect on serum triglycerides, cholesterol

and total bile acids and small intestinal morphology was also insignificant. However, the fecal bile output raised for the CNC group. Results suggested that nanocellulose did not improve lipid metabolisms or change intestinal homeostasis at the test dose. In the third part, CNC was tested for its toxicity on cell viability and the translocation across enterocytes. A novel *in vitro* intestinal mucus model was built to test if the mucus permeability was affected by CNC. It was found that CNC did not permeate through the Caco-2 monolayer or mucus gel layer, nor did it decrease Caco-2 viability. A high concentration of CNC may, however, decrease cholesterol absorption because of the ability of CNC to increase digesta viscosity, decrease mucus permeability, and binding of cholesterol. Our studies provided critical information on nanocellulose on their behavior and functionalities as food additives.

INDEX WORDS: Nanocellulose, cellulose nanofibrils (CNF), TEMPO-CNF, cellulose nanocrystals (CNC), mucoadhesion, *in vitro* digestion, nutrient absorption, short-term consumption, lipid metabolisms, intestinal morphology

BEHAVIOR AND EFFECT OF NANOCELLULOSE ON MUCUS AND MUCOSAL LAYER IN THE GASTROINTESTINAL TRACT

by

YU-JU LIN

BA, National Taiwan University, Taiwan, 2010

MS, National Taiwan University, Taiwan, 2013

A Dissertation Submitted to the Graduate Faculty of The University of Georgia in Partial Fulfillment of the Requirements for the Degree

DOCTOR OF PHILOSOPHY

ATHENS, GEORGIA

2020

BEHAVIOR AND EFFECT OF NANOCELLULOSE ON MUCUS AND MUCOSAL LAYER IN THE GASTROINTESTINAL TRACT

by

YU-JU LIN

Major Professor:	Fanbin Kong
Committee:	Tai L. Guo
	Chad M. Paton
	Jo Anne Shatkin

Electronic Version Approved:

Ron Walcott
Dean of the Graduate School
The University of Georgia
December 2020

DEDICATION

To my dearest parents and family, my husband and my daughter, and women who ever question themselves but truly have a strong vitality and a dream.

ACKNOWLEDGEMENTS

I cannot give enough appreciation to my advisor, Dr. Kong. Dr. Kong gave me endless patience and trust and this was the support that I needed the most. I also appreciate all the opportunities Dr. Kong provided for letting me do all the trials and models, and more experiences such as managing our lab and classes. I think all these combined to become wonderful memories and learning opportunities. I would also like to thank my committee, Dr. Shatkin, Dr. Paton, and Dr. Guo for all the advice and guidance and for walking me through my research. I also especially thank Yingjia Chen for teaching me and letting me learn from her for the animal experiment.

I want to thank every staff and professors in our department and UGA: Dr. Kerr, Dr. Cavender, Dr. Singh, Dr. Pegg, Dr. Dee, Karen, Jessica, Carl, Lisa, Danny, Coverdell Animal Facility, UGA Pathology lab, Meat Science Technology Center, Biomedical Microscopy Core, Georgia Electron Microscopy, as well as Dr. Fox in American University to make my work possible.

My labmates and colleagues (hopefully I am not missing anyone): Duc, Vivien, Nakia, Jiannan, Lingling, Samet, Yiwen, Damla, Ta-Sheng, Zijin, Himanshu, Dr. Xie, Dr. Liu, Dr. Fang, Jin, Xiaodan, Flores, Jeeten, Junyi, Michelle, Po, Bindu, Kay, Peng-Chian, Yura, Xiaoxi, Jo, Jo, Adi, Marvin, Sam, Sarah, Brittany, Nishtha, Natalie, Ana, Lida, Anuj, Carlyn and friends in UGA TSA, Emory University and the University of Virginia. You guys are awesome and I am so lucky to be friends with you.

Last but not least, my family is the most important to me. Every now and then when I felt overwhelmed, they are always there. I am definitely the luckiest one to have my husband, Ching-Wen, and I can say that without him, my degree would not even be possible. My parents, I thank

them for always give me positive feedback and believe in me. And my cutest little daughter, Ella, who joined us in 2019, is the one who boosts my power and strength to succeed in this journey.

Finally, I would like to hug and embrace the stubborn part of me. I thank her for never stop believing and trying. Life definitely has ups and downs, but I am happier than ever. My life goal is to pass loves to others. I will keep doing so.

TABLE OF CONTENT

LIST OF TABLES

LIST OF FIGURES

CHAPTER 1. INTRODUCTION

Nanocellulose, which is nano-sized cellulose derived from woods, vegetables or bacterial byproducts, is a novel environmentally-friendly bio-based nanomaterial. The idea of nanocellulose was developed in the 1970s by ITT Rayonier Eastern Research Division Lab in Whippany, USA as "microfibrillated cellulose" and the first work was published in 1983, which includes the potential use and produced by physical treatment (Turbak, Snyder, & Sandberg, 1983). Since then it has collected attention and there was a boom in research and patents in 2000 (Jorfi & Foster, 2015).

Nanocellulose can be produced from cellulosic raw materials such as plants or be synthesized by microorganisms like bacteria or algae (Rebouillat & Pla, 2013). The first nanocellulose product was obtained from mechanically breaking down wood pulp into nano-size long fibrils, called cellulose nanofibrils (CNF) (Turbak et al., 1983). Due to a lack of chemical modification, CNF usually does not carry charges and has a relatively wide range of length and width. Cellulose nanocrystals (CNC) is another type of nanocellulose made by acid hydrolysis of cellulosic materials, characterized by a shorter, thinner and rod-like shape as opposed to CNF (Moon, Martini, Nairn, Simonsen, & Youngblood, 2011). Both CNF and CNC can undergo further chemical modification. One example is 2,2,6,6-tetramethylpiperidine-1-oxyl (TEMPO) radical-mediated oxidation of CNF and the process opens up the fibrils by substituting carboxyl groups on the fibril surface, resulting in a highly dispersed fibril network (Moon et al., 2011). The product is usually called TEMPO-CNF. Nowadays the manufacturing costs were estimated to be around

USD 1493/ton CMNF (dry equivalent) (cellulose micro- and nanofibrils) (de Assis et al., 2018) and less than USD 5900/ton of CNC (dry equivalent) (de Assis et al., 2017). The global market for nanocellulose and cellulose nanoparticles is expected to reach 808.29 million by 2022 according to the estimation by Stratistics Market Research Counselling (Rajinipriya, Nagalakshmaiah, Robert, & Elkoun, 2018).

There have been wide applications of nanocellulose in the pulp industry. Yet for food use, efforts are underway to obtain more safety information for nanocellulose to be used as a food additive (Ong et al., 2020). Similar to most nanomaterials, the great potential in numerous applications often comes with raising awareness in that the small size poses a safety concern in human health. Especially when incorporated into food as ingredients or packaging materials, questions need to be answered such as the fate of nanocellulose when entering the body as well as the overall impact of nanomaterials on the host.

Mammal gastrointestinal (GI) tract is covered with mucus. This layer is the first barrier for foreign objects to overcome before being taken up and entering the systemic circulation and is so important to protect the host from invasion, including nanomaterials (Ensign, Cone, & Hanes, 2012; Li et al., 2015). Nanocellulose when consumed, whether intentionally added in food or accidentally contaminated from the environment, also inevitably encounters the mucus layer along the GI tract. Understanding how nanocellulose interacts with mucus would elucidate their biological impact, including whether it would stay in the lumen for a longer period or if it would penetrate the mucus layer and reach the epithelium.

Meanwhile, nanocellulose has the potential to become dietary fibers due to the nature of its β-(1→4) glycosidic linkage structure. There are many known benefits of dietary fibers, such as

improved lipid metabolisms, glucose homeostasis, immune system and gut health (Anderson et al., 2009). It would be meaningful to discover any health benefits of nanocellulose.

1.1 Significance of the study

Nanocellulose is an emerging innovative material and the applications in food have drawn attention in recent years. Because of its small size and the involvement of chemical modifications on the molecular surface, its behavior cannot be directly inferred from our prior understanding of cellulose. Its performance in the digestive tract must be tested to evaluate its safety. In the past, scientists as well as the industry sectors have focused on the applications of nanocellulose (Charreau, L Foresti, & Vázquez, 2013) but more in-depth information on how it interacts with the body after consumption is needed to determine the proper uses of nanocellulose. Currently, the industry sector has been seeking novel mucoadhesive materials. More understanding on how nanocellulose reacts to the digestive tract, including the mucosal layer and epithelial cells, can not only pave the way in the development of the mucoadhesive drug delivery system but more importantly, it provides critical information to promote food safety when eating nanocellulose

1.2 Objectives

This project aims to investigate the fate and impacts of nanocellulose on the upper GI tract (i.e. stomach and small intestine). The behavior of nanocellulose after consumption and its interactions with the mucosal layer and nutrients were elucidated.

This project has the following objectives.

1) To assess the mucoadhesive properties of nanocellulose *in vitro* and *ex vivo*

2) To assess the impacts of nanocellulose on intestine and metabolism using a mouse model.
3) To assess the translocation of nanocellulose and impacts on substance diffusion using *in vitro* models.

1.3 Outline

This dissertation includes a general literature review and three research chapters. The literature review will cover current knowledge about nanocellulose, and the behavior of nanocellulose as well as dietary fibers in the digestive tract with mucosal layer and nutrients will be discussed. In the research chapters, three types of nanocellulose, including CNF, CNC, and TEMPO-CNF, were used. The first research chapter investigated the mucoadhesion properties and mechanisms of CNF, CNC, and TEMPO-CNF with *in vitro* and *ex vivo* methods. The second research chapter focuses on *in vivo* evaluation of the effect of long-term consumption of CNF, CNC, and TEMPO-CNF. A six-week trial of mouse model feeding Western diet was conducted to study the sub-chronic effect of different nanocellulose on intestinal physiology and lipid metabolic parameters and compared with regular cellulose. The third research chapter focuses primarily on CNC based on the *in vivo* results obtained in the second research project. An *ex vivo* mucus model was built and the influence of nanocellulose on CNC penetration and substance permeation was tested. *In vitro* Caco-2 model was also used to evaluate the cytotoxicity of CNC by the cell viability test and the penetration of CNC.

1.4 References

Anderson, J. W., Baird, P., Davis, R. H., Jr, Ferreri, S., Knudtson, M., Koraym, A., . . . Williams, C. L. (2009). Health benefits of dietary fiber. *Nutrition Reviews,* 67(4), 188-205.

Charreau, H., L Foresti, M., & Vázquez, A. (2013). Nanocellulose patents trends: a comprehensive review on patents on cellulose nanocrystals, microfibrillated and bacterial cellulose. *Recent patents on nanotechnology,* 7(1), 56-80.

de Assis, C. A., Houtman, C., Phillips, R., Bilek, E. M., Rojas, O. J., Pal, L., . . . Gonzalez, R. (2017). Conversion Economics of Forest Biomaterials: Risk and Financial Analysis of CNC Manufacturing. *Biofuels, Bioproducts and Biorefining,* 11(4), 682-700.

de Assis, C. A., Iglesias, M. C., Bilodeau, M., Johnson, D., Phillips, R., Peresin, M. S., . . . Gonzalez, R. (2018). Cellulose micro- and nanofibrils (CMNF) manufacturing - financial and risk assessment. *Biofuels, Bioproducts and Biorefining,* 12(2), 251-264.

Ensign, L. M., Cone, R., & Hanes, J. (2012). Oral drug delivery with polymeric nanoparticles: The gastrointestinal mucus barriers. *Advanced Drug Delivery Reviews,* 64(6), 557-570.

Jorfi, M., & Foster, E. J. (2015). Recent advances in nanocellulose for biomedical applications. *Journal of Applied Polymer Science,* 132(14).

Li, H., Limenitakis, J. P., Fuhrer, T., Geuking, M. B., Lawson, M. A., Wyss, M., . . . Macpherson, A. J. (2015). The outer mucus layer hosts a distinct intestinal microbial niche. *Nature communications,* 6, 8292.

Moon, R. J., Martini, A., Nairn, J., Simonsen, J., & Youngblood, J. (2011). Cellulose nanomaterials review: structure, properties and nanocomposites. *Chemical Society Reviews,* 40(7), 3941-3994.

Ong, K. J., Ede, J. D., Pomeroy-Carter, C. A., Sayes, C. M., Mulenos, M. R., & Shatkin, J. A. (2020). A 90-day dietary study with fibrillated cellulose in Sprague-Dawley rats. *Toxicology Reports,* 7, 174-182.

Rajinipriya, M., Nagalakshmaiah, M., Robert, M., & Elkoun, S. (2018). Importance of Agricultural and Industrial Waste in the Field of Nanocellulose and Recent Industrial Developments of

Wood Based Nanocellulose: A Review. *ACS Sustainable Chemistry & Engineering,* 6(3), 2807-2828.

Rebouillat, S., & Pla, F. (2013). State of the Art Manufacturing and Engineering of Nanocellulose: A Review of Available Data and Industrial Applications. *Journal of Biomaterials and Nanobiotechnology,* Vol.04No.02, 24.

Turbak, A. F., Snyder, F. W., & Sandberg, K. R. (1983). Microfibrillated cellulose, a new cellulose product: properties, uses, and commercial potential. *J. Appl. Polym. Sci.: Appl. Polym. Symp.;(United States)* (Vol. 37): ITT Rayonier Inc., Shelton, WA.

CHAPTER 2. LITERATURE REVIEW

2.1 Nanocellulose

2.1.1 Classification, production, and characterization

Cellulose is polysaccharides constituted of the repeated cyclic form of glucose $(C_6H_{10}O_5)_n$ units (n= 10,000 to 15,000) connected by β-(1→4) glycosidic linkage. It is the most abundant polysaccharides on earth and can be harvested from a huge variety of sources, including plants, tunicate, algae, and bacteria (R. J. Moon, Martini, Nairn, Simonsen, & Youngblood, 2011). Since this project focuses on wood-based nanocellulose, the following content focuses on the majority of cellulose generated from plants.

Cellulose forms the basic structure of cell walls in plants. In the fibril matrix is the microfibril structure (diameters of 3-20nm). The hydroxyl groups on the surface of glucose units generate strong hydrogen bonding that causes self-association between several long cellulose chains to form elementary fibrils that are composed of the microfibrils. Within the elementary fibrils, the cellulose chain bundles may have alternating disordered (amorphous) regions and crystalline regions. In the crystalline regions, the cellulose arranged in a highly organized order and the hydrogen bonding are so strong and from a dense pack that is hard to break by chemical treatment (Robert J Moon, 2008; Robert J Moon, Frihart, & Wegner, 2006). The cellulose content in different plants vary. For wood, there is about 30–40% cellulose and roughly 1:1 ratio of the crystalline region and amorphous region (Postek et al., 2010).

Nanocellulose is defined as cellulose with at least one dimension lower than 100 nm, usually diameter, and also called cellulose nanomaterials (CNMs) (Foster et al., 2018; Xia et al., 2003). Naturally or by biotechnology means it can be produced by a strain of bacteria, *Komagataeibacter xylinus*, for products like Nata de Coco through static fermentation of coconut water or coconut milk. The nanocellulose produced in this way is called bacterial nanocellulose (BNC) (Gama, Gatenholm, & Klemm, 2012) and has been generally accepted as non-toxic (Helenius et al., 2006). Artificially made nanocellulose is usually generated from plant pulp such as wood, cotton, or hemp (R. J. Moon et al., 2011). The gross product value of plant-based nanocellulose was expected up to $600 billion in 2020 (Endes et al., 2016). The nano-scale downsizing process manages to break down the long cellulose microfibrils and create products that are high in total surface area and high in aspect ratio. Aspect ratio is the measurement of the length over width (diameter) of particles and a higher aspect ratio provides higher reinforcement capacity and hence greater strength. Higher surface area means there is more contact area for the compound to react with substrates. The down-sizing also greatly increases the hydrophilicity of nanocellulose as oppose to cellulose. These properties increase the reactiveness of nanocellulose, making nanocellulose a potential product for industrial use such as wastewater recycling for heavy metal adsorption (Tshikovhi, Mishra, & Mishra, 2020). Nanocellulose as a bio-based material with great strength also makes it a good candidate for food coating and packaging (Khan, Huq, Khan, Riedl, & Lacroix, 2014).

The production of nanocellulose can be seen as a two-steps processing: pretreatment and extraction (Salimi, Sotudeh-Gharebagh, Zarghami, Chan, & Yuen, 2019). Raw materials (cotton, wood, etc) are firstly pretreated to remove impurities such as hemicellulose, lignin, and wax. Alkaline or bleaching is the most common pre-treatment methods and are often combined. NaOH or KOH are the major two solutions in alkaline treatment followed by NaClO2 for bleaching pre-

treatment. The alkaline treatment substitutes the hydrogen in the fiber network with an alkali metal to release the cellulose fibers (Islam, Alam, Patrucco, Montarsolo, & Zoccola, 2014; Kargarzadeh et al., 2018), and the bleach reacts with the chromophoric group on lignin to remove the byproducts as lignin chloride (Abraham et al., 2011; Dufresne, 2017).

The second step is the extraction or isolation of nanocellulose. Depending on the processing methods, several types of mechanically- or chemically-modified nanocellulose are currently available. There can be three major categories of isolation process to produce nanocellulose. First is using mechanically shearing and homogenization of the material pulp. This would break down the cellulose fibrils in random sites and results in a noodle-like shape(R. J. Moon et al., 2011). The second is through acid hydrolysis using sulfuric acid, hydrochloric acid, or phosphoric acid. The acids lyse the amorphous regions and leave the crystalline regions, resulting in a rice-like shape and typically the smallest size of nanocellulose. This kind of nanocellulose is called cellulose nanocrystals (CNC). Thirdly, oxidizing catalysts such as TEMPO (2,2,6,6-tetramethylpiperidine-1-oxyl) or oxidizing reagents such as ammonium persulfate, sodium periodate, and epoxypropyl trimethylammonium chloride (EPTMAC) (Littunen et al., 2016) can be combined with mechanical processing. The result of chemical processing methods, no matter acid hydrolysis or oxidation, changes the surface chemistry of the cellulose chain by giving sites that can be protonated or deprotonated on the surface of the glucose unit according to the environment (solution). This will create repulsion force between the fibrils and decrease self-association and precipitation of nanocellulose, which greatly increase the solubility and stability of the suspension.

Several aforementioned types of nanocellulose are currently commercialized to be produced in bulk. The production and the characteristics of three types of nanocellulose, CNF, CNC, and TEMPO-CNF used in this project are further discussed.

Cellulose nanofibrils (CNF), in a nutshell, is mechanically nano-sized nanocellulose. It may also be called cellulose nanofibers, microfibrillated cellulose (MFC), cellulose filaments (CF), or nanofibrillar cellulose (NFC). There are numerous mechanical down-sizing methods and has been discussed in several reviews (Kargarzadeh et al., 2018; Rajinipriya, Nagalakshmaiah, Robert, & Elkoun, 2018; Salimi et al., 2019), including refining, ultrasonication, grinding, homogenization, grinding, blending, microfluidization, extrusion, cyrocrushing, steam explosion, aqueous counter collision, and radiation. The size varies depending on the source of raw materials and treatment methods. The pass number during the process (cycle time) is also a key factor that affects the morphology of CNF. For example, it was reported that 5-10 passes give the outstanding performance on tensile modulus and strength values for CNF mixed with hydroxypropyl cellulose films, while a higher pass number up to 20 passes breaks down the fibrils into thinner fibers that tend to aggregate due to stronger association between the hydroxyl groups (S.-Y. Lee, Chun, Kang, & Park, 2009). The length of CNF is typically up to several μm; for diameter, it can range from 2-5 nm for CNF extracted from prickly pear fruits using homogenization (Habibi, Mahrouz, & Vignon, 2009) to 12-20 nm for CNF made from soy hull using cyrocrushing technique (Alemdar & Sain, 2008). The aspect ratio can range from 10-100 (Menas et al., 2017). Currently, in the US four companies or institutes are producing CNF: American Process Inc. (now GranBio) and University of Maine with the American Process Inc. (now GranBio) producing the highest amount in a day (0.5 ton/day) (Rajinipriya et al., 2018).

Cellulose nanocrystals (CNC) are also called nanocrystalline cellulose (NCC), cellulose nanowhiskers. A different source of raw materials of CNC has been developed. For examples, coconut husk fibers (Rosa et al., 2010), garlic straw (Kallel et al., 2016), chili leftover (Nagalakshmaiah, kissi, Mortha, & Dufresne, 2016), ground nutshell (Bano & Negi, 2017) have

been used to produce CNC in lab-scale. For industrial production, pulp from wood or cotton is the mainstream source of raw material. The size is typically 2-25 nm in width, 100-750 nm in length and 5-30 in aspect ratio (Foster et al., 2018; Rajinipriya et al., 2018). The production of CNC starts from sending the pulp material to acid hydrolysis where the acids would firstly hydrolyze the glycosidic bonds of the amorphous (non-crystalline) region of the cellulosic materials. Eventually, the acids would react at the reducing ends and the surface of the glucose units. The process would then substitute the alcohol on the C6-carbon with charged groups and gives different characteristics to CNC than CNF. Specifically, sulfuric acid and phosphoric acid attach sulfate half ester and phosphate half ester on the cellulose surface, respectively (Beck-Candanedo, Roman, & Gray, 2005; Camarero Espinosa, Kuhnt, Foster, & Weder, 2013; Ranby, 1949). And hydrochloric acid hydrolysis produces uncharged CNC so the suspension is relatively unstable due to the lack of repulsion on the surface of the crystals (Araki, Wada, & Kuga, 2001). CNC has the advantages of good strength (7.5 GPa in tensile strength) and stiffness (150 GPa in Young's Modulus) which is comparable to commercial fibers like Kevlar® fibers, making it a good candidate as a reinforcement material (Postek et al., 2010).

TEMPO (2,2,6,6-tetramethylpiperidine-1-oxyl) oxidized CNF (TEMPO-CNF) is one of the chemically modified nanocellulose. The oxidation allows the glucose units to carry carboxylate anions on the C6-carbon which leads to interfibrillar repulsion. And the following mechanical dispersion treatment produces a colloidal with high transparency and viscosity (Saito, Kimura, Nishiyama, & Isogai, 2007). The USDA Forest Products Laboratory (FPL) has reported the process of TEMPO-CNF scaling-up production using bleached kraft Eucalyptus machine dried pulp as starting material. Before the TEMPO reaction, the pulp would be soaked with sodium

chlorite and sulfuric acid in water as a pretreatment to remove undesired residues such as lignin, quinones and trace metals. Two pH reaction systems (pH 10 and pH 7) are possible to use TEMPO as the catalyst. The difference was that the pH 10 system used hypochlorite as the terminal oxidant with the aid of sodium bromide, while the pH 7 system used sodium chlorite as the terminal oxidant and took several days at 70°C instead of several hours at room temperature. Bicarbonate/carbonate buffer was also used to maintain the pH in the pH 10 system. The pH 7 TEMPO/sodium chlorite system produced CNF that has fewer carboxyl groups on the surface of the nanofibrils (0.8 mmol -COONa/g dry pulp) but is higher in the degree of polymerization (DP). The pH 10 system, however, was preferred due to shorter processing time, the higher level of carboxylation (1.5mmol -COONa/g dry pulp) and higher transparency of the product. The end product was collected on filters and washed with reverse osmosis (RO) water to remove the reagents. Finally, the suspension was sent to a homogenizer to achieve the dispersion of the fibrils (Reiner & Rudie, 2017). As a result of the combination of chemical and mechanical treatment, the size of TEMPO-CNF is around 5-7 nm in diameter and several μm in length (Qing et al., 2013; Saito et al., 2009). The carboxylic groups on the surface change the properties of TEMPO-CNF by the ionic strength of the surrounding environment and the concentration itself. TEMPO-CNF solution in 0.1 wt% remains homogenous until up to 50 mM NaCl and forms hydrogel at 100 mM NaCl. For 200 mM NaCl and above, the hydrogel may separate into aggregates and supernatant. In the case of the presence of divalent ions such as $MgCl_2$ or $CaCl_2$, the gel forms at a lower salt concentration at 2-4 mM (Fukuzumi, Tanaka, Saito, & Isogai, 2014). And the steady-state shear viscosity of TEMPO-CNF increases slowly with a concentration below 0.1 wt% and thicken quickly above 0.3 wt% (Geng et al., 2017).

2.1.2 Current applications of nanocellulose in food-related use

Nanocellulose generated from wood has attracted great interest in both the academic and industry sectors in applying in food-related use (錯誤! 找不到參照來源。). As the raw material is a source for paper, there were many studies extensively studying and reviewing nanocellulose-based nano-composite for packaging, especially functional food packaging (Azeredo, Rosa, & Mattoso, 2017; Bharimalla, Deshmukh, Vigneshwaran, Patil, & Prasad, 2017; Khan et al., 2014; Tang, Kumar, Alavi, & Sandeep, 2012; Vilarinho, Sanches Silva, Vaz, & Farinha, 2018). In general, nanocellulose-based bio-composites have been considered environmentally friendly because it is bio-degradable and sustainable. The addition of nanocellulose into synthetic biopolymers, such as poly-lactic acid, poly(3-hydroxybutyrate-co-3-hydroxy valerate) (PHBV) and polyvinyl alcohol (PVA) was found to provide extra mechanical strength, barrier properties against oxygen and moisture and thermal stability (Fortunati et al., 2012) (Yu et al., 2012) (George, Bawa, & Siddaramaiah, 2010).

As nanocellulose forms hydrogel in water, the addition of nanocellulose may improve the texture and rheology of food. MFC was first used as a thickener in foods. The results show 0.1-2% of MFC improved the smoothness of puddings and gravy (Turbak, Snyder, & Sandberg, 1982, 1983a). It was also shown that 0.3-2% of cellulosic microfibrils form a thixotropic network in the filling of bread (Kleinschmidt, Roberts, Fuqua, & Melchion, 1988). Qi et al. (2020) reported the use of CNF and CNC in pork sausage not only improved fat and water binding capacity but also the final product had higher hardness, springiness and chewiness. CNF was also used as a thickener in mayonnaise. And it was found at 0.42% of CNF the rheology and visual stability of the product were improved (Heggset et al., 2020). Nanocellulose was also able to improve the stability of oil-

in-water emulsions by using 0.25-2% of MFC in salad dressing (Turbak, Snyder, & Sandberg, 1983b). A recent study showed that a higher level of homogenization of MFC could effectively decrease the size, therefore increase its emulsifying effect. Along with a decreased degree of polymerization, viscoelasticity and viscosity. The most impressive part is when MFC was added up to 0.1%, the emulsion stability was unaffected by environmental stress such as heat, NaCl concentration and pH (Winuprasith & Suphantharika, 2013). This greatly increased the possibility of nanocellulose in the application in foods where the system could go through high temperature or high salt. Nanocellulose generates its emulsification effect by forming a "Pickering emulsion" which is different from the emulsions formed by bipolar surfactants. In a Pickering emulsion, solids accumulate at the oil-water interface which then forms a barrier to prevent emulsion droplets against coalescence (Pickering, 1907). TEMPO-CNF has been combined with electrolytes and xanthan gum to test its potential as a food thickener. The results showed the thickening effect of TEMPO-CNF was highly dependent on the environmental ionic strength when used with Xanthan (Aaen, Simon, Wernersson Brodin, & Syverud, 2019). Another research also showed TEMPO-CNF was more ineffective as a stabilizer in oil-in-water emulsion with 1 wt% NaCl or 0.2 wt% acetic acid. The charge density on TEMPO-CNF was suggested to play the role to the stability corresponding to the environment (Aaen, Brodin, Simon, Heggset, & Syverud, 2019).

Due to the nature of cellulose as a non-digestible carbohydrate, there is also the potential for nanocellulose as a fat replacer in producing low-calorie foods. MFC was first suggested to be used in low-calorie toppings (Turbak et al., 1982). There was the usage of 0.25-1% CNF in ice cream which successfully lowered the fat content of ice cream to 1% without affecting its texture (Ford, 2015). It may also be incorporated into food or supplements as a coating or encapsulation reagent. Both CNF and CNC have been developed as an edible coating for fresh produce such as

blueberries and helped retain moisture and protect pigments from UV damage (Zhao, Simonsen, Cavender, Jung, & Fuchigami, 2019). CNC extracted from banana pseudostems was added into starch-based edible films. The results suggested adding CNC could improve water vapor permeability and mechanical strength for the edible film and maybe further applied in food packaging (Jeevahan & Chandrasekaran, 2019).

Nanocellulose may also have a controlled-release property which could help improve the delivery of functional compounds. The surface charges of modified nanocellulose would be merit in reacting to pH or ionic changes in the environment. For example, CNC was used to bind water-soluble drugs and extended the release time of the drugs. A surfactant, cetyltrimethylammonium bromide (CTAB) was attached on the surface of CNC and showed controlled-release properties of hydrophobic drugs (Burt, Jackson, & Hamad, 2014). CNC was also cationized by 2,3-epoxypropyl trimethylammonium chloride and mixed with sodium alginate to make double-membrane encapsulation. The result showed good encapsulation efficiency with the rapid release of antibiotics, suggesting a promising potential for oral drug applications (Lin, Gèze, Wouessidjewe, Huang, & Dufresne, 2016). TEMPO-CNF was mixed with gelatin and dialdehyde starch as a biocompatible nanocomposite and freeze-dried to form a cryogel for controlled-release of 5-fluorouracil. The TEMPO-CNF ratio in the mixture had a determining effect on the structure of the cryogels and the release profile as well as the drug loading efficiency (J. Li et al., 2019)

Table 2.1. Examples of current research of nanocellulose in food applications

Types of NC	Source of fiber	Chemical treatment and surface modification/	Characteristics	Uses and food products	Conc.	Performance and results	Ref.
MFC	Wood cellulose pulps			As thickener, flavor carrier and suspension stabilizer in foods like puddings, gravy and low-calorie toppings	0.1-25 wt%	Improved smoothness and consistency in texture	(Turbak et al., 1982)
MFC	Wood cellulose pulps			Ground meat	0.3 wt% in water	MFC helps prevent cooking loss of juices	(Turbak et al., 1983a)
MFC	Wood cellulose pulps			Stabilizer in oil-in-water emulsion and fat-replacer in no-oil salad dressing	0.25-2 wt%	MFC forms stable oil-in-water emulsion	(Turbak et al., 1983b)
MFC	Fully bleached spruce sulfite cellulose	Hydrophobization with Chlorodimethyl isopropylsilane (CDMIPS)	Dss 0.6-1.1	Oil-in-water emulsions	0.05-0.5 wt%	Excellent stability in preventing coalescence	(Andresen & Stenius, 2007)
MFC	Mixed softwood bleached kraft pulp	Hydrophobization with Chlorodimethyl isopropylsilane (CDMIPS)	Dss 0.06-0.5	Oil-in-water emulsions	0.05-0.2 wt%	Prevented gravity-induced sedimentation and coalescence	(Xhanari, Syverud, & Stenius, 2011)
MFC	Mangosteen (Garcinia mangostana L.) rind	1, 5, and 20 passes of homogenization	DP ranges from 1003-711	Oil-in-water emulsions	0.49 wt%	More homogenization passes to improve the emulsion stability	(Winuprasith & Suphantharika, 2013)
Cellulosic fibrils and microfibrils				Flow control product filling in the dough product	0.1 to 5 wt% (prefer 0.3-2%)	Forms thixotropic network in the filling	(Kleinschmidt et al., 1988)
CNF and CNC			3 to several hundred nm in width; CNF with aspect ratio >50 or CNC with aspect ratio >10	Edible films or coatings for foods especially fresh produce (ex. Blueberries and apples)	1 wt%	Protect moisture and nutrients loss and UV damage to pigments	(Zhao et al., 2019)

CNF	Bleached softwood kraft pulp			Fat replacer in ice cream	0.25-1 wt%	The lower fat content of ice cream to 1% with a similar texture to regular ice cream	(Ford, 2015)
Enzymatically pretreated CNF (E-CNF) and TEMPO-CNF	Never-dried, chlorine free-bleached sulfite dissolving pulp	CNF-E was pretreated with endoglucanase, TEMPO-CNF was prepared with TEMPO-oxidation	Total Charge (mmol/g): CNF-E 0.044 ± 0.003, CNF-T 1.49 ± 0.02	Rapeseed Oil emulsion	0.50 wt%	Both kept emulsion stable for 1one month. 1 wt% NaCl or 0.2 wt% acetic acid decreased stability of CNF-T stabilized emulsions while did not affect CNF-E stabilized emulsions	(Aaen, Brodin, et al., 2019)
CNFs	Never-dried, bleached softwood sulfite dissolving pulp	endoglucanase pretreated pulp and pass three times through a Microfluidizer		Thickener in mayonnaise	0.25, 0.42 wt%	Improved rheological properties and visual stability	(Heggset et al., 2020)
CNF and CNC	Cotton and sisal		Two different sources of CNF were 4-10 nm in diameter and 1-3 μm in length. CNC from cotton was 4-10 in diameter and 100-500 nm in length	The emulsifier in pork sausage	2 wt%	Increased fat and water binding capacities; increased hardness, springiness, and chewiness	(Qi et al., 2020)
CNC	MCC	sulfuric acid hydrolysis		As a reinforcement reagent in composites mixed with bacterial polyester poly(3-hydroxybutyrate-co-3-hydroxyvalerate) (PHBV)	1-20 wt%	Greatly improves tensile strength and Young's modulus when mixed with 10% CNC	(Yu et al., 2012)
CNC	MCC	CNC and surfactant-modified CNC		As a reinforcement reagent in PLA nano-biocomposites	1 wt%, 5 wt%	Reduced water permeability with good oxygen barrier properties. Overall migration level was better than normative limits.	(Fortunati et al., 2012)
CNC	MCC	sulfuric and hydrochloric acid hydrolysis		As a reinforcement reagent in composites mixed	10-12 wt%	Both CNC-S and CNC-H improved the strength of the composites. CNC-H	(Yu et al., 2013)

				with bacterial polyester poly(3-hydroxybutyrate-co-3-hydroxyvalerate) (PHBV)		had better performance due to more intermolecular hydrogen bonding interactions.	
CNC	Banana pseudo stems			Starch-based edible films,	2-10 wt%	Improved water vapor permeability and mechanical strength, decreased solubility	(Jeevahan & Chandrasekaran, 2019)
TEMPO- CNF	Dissolving pulp	TEMPO oxidation	Three different TEMPO-CNF has 649 ± 16, 1068 ± 43 and 1352 ± 5 μmol/g in charge density	Electrolytes and xanthan	0.11-1.08 wt%	Low electrolytes contribute to elevated viscosity and modulus. Effect on viscosity and modulus of xanthan with TEMPO-CNF greatly depends on the environment	(Aaen, Simon, et al., 2019)
TEMPO-CNF	Softwood pulp	TEMPO oxidation		Mixed with gelatin as cryogels as a carrier of 5-fluorouracil	0.06-0.6 wt%	Slowed release of for up to 12 hrs	(J. Li et al., 2019)

Abbreviations: MFC, microfibrillated cellulose; DSS, degree of surface substitution; DP, degree of polymerization; CNC-S, CNC prepared by sulfuric acid hydrolysis; CNC-H, CNC prepared by hydrochloric acid hydrolysis; CHO-CNC, aldehyde-functionalized CNC; MCC, Microcrystalline cellulose

2.1.3 Toxicity of nanocellulose by ingestion

Cellulose and modified cellulose such as microcrystalline cellulose, methylcellulose, hydroxypropyl cellulose are some of the most common additives for both food and pharmaceuticals that already exist in the market. The United States Food and Drug Administration (U.S. FDA) has included many cellulose analogs in the Food Additives Status List[1]. Among those cellulosic compounds, many are considered to be generally recognized as safe (GRAS), such as microcrystalline cellulose and carboxymethylcellulose. Some are addressed with use limitations, such as hydroxypropyl cellulose. The current status of cellulosic compounds as food additives and their GRAS status were summarized in Table 2.2. The safety or effects of nano-sized cellulose, however, may require re-evaluation to be used as food additives considering its unique properties or unless proven to have similar biological effects as cellulose. The small size provides an extremely high surface area, which makes nanocellulose different from current cellulose products in some physicochemical properties especially the reactivity (Gómez H et al., 2016; Saptarshi, Duschl, & Lopata, 2013).

Table 2.2. Summary of cellulosic compounds as food additives and GRAS status from U.S. FDA

Name of the additives	**Kind or effect of food additive**	**GRAS?**
Carboxymethylcellulose	stabilizer	y
Cellulose gum	stabilizer	y
Cellulose triacetate	Miscellaneous (fixing agent)	
Diethylamino-cellulose	Miscellaneous (fixing agent)	

[1] U.S. FDA Food Additives Status List https://www.fda.gov/food/food-additives-petitions/food-additive-status-list#abb

Ethyl cellulose	Miscellaneous (binder or filler)	y
Hemicellulose extract	Feed	
Hydroxypropyl cellulose	Emulsifier, stabilizer	
Hydroxypropyl methylcellulose	Emulsifier	y[a]
Methylcellulose (USP methylcellulose)	Miscellaneous	y[b]
Methyl ethyl cellulose	Miscellaneous (aerating, emulsifying and foaming agent)	
Microcrystalline cellulose	Miscellaneous	y
Regenerated cellulose	Miscellaneous (ion-exchange resin)	
Sodium carboxymethylcellulose (cellulose gum)	stabilizer	y[c]

Abbreviations: GRAS, generally recognized as safe
The GRAS status of hydroxypropyl methylcellulose was noted on the U.S. FDA GRAS Notice Inventory[2]
[b] Expect methoxy content 27.5 & 31.5% dry wt basis
[c] For sodium salt form higher than 99.5% dry wt basis

The toxicity of nanocellulose is still under investigation. There have been studies focusing on types, size and surface modifications of nanocellulose in terms of their toxicity.

CNF is manufactured by mechanical forces such as ultrafine grinder or blender without chemical modification and there are generally no charges on the surface and may correlate to less cytotoxicity (Huang, Cambre, & Lee, 2017). Studies have found no cytotoxicity on mouse macrophages (RAW 264.7) and no inflammatory effects on human peripheral blood-derived monocytes after 6 hours of exposures (Vartiainen, Pöhler, Sirola, Pylkkänen, & Cellulose, 2011). In the HeLa cell experiment, it was found the fractions of CNF with the smallest size had no sub-

[2] https://www.fda.gov/food/generally-recognized-safe-gras/gras-notice-inventory

lethal effects or genotoxicity but showed inhibition growth effect by total protein content (TPC) assay (Pitkanen et al., 2014). The toxicity of CNF via GI route has also been examined and generally low or no direct cytotoxicity was found. CNF showed a dose-dependent effect on decreasing cell viability on Caco-2 above 1000 mg/mL (Tibolla, Pelissari, Martins, Vicente, & Menegalli, 2018) and 500 mg/mL for Caco-2 and two different epithelial cells (LNCaP and TRAMP-C2, both are prostate epithelial cells) (Chen, Lin, Nagy, Kong, & Guo, 2020). G. DeLoid et al. (2019) tested CNF on a tri-culture intestinal cell model (HT29-MTX, Caco-2, Raji B cells) and found no significant effect on cytotoxicity while reactive oxygen species were found up to 1.5%, which was double confirmed by Pradhan et al. (2020). Our lab previously demonstrated that CNF may delay the digestion or absorption of glucose, fat, protein and minerals *in vitro* (Liu, Kerr, & Kong, 2019; Liu, Kerr, Kong, Dee, & Lin, 2018; Liu & Kong, 2019a, 2019c) and in cell experiment it was seen that CNF blocked the cellular uptake of the viability test dye (Chen et al., 2020). The level of the interfering effects seen in *in vitro* experiments then needs to be examined to understand if it causes toxicity in real life. For *in vivo* results, mice fed with up to 21% wt CNF diet showed normal biochemical analyses compared to controls (Andrade et al., 2015). Recent research focuses found no observable toxicity in rats feeding 2 to 4% CNF in the diet daily for 90 days and a no-observed-adverse-effect level (NOAEL) was reported up to 2 to 2.5 g/kg/day (Ong et al., 2020) and also no adverse effect in clinical pathology for consuming 1% (w/w) CNF twice weekly for five weeks (G. DeLoid et al., 2019). An adverse effect of CNF was found when an imbalanced diet (Western diet) was fed to the mice. A decrease of lean body mass was seen after 30 mg/kg body weight of CNF daily for 6 weeks. In the same study, it was also found that CNF disrupted glucose homeostasis. It was concluded that although CNF may not have direct toxicity on the clinical-pathological parameters and may have a protective effect from nonalcoholic fatty

liver, CNF may not provide all the ideal health benefits of fiber consumption while having a suboptimal diet (Chen et al., 2020).

The toxicity of CNC has been discussed in several review literature (Roman, 2015; Seabra, Bernardes, Fávaro, Paula, & Durán, 2018; Ventura et al., 2020). Roman (2015) reviewed the toxicity of CNC and concluded from previous studies that CNC showed inconsistent cytotoxicity from various cell models, but she speculated CNC may not be uptake by enterocytes because of its hydrophilicity and size. On the contrary, uptake of CNC was seen in lung alveolar epithelial cell line A549 after 72 hours of exposure. Note that drying processes (freeze-drying and spray drying) may change the structure and chemical properties of CNC and caused a different level of uptake, toxicity and inflammatory response, although uptake of CNC was only seen in gel form and rehydrated forms (Menas et al., 2017; Y. Peng et al., 2013). It was also suggested cationic modified CNC would be uptake by human embryonic kidney cells (HEK 293) but such uptake was not seen in anionic modified CNC (Mahmoud et al., 2010). For *in vivo* results, CNC was tested for toxicity on embryonic zebrafish. No significant difference in mortality rate was found, but accumulation was observed when given 100-500 mg/L to developing zebrafish (Harper et al., 2016).

The GI cellular cytotoxicity of CNC *in vitro* has been assessed in different intestinal cell models using Caco-2, HCT116 and tri-culture model (Caco-2, HT29-MTX, Raj B). Hanif, Ahmed, Shin, Kim, and Um (2014) reported cytotoxicity was seen above 500 μg/mL using WST-1 assay in HCT 116 after 24 hours of incubation, although it seemed not correlated with the size of different CNC. (Xiao et al., 2019) reported decreased cell viability at above 2 mg/mL after 24 hours incubation using Caco-2 cell model and the same cell line was found to have decreased mitochondria activity only for higher charge density groups carrying above 4.7 mmol/g -COOH

but all CNC affect the membrane integrity of cells (Hosseinidoust, Alam, Sim, Tufenkji, & van de Ven, 2015). G. DeLoid et al. (2019) reported that no adverse effect on monolayer integrity but elevated cytotoxicity (by LDH assay for CNC in *in vitro* intestinal digesta) and ROS (for CNC in fasting model) was seen at 15 mg/mL of CNC with an average diameter of 25 nm in Caco-2, HT29-MTX, Raj B tri-culture model.

In vitro GI cellular uptake of CNC was also seen in Caco-2 cells for as quick as three hours and was found to be time- and dose-dependent. The uptake also increased with higher charge density (Hosseinidoust et al., 2015). For *in vivo* result, acute oral toxicity was tested with Crl:CD(SD)BR rats and NOAEL was determined up to 2 g/kg of CNC suspension (O'Connor, Berry, & Goguen, 2014). More toxicology studies of CNC will be needed for mid-term and long-term ingestion.

As for TEMPO-CNF, little is known about its toxicity so far. It was found that no sub-lethal impacts on developing zebrafish (Harper et al., 2016). Ames test using *Salmonella typhimurium* and cytotoxic test by MTT assay using normal cell line GM07492A and human metabolizing cells (HepG2) revealed no cytotoxicity up to 0.12 wt% and still around 75% of cell viability by 0.5 wt% (de Lima Pizi Cândido, Fregonezi, Carvalho, Trovatti, & Resende, 2020). Due to the lack of knowledge, it is needed to address the toxicity of Tempo-oxidized CNF.

2.2 Behavior and interaction of nanocellulose and dietary fiber on the mucosal layer in the GI tract

2.2.1 Structure of gastrointestinal mucus and mucosal layer

The GI wall can generally be divided into four layers: mucosa, submucosa, muscular layer, and serosa (Reinus & Simon, 2014). On top of the mucosal layer is the mucus layer. Underneath the mucosal layer is Submucosa. It is a layer of connective tissue with lymph vessels and large blood vessels. Beneath the submucosa is the muscularis propria, which is composed of circular and longitudinal layers of smooth muscle to support the hollow structure of the GI tract and does the contraction and movement of the bowl. The outmost layer is Serosa, or adventitia. It is a layer of connective tissue. This is where separate but connect the organ to the other body parts (Betts, 2013). Since this study focuses only on the mucus layer and mucosal layer, they are further discussed below.

Mucus layer

Mucus covers the internal epithelium along with the gastrointestinal (GI) tract on top of the mucosa. The thickness of mucus ranges from hundreds of micrometers in the stomach (Huh, Bhutani, Farfan, & Bolch, 2003) to a thinner layer of several micrometers in the small intestine (Atuma, Strugala, Allen, & Holm, 2001). It is so important as both lubrication during digestion and a physical barrier from intestinal bacteria invasion, meanwhile providing habitat for luminal microbiota (H. Li et al., 2015).

The main component of mucus is mucin, a family of glycoproteins, and is secreted by goblet cells on the mucosa. This macromolecule has a protein backbone containing tandem repeats rich in proline (P), threonine (T), and serine (S) (PTS domains) that can be glycosylated with sugar units such as acetylglucosamine, acetylgalactosamine and other sugar residues. When mucins are released from goblet cells, it attracts water and forms a gel network by the cysteine cross-linking, and this cross-linkage gradually cleaves when near gut lumen by acid, proteolytic enzymes such as pepsin and mucolytic bacteria, thus forming a more loosen outer layer of mucus gel (Allen &

Carroll, 1985; Atuma et al., 2001; M. E. Johansson, Larsson, & Hansson, 2011). The mucus gel, therefore, can be considered as a porous adsorbent with an estimated 1μm cut-off, and that particles smaller than 1μm would be easier to diffuse into the mucus layer (Ponchel, Montisci, Dembri, Durrer, & Duchêne, 1997).

The important function of the mucus layer as the first host defense of a biological entity is because the gel structure is a physical and chemical barrier to microorganisms in the GI tract. With the constantly secreted mucin in the intestinal tract, and invading microorganisms must first penetrate this mucus layer to contact the epithelium and then either colonize or release toxins to break the epithelial integrity (Salyers, Whitt, & Whitt, 1994). The mucus layer not only contains mucin and water but also it is a matrix that is loaded with antimicrobial molecules. For example, α-1-4-linked N-acetyl-glucosamine is a gastric mucin oligosaccharide and was found to inhibit the synthesis of the cell wall of *Helicobacter pylori* (Kawakubo et al., 2004). In the mucus, some molecules are secreted by the enterocytes or immune cells from the mucosa, such as histatins, statherin, and secretory IgA (Royle et al., 2003) (Bobek & Situ, 2003; Bruno et al., 2005). Hence if the mucus-secreting function is aberrant, gut health would be affected. It was found one of the mucin gene knock-out mice ($MUC2^{-/-}$), had a higher chance of colitis, adenomas in the small intestine, and rectal tumors (Van der Sluis et al., 2006; Velcich et al., 2002). In human, reduced glycosylation of intestinal mucus may result in a thinner mucus layer of the colon and was found to correlated to inflammatory bowel disease (IBD) (Theodoratou et al., 2014). Children diagnosed with IBD also had lower goblet cell density and thinner mucus layer in the colon (Shaoul, Okada, Cutz, & Marcon, 2004).

Mucosa

The mucosa layer is composed of three layers: epithelium, lamina propria, muscularis mucosae. The first layer, epithelium, is unique in each GI organs but is the same place where the absorption and secretion happen. And it is also an important wall to protect of the biological entities. The epithelium is composed of cells with different functions and varies in each GI organs. For the stomach, there are neck cells that secret mucus to protect the epithelium, chief cells that secret enzymes like pepsinogen, parietal cells that secrete hydrochloric acids, and enteroendocrine cells that secrete endocrines such as gastrin. For the small intestine, the majority are enterocytes that absorb nutrients and water. There are also cells like goblet cells that secrete mucus and antifungal peptides, Paneth cells that secrete antimicrobial peptides, enteroendocrine cells that secret endocrine to stimulate digestion, microfold cells (M cells) that mediate transcytosis, and some lymphatic cells such as dendritic cells that move between the epithelium and the lumen in the Peyer's Patch. For the large intestine, there are mainly enterocytes and goblet cells. The lamina propria is composed of a layer of loose connective tissue and rich in lymph vessels and blood vessels. The muscularis mucosae are composed of two layers of smooth muscle, one inner circular and one outer longitudinal (Reinus & Simon, 2014).

2.2.2 Mucoadhesion

Mucoadhesion describes the behavior in which a substance adsorbs onto the mucus layer, thus extending the time it remains in particular organs. Mucoadhesion happens when a foreign substance contacts with the mucus layer and forms bindings between the two components that cause attachment (Khutoryanskiy, 2011; Rajput, Majmudar, Patel, Thakor, & Rajgor, 2010). It has drawn attention in mostly drug delivery applications in the past for the advantage of increased drug

residence time, improved drug bioavailability, and reduced administration frequency (Andrews, Laverty, & Jones, 2009).

The attachment of liquid or paste to mucus is a continuous motion that involves contact of the droplet to the mucosal surface, adsorption, spreading and interpenetration of the polymer chains. The electrostatic force, hydrogen bonds, covalent bonds, and hydrophobic attraction are possible molecular interactions between mucin and mucoadhesive materials (Derjaguin, Aleinikova, & Toporov, 1994; Derjaguin, Toporov, Muller, & Aleinikova, 1977; Kinloch, 1980). In the GI tract, however, many environmental and physical factors could significantly change the physical and chemical properties of a mucoadhesive material compared to other parts of the body covered with mucus. For example, the extreme pH in the stomach, the short turnover time of mucus in the GI tract, the GI motility, and the absorption-driven water movement all play important roles in whether and how long a mucoadhesive material could attach to the mucus (Ahuja, Khar, & Ali, 2008; Fabiano, Zambito, & Bernkop-Schnurch, 2017).

Mucoadhesive polymers typically have characteristics including anionic groups such as carboxylic groups and sulfate groups, high molecular weight, with flexible chains and suitable surface tension allowing them to spread onto mucus and forms attachment (J. W. Lee, Park, & Robinson, 2000; Park & Robinson, 1984; Peppas & Buri, 1985). It is also suggested that higher surface-area-to-volume particles increase the chance of forming greater attractive than repulsive force especially in the case when the surface molecules and the particles are carrying opposite charges (Smart, 2005). Several cellulose and derivates have been tested for their mucoadhesive properties. A previous study using porcine small intestine to test the detachment force of hydroxypropyl cellulose (non-ionic) and carboxymethylcellulose (anionic) with three different viscosities showed little or no mucoadhesiveness (Lehr, Bouwstra, Schacht, & Junginger, 1992).

Sodium carboxymethylcellulose (SCMC) and hydroxypropyl methylcellulose (HPMC) were made into buccal adhesive patches in a previous study(Cavallari, Brigidi, & Fini, 2015). Results showed that a mixture containing SCMC with different types of HPMC showed a different level of tensile strength to detach from the porcine oral mucosa. The authors concluded the lower methoxy to propoxy substituents and higher viscosity might be the cause of the difference.

2.2.3 Effect of fibers and dietary factors on mucus and mucosa layer

The homeostasis of intestinal mucus would rely on several factors. On the production side, the secretion of mucin from goblet cells and the glycosylation of mucin protein would determine the rate and the strength of the mucus. On the degradation side, the proteolysis from the intestinal microorganism, hydrolysis and digestion all affect the turnover of the mucus. These factors all weigh in the equilibrium for the mucus layer to protect from pathogen invasion but still facilitate nutrient absorption (Glade & Meguid, 2016).

Diet was reported to be an important factor for glycoconjugates patterns, types, and density of mucins in the small and large intestine by using germ-free mice, humanized gnotobiotic mice, and conventionally-raised mice with cellulose or crude cereals as fiber sources. The number of goblet cells containing sialomucin was higher in humanized mice than in germ-free mice in the large intestine, while more goblet cells containing sulfomucin were found in the small intestine of humanized mice than conventionally-raised rats. The same authors also found that the inoculation of human microflora to germ-free mice changed the morphology of intestinal villi by reducing the villi height and crypt depth in the small intestine. It was concluded that the changes of both dietary composition and microflora affected the composition of mucins secreted by goblet cells (R.

Sharma & U. Schumacher, 1995; Ram Sharma & Udo Schumacher, 1995; Sharma, Schumacher, Ronaasen, & Coates, 1995).

Effect on the large intestine

The effect of fibers on the large intestine has been widely studied. The mucus layer in the large intestine are two layers and the inner layer is denser and firmly attached to the intestinal epithelium, in which there are barely microorganisms for healthy guts (Ermund, Schütte, Johansson, Gustafsson, & Hansson, 2013; Malin E V Johansson et al., 2014; Malin E. V. Johansson et al., 2008). The mucosa in the large intestine is different from the small intestine in that there is a lack of protruding villi. Instead, the mucosa in the large intestine is a smooth surface with underlying crypts. Also, there are many different types of cells in the small intestine, e.g. epithelium cell, goblet cells, Paneth cells, M cells, while the large intestine is mostly just enterocytes and goblet cells (Betts, 2013).

The colonic microbiota, other than using glycan in the mucus as one of its energy sources (Desai et al., 2016; Martens, Chiang, & Gordon, 2008), largely ferment the dietary fibers as their nutrition sources and produce metabolites, such as short-chain fatty acids (SCFA). The SCFA profile produced by colonic microbiota then mediates the differentiation of goblet cells and the types of mucins they produced (Wrzosek et al., 2013). SCFAs are saturated fatty acids that have one to five carbons, and the majority SCFAs in the gut are acetate, propionate, and butyrate (Dalile, Van Oudenhove, Vervliet, & Verbeke, 2019; Ruppin, Bar-Meir, Soergel, Wood, & Schmitt, 1980). SCFAs were found to stimulate MUC2, the major mucin glycoprotein, secretion *in vitro* by upregulating Prostaglandin E1 (PGE1), and PGE2 secretion from subepithelial myofibroblasts *(Willemsen, Koetsier, van Deventer, & van Tol, 2003).* It was also proven *in vivo* that the infusion of SCFAs into the colon increased the release of mucus (Shimotoyodome, Meguro, Hase,

Tokimitsu, & Sakata, 2000). SCFAs can also be used as nutrition sources for the proliferation of intestinal epithelial cells, so a diet low in fibers generally does not promote a healthy gut (Roediger, 1980; Sakata, 1987).

Lack of fibers in diets, or Western style diet, was found to induce mucus defects, shown as increased permeability of the mucus layer and thinning of mucus layer (Schroeder et al., 2018). Without fibers as the external source of food for the gut microbiota, the microbiota composition changed and promote the growth of pathogenic species, such as *Citrobacter rodentium*, and mucus-degrading species, such as *A. muciniphila* and *B. intestinihominis* (Desai et al., 2016). As a result, a compensated mucus layer lacks the barrier function and provides more accessibility of epithelium to the pathogenic bacteria, leading to imbalanced microbial composition and intestinal dysfunction, inflammation and GI disorders including inflammatory bowel disease (IBD) (Lobionda, Sittipo, Kwon, & Lee, 2019), obesity (Shen, Obin, & Zhao, 2013) and in some cases may link to mental illnesses such as eating disorders, anxiety (Kleiman et al., 2015) or autism spectrum disorder (ASD) (Kang et al., 2013).

The addition of fibers in diet, on the other hand, may change the intestinal morphology with health benefits. The dietary fibers that are indigestible and have been proven to stimulate the growth of known beneficial gut microbes, i.e. probiotics, may also be called prebiotics (J. Slavin, 2013; Whisner & Castillo, 2018). The consumption of prebiotics is associate to improve host immunity (Schley & Field, 2002), mineral absorption (Bongers & van den Heuvel, 2003; Whisner & Castillo, 2018), stress resilience and memory (Romo-Araiza et al., 2018; Thompson et al., 2020), and intestinal diseases including infant diarrhea (Shahramian et al., 2018), IBD (Ewaschuk & Dieleman, 2006), etc.

The mechanisms of the health benefits of prebiotics have been summarized in the literature (Sanders, Merenstein, Reid, Gibson, & Rastall, 2019). Firstly, prebiotics typically has good water binding ability as well as can serve as a bulking agent in the stool, and therefore soften stools and improve bowel habit. Secondly, prebiotics promotes the growth of probiotics, which then suppresses the growth of harmful or pathogenic bacteria by competing nutrients and space in the lumen and mucus layer and secreting antimicrobial molecules. Thirdly, the fermentation of prebiotics by probiotics produces SCFAs and reduces the overall pH in the lumen. Lower pH not only helps the suppression of pathogenic bacteria but also enhances minerals bioavailability by increasing the solubility. Fourthly, it was proposed that prebiotics may modulate goblet cells and epithelial cells in a probiotics-independent way. Galacto-oligosaccharides (GOS) was added to goblet cell-like LS174T cell line and was found to up-regulate *MUC2* gene expression and the gene expression of several goblet cells secretory products, including trefoil factor 3 (*TFF3*), carbohydrate (N-acetylglucosamine-6-O) sulfotransferase 5 (*CHST5*), and resistin-like molecule beta (*RETNLB*)(Bhatia et al., 2015). In another research using GOS to treat Caco-2 monolayers, results showed that a commercial GOS syrup protected the monolayer integrity and lowered the release of interleukin 8 (IL-8), an inflammatory marker secreted by Caco-2, from damage induced by fungal toxins (Akbari et al., 2017).

Because fibers play an important role in the healthy/inflammation status of the gut and the stimulation function of SCFAs in mucosal cell proliferation, the large intestine morphology may also be affected. For example, the supplement of inulin was found to increase the crypt depth, goblet cells per crypt, and mucus thickness in the distal colon in humanized gnotobiotic rats (Kleessen, Hartmann, & Blaut, 2003). The increase of villi length and crypt depth also means there

was a higher intestinal surface area, which was suggested as one of the mechanisms of increased mineral absorptions (Raschka & Daniel, 2005; Scholz-Ahrens & Schrezenmeir, 2002).

Effect on the small intestine

Like previously mentioned, the small intestine morphology differs from the large intestine in the villi structure and the diversity of cell composition. The microbiota in the small intestine also has different characteristics than that in the large intestine. It was found that in the gut of a human adult, 10^{10} to 10^{12} colony-forming units (CFUs)/mL of microorganisms reside in the colon while there are only 10^{3} to 10^{4} CFU/mL in the jejunum and 10^{7} to 10^{9} CFU/mL in the ileum. There are also more aerobes than anaerobes in the small intestine due to the higher oxygen level as a result of peristalsis (Simon & Gorbach, 1986). Nonetheless, the gut-microbiota homeostasis is still crucial to the health of the hosts and can be regulated via diet (El Aidy, van den Bogert, & Kleerebezem, 2015).

The effect of fibers on the morphology of the small intestine in the literature has been summarized in Table 2.3. Different dietary fibers have been tested for their effect on small intestine morphology and mucin production. For example, pectin has been tested in rats in concentration varied from 2.5% to 20% while the effect on the villi morphology was controversial. Pectin was shown to affect the development of villi after adulthood when added into the diet by 10% in newly weaned rats and decreased villus height in adult rats (Jacobs, 1983; Tasman-Jones, Owen, & Jones, 1982). Other studies found pectin increased villus length and height in the small intestine (Chun, Bamba, & Hosoda, 1989; Sigleo, Jackson, & Vahouny, 1984). In most cases, dietary fibers increased villus height or villus width and this effect seemed more pronounced in jejunum and ileum especially when compared to low- or free-fiber diet (Chun et al., 1989; Jin, Reynolds,

Redmer, Caton, & Crenshaw, 1994; Sigleo et al., 1984). The increase in villus total area can increase the efficiency of nutrient absorption when the nutrient influx was also tested or higher weight gain was observed (Chun et al., 1989; Sigleo et al., 1984), although the relationship has not yet to be discussed as widely as in the large intestine. The effect on the crypt depth of the small intestine was more similar in studies using pectin, oat bran, guar gum, inulin, wheat straw as dietary fiber sources (Chun et al., 1989; Jacobs, 1983; Jin et al., 1994; Kleessen et al., 2003; Sharma et al., 1995). Crypt is the harbor where the proliferation of new cells happen and greatly determine the homeostatic turnover of the epithelium (Parker et al., 2017), so the enlargement of the crypts would suggest cell proliferation in the small intestine was enhanced by fibers, which was shown in several studies where fibers increased cell proliferation and cell migration (Chun et al., 1989; Hino et al., 2012; Jacobs, 1983; Jin et al., 1994).

The properties of fibers have been proposed to be associated with their biological effect on GI mucosa. Morita and colleagues tested the effect of soluble and insoluble fibers and found both soluble and insoluble fibers increased the production of sialylated and sulfated mucins in the small intestine, with a stronger linear association for sialylated mucin. The authors also found the settling volume, the volume expended after fibers were added into water, was associated with the total mucin content in the small intestine. The viscosity of the fibers was also found to correlate with goblet cell numbers and luminal mucin, although the MUC2 gene was not affected. They concluded that insoluble fibers could display a bulking effect and soluble fibers could generate high viscosity could both stimulate goblet cells in the small intestine (Hino et al., 2012; Ito et al., 2009; Tanabe, Ito, Sugiyama, Kiriyama, & Morita, 2006; Tanabe, Sugiyama, Matsuda, Kiriyama, & Morita, 2005).

Table 2.3. Examples of the literature of influences of fibers on small intestinal morphology

Animal	Dietary fiber	Conc.	Control diet	Villi	Crypt	Cell growth	Goblet cell/mucin	Other physiology	References
Newly weaned rats	cellulose or pectin	10%	Fiber-free diet	Pectin caused less well-developed villi and fewer villi per cm2 after adulthood				Cellulose showed a similar effect as no-fiber or cholestyramine-diet	(Tasman-Jones et al., 1982)
Rats	oat bran, pectin, and guar	10-20% fiber	Fiber-free diet	Pectin decreased villus height	Pectin increased crypt length	Pectin and guar increase cell migration		Guar diet increased mucosal mass and weight, total RNA and DNA	(Jacobs, 1983)
Adult male rats	methoxylated pectin or cellulose	10%	Low-fiber diet	Increased villus length and width				Higher weight gain and food intake; increased nutrient influx	(Sigleo et al., 1984)
Rats	pectin	2.5 (w/w)	Fiber-free liquid diet	Increased villus height in jejunum and ileum	Increased crypt depth in jejunum and ileum	Increased cell proliferation in the crypt in jejunum and ileum		Increase maltose absorption in the ileum	(Chun et al., 1989)
Rats	guar gum or citrus fiber	5%	Fiber-free diet				Citrus fiber increased mucin production in the stomach and intestine		(Satchithanandam, Vargofcak-Apker, Calvert, Leeds, & Cassidy, 1990)
Growing pigs	wheat straw	10%	Low-fiber diet	Width increase in jejunum and ileum	Depth increase in jejunum and ileum	Increase cell proliferation in the crypt in jejunum; increased death in jejunum and ileum		Increase RNA in the colon	(Jin et al., 1994)
GF rats, conventional rat flora	commercial diet, fibers source from cereal	Crude fiber content 4.1%	Cellulose	Conventional diet increased villus length	Conventional diet increased crypt depth		Denser neutral mucins in the upper crypts		(Sharma et al., 1995)

rats, HFA rats	products (barley, maize, wheat and wheat feed)								
GF rats, DA rats, HFA rats	Inulin	50g/kg	Commercial diet	Inulin increased villi length	Inulin increased crypt depth			Effect not seen in GF rats; thicker mucus and more goblet cells in the colon in DA and HFA rats	(Kleessen et al., 2003)
Rats	PSF, wheat bran, beet fiber, and corn husk	50 g/kg diet	Fiber-free diet				Higher SV was associated with sialic acid content and protein content of mucin	The production of mucin need a chronic exposure of fibers	(Tanabe et al., 2005)
Rats	5% PSF, 5% FOS, 5% PSF + 5% FOS, or 10% beet fiber		Fiber-free diet				PSF, PSF + FOS, and beet fiber but not FOS increased mucin content in the small intestine	FOS, PSF+FOS and beet fibers but not PSF increased mucin content in the cecum. Gastric mucin was not affected in all groups	(Tanabe et al., 2006)
Rats	konjac mannan with low, medium, high MW, guar gums (high or low MW), psyllium, or pectin	50 g/kg diet	Fiber-free diet				Mucin content and goblet cell number increased with fibers with higher viscosity except for pectin	The increase of mucin is independent of MUC gene expression	(Ito et al., 2009)
Rats	soluble fiber: konjac mannan (KM), psyllium, or guar gum; 50 g/kg; or insoluble fiber: polystyrene					Beet fiber increased epithelial cell migration	Increased in the ileum and increased sialylated mucin while		(Hino et al., 2012)

	foam, wheat bran, or cornhusk; 80 g/kg	less sulfated mucin

Abbreviations: GF rats, germ-free rats; DA rats, rats harboring *Bacteroides vulgatus* and *Bifidobacterium longum* (diassociated rats); HFA rat, rats with a human fecal flora; MW, molecular weight; polystyrene foam (PSF); fructooligosaccharide (FOS); settling volume (sv)

Effect on the stomach

It is clear diet is an important factor in gastric health. Inadequate use of salt, soy sauce, and alcohol are some examples that are known to increase risks of gastric mucosal injury (Kato, Nomura, Stemmermann, & Chyou, 1992). In an epidemiological study, dietary fiber intake was found to be associated with lower stomach cancer risk (Bravi et al., 2009). Gastric luminal mucin was found to increase when 5% guar gum or citrus fiber was added into the diet in rats for 4 weeks (Satchithanandam et al., 1990). While in a rat study feeding 5% polystyrene foam (PSF), 5% fructooligosaccharide (FOS), 5% PSF + 5% FOS or 10% beet fiber, results showed no significant difference to gastric mucins, while the same concentration was able to increase intestinal mucins (Tanabe et al., 2006).

Interestingly, different dietary fibers were proposed in coating the gastric lumen provide a physical barrier for drug delivery purposes. It was found for gum karaya, methyl cellulose and pectin had a good performance in blocking glucose permeation across the mucus layer *in vitro* at pH 1.0 condition. Although these fibers did not form a stable gel layer for a long enough period for use in pharmaceuticals, it shows a potential application for fibers targeting the stomach site (Y. Lee et al., 2018). A few earlier pieces of research evaluated the potential of chitosan as the mucoadhesive encapsulating agent for drug delivery to the stomach. (Patel & Patel, 2007; Säkkinen et al., 2004) Chitosan carries positive charges under an acidic condition that generates strong electrostatic attraction force with negatively charged sialylated mucins and may be further modified to improve its mucoadhesive properties for a more specific site of delivery (Ways, Lau, & Khutoryanskiy, 2018).

2.2.4 Effect of nanocellulose and dietary fibers on lipid metabolism

Dietary fibers have been associated with many health benefits such as improving gut health, lowering risk in metabolic syndrome, and heart disease (Dhingra, Michael, Rajput, & Patil, 2012; Mudgil & Barak, 2013). Fibers can affect both the digestion and absorption of macro- and micro-nutrients. More so, fibers may provide a protective effect even in unhealthy diet conditions. Research combining a high-fat diet with higher fiber consumption was found to reduce inflammation (Jakobsdottir, Xu, Molin, Ahrné, & Nyman, 2013). As nowadays fibers are usually recommended to combat obesity, the impact of nanocellulose on lipid metabolism would be of interest to study. The general background of lipid metabolism can be referred to as recent review literature (Betts, 2013; Lairon, Play, & Jourdheuil-Rahmani, 2007). The mechanisms of fibers affecting lipid metabolisms can be roughly considered from three aspects, digestion, intestinal absorption and postprandial modulation (Lairon et al., 2007).

During digestion, fibers may increase the viscosity, or bulk up the content to slow down the lipolysis in the stomach and small intestine by limiting lipid emulsification (B. Pasquier et al., 1996; Bérengère Pasquier et al., 1996). Fibers may physically encapsulate fat within cell walls to prevent digestion (Levine & Silvis, 1980), decrease lipid micellization by adsorbing bile acids to interfere with digestion (Ebihara & Schneeman, 1989). Some fibers such as chitosan may form aggregates with lipid globules to delay lipolysis (Ausar, Landa, Bianco, Castagna, & Beltramo, 2001). When the lipid micelles are on the brush border for absorption by enterocytes, viscosity was considered as the major mechanism for lowering lipid trafficking. Some evidence also suggested that some dietary fibers like oat-bran may alter the chylomicron output to the systemic circulation and reduce the postprandial chylomicron triglycerides, cholesterol and phospholipid (Lia et al., 1997). Postprandial modulation of fibers on lipid metabolism are the indirect ways of mediation other than lipid digestion and absorption, possibly can relate to improved glycemic

control and changes on microbiota. For example, resistant starch was found to improve insulin sensitivity and given it did not affect glucose absorption (Robertson, Bickerton, Dennis, Vidal, & Frayn, 2005). The changes of SCFAs from the fermentation of dietary fibers by microbiota is also important due to they serve as substrates for lipogenesis and cholesterol synthesis (Besten et al., 2013) and are signaling molecules for GPR43/FFAR2 (G-protein-coupled receptors 41, or free fatty acid receptor 2) and GPR41/FFAR3 and PPARγ receptors (Schoeler & Caesar, 2019). Human studies also confirmed that inulin increased *Bifidobacterium* spp. and decreased *Bacteroides vulgatus* accompanied by a significant reduction in body weight z-score, percent body fat, and percent trunk fat (Nicolucci et al., 2017).

The effect of dietary fibers with bile salt metabolisms is further emphasized here. Bile acids are made mainly from cholate, deoxycholate, and chenodeoxycholate with conjugation with glycine, taurine, or other amino acids. Bile acids are made in the liver and stored in the gall bladder. It is secreted into the duodenum and coats lipid droplets on the surface interface and forms micelles for lipids to be uptake by enterocytes (Maldonado-Valderrama, Wilde, Macierzanka, & Mackie, 2011). It was reported that soluble fibers such as β-glucan in oat and guar gum reduced plasma cholesterol level and more fecal bile acids were seen (Ellegård & Andersson, 2007; Moriceau et al., 2000). Fibers may bind bile acids and the viscosity could physically retard the mass transfer of lipolysis and absorption (Gunness & Gidley, 2010). The remaining bile acids then arrive at the large intestine and are utilized by microbiota. The composition and pool size of bile acids are affected by and also regulate the microbiota profile as well as the metabolites (secondary bile acids) and so forth to the host phenotype in insulin secretion and triglyceride metabolisms (Ridlon, Kang, Hylemon, & Bajaj, 2014; Schoeler & Caesar, 2019). The depleted bile acids pool then initial bile synthesis from cholesterol, causing drops on blood cholesterol level.

Cellulose is considered insoluble fibers and cannot increase chyme viscosity (Dhingra et al., 2012) and hence may not be as effective in delaying gastric emptying (Berthold, Unverdorben, Degenhardt, Unverdorben, & Gouni-Berthold, 2008). The major biological functionalities for cellulose include increasing bowel movement and stool weight (Eastwood, Kirkpatrick, Mitchell, Bone, & Hamilton, 1973; J. L. Slavin & Marlett, 1980). Cellulose was also shown to have low to no adsorption of bile acids and cholesterol at a higher amount (Gallaher & Schneeman, 1986; Story, 1986; Sundaravalli, Shurpalekar, & Rao, 1971). The fermentability of cellulose was low, although it still has a beneficial impact on host immunity and such effect is microbiota-dependent (Berer et al., 2018; Morowitz et al., 2017). On the contrary, nanocellulose, whether with surface modification or not, has distinct physical and chemical properties from cellulose, and the impact on lipid metabolism is reviewed as the following.

The viscoelastic properties of nanocellulose showed significant results in *in vitro* studies on lipid digestion and absorption. Depending on the concentration of nanocellulose and the site of digestion, which is important in ionic strength and pH, nanocellulose may form a gel network or be well-dispersed in the lumen to physically hinder the lipase or bile salts to interact with dietary lipids. CNF was found to be entangled and stabilizing the emulsion in the gastric phase *in vitro* which may result in less lipolysis (Liu et al., 2019). A similar effect was seen for CNC that forms a gel in the gastric phase and caused decrease efficiency of lipids when using CNC as an emulsifier (Scheuble et al., 2018). TEMPO-CNF was also found to aggregate and cause phase separation in the stomach and decreased the initial release of fatty acids, and was later found to delay the release of fatty acids of milk *in vitro* in the intestinal digestion (Liu et al., 2019; Liu & Kong, 2019a).

The emulsifying properties of nanocellulose also generate a great affinity for adhesion of nanocellulose on the lipid droplets. The adhesion of nanocellulose on the surface of the lipid

droplets essentially changes the micelle properties and could impact lipid digestion. Such an effect was investigated in the literature. For example, 0.7% w/w CNF formed a gel network that limited the movement of lipid droplets and lowered the release of CNF encapsulated vitamin D3 emulsion and free fatty acids (Winuprasith et al., 2018). Similar results of decreased free fatty acids release were reported by G. M. DeLoid et al. (2018) when mixing 0.75% w/w CNF with heavy cream. For CNC, it may bind to the interface of lipid droplet via electrostatic forces and hydrogen bonding, causing less available area for bile acids or lipase to digest lipids (Bai et al., 2019; Mackie et al., 2019; Sarkar, Li, Cray, & Boxall, 2018).

Another major functionality of fibers nanocellulose could decrease lipid digestion is through the binding of bile acids in the small intestine and excretion in the feces. Bile acids are essential emulsifiers for dietary lipids to break down into micelles to diffuse into enterocytes. CNF and CNC have been found to potentially bind bile salts. Specifically, G. M. DeLoid et al. (2018) investigated the binding energy of CNF to bile salts by discrete molecular dynamics (DMD) simulations and a result of $(2.1 \pm 0.7$ kcal/mol) was above the systemic thermal energy, indicating it may bind in a dynamic/kinetic fashion. CNC was added in an oil-in-water emulsion system for *in vitro* digestion. The digesta after the intestinal phase was added into a Ussing Chamber mounted with murine ileum. The bile acids concentration in the apical side was higher for the CNC group, suggesting sequestration of bile acids by CNC (Mackie et al., 2019). This could also ameliorate hypercholesterolemia because the loss of bile acids would stimulate the liver to recycle more cholesterol from the bloodstream to produce bile acids (Ebihara & Schneeman, 1989).

There are other possible mechanisms for affecting lipid digestion and absorption. Some fibers such as pectin and psyllium may show inhibition on lipase activity (Isaksson, Lundquist, & Ihse, 1982). Although not yet seen on CNC or TEMPO-CNF, 0.4-1% of CNF was found to show

an inhibiting effect on lipase (Liu & Kong, 2019b). Blocking the mucus pore by CNC and affecting the permeability of the mucus layer may also play a role in decreasing the absorption of lipids (Mackie et al., 2019). Note that the extent of the effect on decreasing lipid digestion and absorption is still unsure. Given the initial rate of lipolysis was lower for CNF, CNC, and TEMPO-CNF in *in vitro* investigation, the endpoint lipolysis level was not significant compared to the cellulose group or no fiber group. *In vivo* study feeding mice with regular purified rodent diet (AIN-93) plus up to 21% w/w of CNF showed no significant change on serum triglycerides or total cholesterol and no hepatic damages as well (Andrade et al., 2015). The beneficial effect might be more obvious when a high-fat diet such as the Western diet is consumed. It was seen that CNF (30 mg CNF/kg body weight given once daily by oral gavage) attenuated Western diet-induced fatty liver although no effect on the serum triglyceride level was seen. A promising effect was seen on healthy adults taking 200 mL of medium-chain triglyceride (MCT) oil emulsion containing 4 wt% of CNC. A lower A_{max} (the maximum positive (or negative) amplitude) values for plasma triglyceride and cholecystokinin was seen (Scheuble et al., 2018).

The impact of nanocellulose on lipid digestion via mediating microbiota has not been fully investigated. And there is a lack of studies to look at the association between microbiota changes by nanocellulose to modulation of lipid metabolisms. Although CNC was found to be partially degradable by OECD (Organisation for Economic Co-operation and Development) standardized procedure although the condition was using microorganisms from sewage treatment plants under aerobic conditions (Kümmerer, Menz, Schubert, & Thielemans, 2011) , whether human microbiota can digest CNC still need more studies. The fermentability of both CNC and MCC was found to be higher than the no-fiber group and correlated with particle size both *in vitro* and *in vivo* and is suggested could be used as prebiotics and lowered pH by producing SCFA and promoted growth

of *Bifidobacterium* (Nsor-Atindana et al., 2020). Less is known for TEMPO-CNF although it is considered biodegradable when submerged in phosphate-buffered saline (PBS, pH = 7.4) (Luo et al., 2013; S. Peng et al., 2012). The effect of different nanocellulose on microbiota and how it affects the epigenetic modulation of lipid metabolisms could be further studied.

2.3 References

Aaen, R., Brodin, F. W., Simon, S., Heggset, E. B., & Syverud, K. (2019). Oil-in-Water emulsions stabilized by cellulose nanofibrils—The effects of ionic strength and pH. *Nanomaterials,* 9(2), 259.

Aaen, R., Simon, S., Wernersson Brodin, F., & Syverud, K. (2019). The potential of TEMPO-oxidized cellulose nanofibrils as rheology modifiers in food systems. *Cellulose,* 26(9), 5483-5496.

Abraham, E., Deepa, B., Pothan, L. A., Jacob, M., Thomas, S., Cvelbar, U., & Anandjiwala, R. (2011). Extraction of nanocellulose fibrils from lignocellulosic fibres: A novel approach. *Carbohydrate Polymers,* 86(4), 1468-1475.

Ahuja, A., Khar, R. K., & Ali, J. (2008). Mucoadhesive Drug Delivery Systems. *Drug Development and Industrial Pharmacy,* 23(5), 489-515.

Akbari, P., Fink-Gremmels, J., Willems, R. H. A. M., Difilippo, E., Schols, H. A., Schoterman, M. H. C., . . . Braber, S. (2017). Characterizing microbiota-independent effects of oligosaccharides on intestinal epithelial cells: insight into the role of structure and size. *European Journal of Nutrition,* 56(5), 1919-1930.

Alemdar, A., & Sain, M. (2008). Isolation and characterization of nanofibers from agricultural residues – Wheat straw and soy hulls. *Bioresource Technology,* 99(6), 1664-1671.

Allen, A., & Carroll, N. J. H. (1985). Adherent and soluble mucus in the stomach and duodenum. *Digestive Diseases and Sciences,* 30(11 Suppl), 55S-62S.

Andrade, D. R., Mendonca, M. H., Helm, C. V., Magalhaes, W. L., de Muniz, G. I., & Kestur, S. G. (2015). Assessment of Nano Cellulose from Peach Palm Residue as Potential Food Additive: Part II: Preliminary Studies. *J Food Sci Technol,* 52(9), 5641-5650.

Andresen, M., & Stenius, P. (2007). Water-in-oil Emulsions Stabilized by Hydrophobized Microfibrillated Cellulose. *Journal of Dispersion Science and Technology,* 28(6), 837-844.

Andrews, G. P., Laverty, T. P., & Jones, D. S. (2009). Mucoadhesive polymeric platforms for controlled drug delivery. *European Journal of Pharmaceutics and Biopharmaceutics,*

71(3), 505-518.

Araki, J., Wada, M., & Kuga, S. (2001). Steric Stabilization of a Cellulose Microcrystal Suspension by Poly(ethylene glycol) Grafting. *Langmuir,* 17(1), 21-27.

Atuma, C., Strugala, V., Allen, A., & Holm, L. (2001). The adherent gastrointestinal mucus gel layer: thickness and physical state in vivo. *American Journal of Physiology-Gastrointestinal and Liver Physiology,* 280(5), G922-929.

Ausar, S. F., Landa, C. A., Bianco, I. D., Castagna, L. F., & Beltramo, D. M. (2001). Hydrolysis of a Chitosan-induced Milk Aggregate by Pepsin, Trypsin and Pancreatic Lipase. *Bioscience, Biotechnology, and Biochemistry,* 65(11), 2412-2418.

Azeredo, H. M. C., Rosa, M. F., & Mattoso, L. H. C. (2017). Nanocellulose in bio-based food packaging applications. *Industrial Crops and Products,* 97, 664-671.

Bai, L., Lv, S., Xiang, W., Huan, S., McClements, D. J., & Rojas, O. J. (2019). Oil-in-water Pickering emulsions via microfluidization with cellulose nanocrystals: 2. In vitro lipid digestion. *Food Hydrocolloids,* 96, 709-716.

Bano, S., & Negi, Y. S. (2017). Studies on cellulose nanocrystals isolated from groundnut shells. *Carbohydrate Polymers,* 157, 1041-1049.

Beck-Candanedo, S., Roman, M., & Gray, D. G. (2005). Effect of Reaction Conditions on the Properties and Behavior of Wood Cellulose Nanocrystal Suspensions. *Biomacromolecules,* 6(2), 1048-1054.

Berer, K., Martínez, I., Walker, A., Kunkel, B., Schmitt-Kopplin, P., Walter, J., & Krishnamoorthy, G. (2018). Dietary non-fermentable fiber prevents autoimmune neurological disease by changing gut metabolic and immune status. *Scientific Reports,* 8(1), 10431.

Berthold, H. K., Unverdorben, S., Degenhardt, R., Unverdorben, M., & Gouni-Berthold, I. (2008). Effect of a cellulose-containing weight-loss supplement on gastric emptying and sensory functions. *Obesity,* 16(10), 2272-2280.

Besten, G. d., Lange, K., Havinga, R., Dijk, T. H. v., Gerding, A., Eunen, K. v., . . . Reijngoud, D.-J. (2013). Gut-derived short-chain fatty acids are vividly assimilated into host

carbohydrates and lipids. *American Journal of Physiology-Gastrointestinal and Liver Physiology,* 305(12), G900-G910.

Betts, J. G. (2013). *Anatomy and Physiology*. Minneapolis, MN: Open Textbook Library, OpenStax.

Bharimalla, A. K., Deshmukh, S. P., Vigneshwaran, N., Patil, P. G., & Prasad, V. (2017). Nanocellulose-Polymer Composites for Applications in Food Packaging: Current Status, Future Prospects and Challenges. *Polymer-Plastics Technology and Engineering,* 56(8), 805-823.

Bhatia, S., Prabhu, P. N., Benefiel, A. C., Miller, M. J., Chow, J., Davis, S. R., & Gaskins, H. R. (2015). Galacto-oligosaccharides may directly enhance intestinal barrier function through the modulation of goblet cells. *Molecular Nutrition & Food Research,* 59(3), 566-573.

Bobek, L. A., & Situ, H. (2003). MUC7 20-Mer: Investigation of Antimicrobial Activity, Secondary Structure, and Possible Mechanism of Antifungal Action. *Antimicrobial Agents and Chemotherapy,* 47(2), 643-652.

Bongers, A., & van den Heuvel, E. G. H. M. (2003). Prebiotics and the Bioavailability of Minerals and Trace Elements. *Food Reviews International,* 19(4), 397-422.

Bravi, F., Scotti, L., Bosetti, C., Bertuccio, P., Negri, E., & La Vecchia, C. (2009). Dietary fiber and stomach cancer risk: a case–control study from Italy. *Cancer Causes & Control,* 20(6), 847-853.

Bruno, L. S., Li, X., Wang, L., Soares, R. V., Siqueira, C. C., Oppenheim, F. G., . . . Offner, G. D. (2005). Two-hybrid analysis of human salivary mucin MUC7 interactions. *Biochimica et Biophysica Acta (BBA) - Molecular Cell Research,* 1746(1), 65-72.

Burt, H. M., Jackson, J. K., & Hamad, W. Y. (2014). Binding drugs with nanocrystalline cellulose (ncc). Google Patents.

Camarero Espinosa, S., Kuhnt, T., Foster, E. J., & Weder, C. (2013). Isolation of Thermally Stable Cellulose Nanocrystals by Phosphoric Acid Hydrolysis. *Biomacromolecules,* 14(4), 1223-1230.

Cavallari, C., Brigidi, P., & Fini, A. (2015). Ex-vivoand in-vitro assessment of mucoadhesive patches containing the gel-forming polysaccharide psyllium for buccal delivery of chlorhexidine base. *International Journal of Pharmaceutics,* 496(2), 593-600.

Chen, Y., Lin, Y.-J., Nagy, T., Kong, F., & Guo, T. L. (2020). Subchronic exposure to cellulose nanofibrils induces nutritional risk by non-specifically reducing the intestinal absorption. *Carbohydrate Polymers,* 229, 115536.

Chun, W., Bamba, T., & Hosoda, S. (1989). Effect of Pectin, a Soluble Dietary Fiber, on Functional and Morphological Parameters of the Small Intestine in Rats. *Digestion,* 42(1), 22-29.

Dalile, B., Van Oudenhove, L., Vervliet, B., & Verbeke, K. (2019). The role of short-chain fatty acids in microbiota–gut–brain communication. *Nature Reviews Gastroenterology & Hepatology,* 16(8), 461-478.

de Lima Pizi Cândido, A., Fregonezi, N. F., Carvalho, A. J. F., Trovatti, E., & Resende, F. A. (2020). TEMPO-Oxidized Cellulose Nanofibers In Vitro Cyto-genotoxicity Studies. *BioNanoScience,* 10(3), 766-772.

DeLoid, G., Cao, X., Molina, R. M., Silva, D. I., Bhattacharya, K., Ng, K. W., . . . Demokritou, P. (2019). Toxicological effects of ingested nanocellulose in in vitro intestinal epithelium and in vivo rat models. *Environmental Science: Nano*.

DeLoid, G. M., Sohal, I. S., Lorente, L. R., Molina, R. M., Pyrgiotakis, G., Stevanovic, A., . . . Bousfield, D. W. (2018). Reducing intestinal digestion and absorption of fat using a nature-derived biopolymer: Interference of triglyceride hydrolysis by nanocellulose. *ACS nano,* 12(7), 6469-6479.

Derjaguin, B. V., Aleinikova, I. N., & Toporov, Y. P. (1994). On the Role of Electrostatic Forces in the Adhesion of Polymer Particles to Solid-Surfaces. *Progress in Surface Science,* 45(1-4), 119-123.

Derjaguin, B. V., Toporov, Y. P., Muller, V. M., & Aleinikova, I. N. (1977). On the relationship between the electrostatic and the molecular component of the adhesion of elastic particles to a solid surface. *Journal of Colloid and Interface Science,* 58(3), 528-533.

Desai, M. S., Seekatz, A. M., Koropatkin, N. M., Kamada, N., Hickey, C. A., Wolter, M., . . . Martens, E. C. (2016). A Dietary Fiber-Deprived Gut Microbiota Degrades the Colonic

Mucus Barrier and Enhances Pathogen Susceptibility. *Cell,* 167(5), 1339-1353.e1321.

Dhingra, D., Michael, M., Rajput, H., & Patil, R. T. (2012). Dietary fibre in foods: a review. *Journal of Food Science and Technology,* 49(3), 255-266.

Dufresne, A. (2017). *Nanocellulose: from nature to high performance tailored materials*: Walter de Gruyter GmbH & Co KG.

Eastwood, M. A., Kirkpatrick, J. R., Mitchell, W. D., Bone, A., & Hamilton, T. (1973). Effects of Dietary Supplements of Wheat Bran and Cellulose on Faeces and Bowel Function. *British Medical Journal,* 4(5889), 392-394.

Ebihara, K., & Schneeman, B. O. (1989). Interaction of bile acids, phospholipids, cholesterol and triglyceride with dietary fibers in the small intestine of rats. *The Journal of Nutrition,* 119(8), 1100-1106.

El Aidy, S., van den Bogert, B., & Kleerebezem, M. (2015). The small intestine microbiota, nutritional modulation and relevance for health. *Current Opinion in Biotechnology,* 32, 14-20.

Ellegård, L., & Andersson, H. (2007). Oat bran rapidly increases bile acid excretion and bile acid synthesis: an ileostomy study. *European Journal of Clinical Nutrition,* 61(8), 938-945.

Endes, C., Camarero-Espinosa, S., Mueller, S., Foster, E. J., Petri-Fink, A., Rothen-Rutishauser, B., . . . Clift, M. J. D. (2016). A critical review of the current knowledge regarding the biological impact of nanocellulose. *Journal of Nanobiotechnology,* 14(1), 78.

Ermund, A., Schütte, A., Johansson, M. E. V., Gustafsson, J. K., & Hansson, G. C. (2013). Studies of mucus in mouse stomach, small intestine, and colon. I. Gastrointestinal mucus layers have different properties depending on location as well as over the Peyer's patches. *American Journal of Physiology-Gastrointestinal and Liver Physiology,* 305(5), G341-G347.

Ewaschuk, J. B., & Dieleman, L. A. (2006). Probiotics and prebiotics in chronic inflammatory bowel diseases. *World journal of gastroenterology,* 12(37), 5941-5950.

Fabiano, A., Zambito, Y., & Bernkop-Schnurch, A. (2017). About the impact of water movement

on the permeation behaviour of nanoparticles in mucus. *International Journal of Pharmaceutics,* 517(1-2), 279-285.

Ford, D. A. (2015). Pilot Study: Nanocellulose as a Fat Replacer in Ice Cream. *Food Science and Human Nutrition* (Vol. Master of Science (MS)): University of Maine.

Fortunati, E., Peltzer, M., Armentano, I., Torre, L., Jiménez, A., & Kenny, J. M. (2012). Effects of modified cellulose nanocrystals on the barrier and migration properties of PLA nano-biocomposites. *Carbohydrate Polymers,* 90(2), 948-956.

Foster, E. J., Moon, R. J., Agarwal, U. P., Bortner, M. J., Bras, J., Camarero-Espinosa, S., . . . Youngblood, J. (2018). Current characterization methods for cellulose nanomaterials. *Chemical Society Reviews,* 47(8), 2609-2679.

Fukuzumi, H., Tanaka, R., Saito, T., & Isogai, A. (2014). Dispersion stability and aggregation behavior of TEMPO-oxidized cellulose nanofibrils in water as a function of salt addition. *Cellulose,* 21(3), 1553-1559.

Gómez H, C., Serpa, A., Velásquez-Cock, J., Gañán, P., Castro, C., Vélez, L., & Zuluaga, R. (2016). Vegetable nanocellulose in food science: A review. *Food Hydrocolloids,* 57, 178-186.

Gallaher, D., & Schneeman, B. O. (1986). Intestinal interaction of bile acids, phospholipids, dietary fibers, and cholestyramine. *American Journal of Physiology-Gastrointestinal and Liver Physiology,* 250(4), G420-G426.

Gama, M., Gatenholm, P., & Klemm, D. (2012). *Bacterial nanocellulose: a sophisticated multifunctional material*: CRC press.

Geng, L., Peng, X., Zhan, C., Naderi, A., Sharma, P. R., Mao, Y., & Hsiao, B. S. (2017). Structure characterization of cellulose nanofiber hydrogel as functions of concentration and ionic strength. *Cellulose,* 24(12), 5417-5429.

George, J., Bawa, A. S., & Siddaramaiah. (2010). Synthesis and Characterization of Bacterial Cellulose Nanocrystals and their PVA Nanocomposites. *Advanced Materials Research,* 123-125, 383-386.

Glade, M. J., & Meguid, M. M. (2016). A glance at … dietary emulsifiers, the human intestinal

mucus and microbiome, and dietary fiber. *Nutrition,* 32(5), 609-614.

Gunness, P., & Gidley, M. J. (2010). Mechanisms underlying the cholesterol-lowering properties of soluble dietary fibre polysaccharides. *Food & Function,* 1(2), 149-155.

Habibi, Y., Mahrouz, M., & Vignon, M. R. (2009). Microfibrillated cellulose from the peel of prickly pear fruits. *Food chemistry,* 115(2), 423-429.

Hanif, Z., Ahmed, F. R., Shin, S. W., Kim, Y.-K., & Um, S. H. (2014). Size- and dose-dependent toxicity of cellulose nanocrystals (CNC) on human fibroblasts and colon adenocarcinoma. *Colloids and Surfaces B: Biointerfaces,* 119, 162-165.

Harper, B. J., Clendaniel, A., Sinche, F., Way, D., Hughes, M., Schardt, J., . . . Harper, S. L. (2016). Impacts of chemical modification on the toxicity of diverse nanocellulose materials to developing zebrafish. *Cellulose,* 23(3), 1763-1775.

Heggset, E. B., Aaen, R., Veslum, T., Henriksson, M., Simon, S., & Syverud, K. (2020). Cellulose nanofibrils as rheology modifier in mayonnaise – A pilot scale demonstration. *Food Hydrocolloids,* 108, 106084.

Helenius, G., Backdahl, H., Bodin, A., Nannmark, U., Gatenholm, P., & Risberg, B. (2006). In vivo biocompatibility of bacterial cellulose. *Journal of Biomedical Materials Research Part A,* 76(2), 431-438.

Hino, S., Takemura, N., Sonoyama, K., Morita, A., Kawagishi, H., Aoe, S., & Morita, T. (2012). Small Intestinal Goblet Cell Proliferation Induced by Ingestion of Soluble and Insoluble Dietary Fiber Is Characterized by An Increase in Sialylated Mucins in Rats. *The Journal of Nutrition,* 142(8), 1429-1436.

Hosseinidoust, Z., Alam, M. N., Sim, G., Tufenkji, N., & van de Ven, T. G. M. (2015). Cellulose nanocrystals with tunable surface charge for nanomedicine. *Nanoscale,* 7(40), 16647-16657.

Huang, Y.-W., Cambre, M., & Lee, H.-J. (2017). The Toxicity of Nanoparticles Depends on Multiple Molecular and Physicochemical Mechanisms. *International journal of molecular sciences,* 18(12), 2702.

Huh, C. H., Bhutani, M. S., Farfan, E. B., & Bolch, W. E. (2003). Individual variations in mucosa and total wall thickness in the stomach and rectum assessed via endoscopic ultrasound. *Physiological measurement,* 24(4), N15-22.

Isaksson, G., Lundquist, I., & Ihse, I. (1982). In vitro Inhibition of Pancreatic Enzyme Activities by Dietary Fiber. *Digestion,* 24(1), 54-59.

Islam, M. T., Alam, M. M., Patrucco, A., Montarsolo, A., & Zoccola, M. (2014). Preparation of nanocellulose: A review. *AATCC Journal of Research,* 1(5), 17-23.

Ito, H., Satsukawa, M., Arai, E., Sugiyama, K., Sonoyama, K., Kiriyama, S., & Morita, T. (2009). Soluble Fiber Viscosity Affects Both Goblet Cell Number and Small Intestine Mucin Secretion in Rats. *The Journal of Nutrition,* 139(9), 1640-1647.

Jacobs, L. R. (1983). Effects of dietary fiber on mucosal growth and cell proliferation in the small intestine of the rat: a comparison of oat bran, pectin, and guar with total fiber deprivation. *The American Journal of Clinical Nutrition,* 37(6), 954-960.

Jakobsdottir, G., Xu, J., Molin, G., Ahrné, S., & Nyman, M. (2013). High-fat diet reduces the formation of butyrate, but increases succinate, inflammation, liver fat and cholesterol in rats, while dietary fibre counteracts these effects. *PLoS One,* 8(11), e80476.

Jeevahan, J., & Chandrasekaran, M. (2019). Influence of Nanocellulose Additive on the Film Properties of Native Rice Starch-based Edible Films for Food Packaging. *Recent Pat Nanotechnol,* 13(3), 222-233.

Jin, L., Reynolds, L. P., Redmer, D. A., Caton, J. S., & Crenshaw, J. D. (1994). Effects of dietary fiber on intestinal growth, cell proliferation, and morphology in growing pigs2. *Journal of Animal Science,* 72(9), 2270-2278.

Johansson, M. E., Larsson, J. M., & Hansson, G. C. (2011). The two mucus layers of colon are organized by the MUC2 mucin, whereas the outer layer is a legislator of host-microbial interactions. *Proceedings of the National Academy of Sciences,* 108 Suppl 1, 4659-4665.

Johansson, M. E. V., Gustafsson, J. K., Holmén-Larsson, J., Jabbar, K. S., Xia, L., Xu, H., . . . Hansson, G. C. (2014). Bacteria penetrate the normally impenetrable inner colon mucus layer in both murine colitis models and patients with ulcerative colitis. *Gut,* 63(2), 281-291.

Johansson, M. E. V., Phillipson, M., Petersson, J., Velcich, A., Holm, L., & Hansson, G. C. (2008). The inner of the two Muc2 mucin-dependent mucus layers in colon is devoid of bacteria. *Proceedings of the National Academy of Sciences,* 105(39), 15064-15069.

Kümmerer, K., Menz, J., Schubert, T., & Thielemans, W. (2011). Biodegradability of organic nanoparticles in the aqueous environment. *Chemosphere,* 82(10), 1387-1392.

Kallel, F., Bettaieb, F., Khiari, R., García, A., Bras, J., & Chaabouni, S. E. (2016). Isolation and structural characterization of cellulose nanocrystals extracted from garlic straw residues. *Industrial Crops and Products,* 87, 287-296.

Kang, D.-W., Park, J. G., Ilhan, Z. E., Wallstrom, G., LaBaer, J., Adams, J. B., & Krajmalnik-Brown, R. (2013). Reduced Incidence of Prevotella and Other Fermenters in Intestinal Microflora of Autistic Children. *PLoS One,* 8(7), e68322.

Kargarzadeh, H., Mariano, M., Gopakumar, D., Ahmad, I., Thomas, S., Dufresne, A., . . . Lin, N. (2018). Advances in cellulose nanomaterials. *Cellulose,* 25(4), 2151-2189.

Kato, I., Nomura, A. M. Y., Stemmermann, G. N., & Chyou, P.-H. (1992). A Prospective Study of Gastric and Duodenal Ulcer and Its Relation to Smoking, Alcohol, and Diet. *American Journal of Epidemiology,* 135(5), 521-530.

Kawakubo, M., Ito, Y., Okimura, Y., Kobayashi, M., Sakura, K., Kasama, S., . . . Nakayama, J. (2004). Natural Antibiotic Function of a Human Gastric Mucin Against Helicobacter pylori Infection. *Science,* 305(5686), 1003-1006.

Khan, A., Huq, T., Khan, R. A., Riedl, B., & Lacroix, M. (2014). Nanocellulose-Based Composites and Bioactive Agents for Food Packaging. *Critical Reviews in Food Science and Nutrition,* 54(2), 163-174.

Khutoryanskiy, V. V. (2011). Advances in mucoadhesion and mucoadhesive polymers. *Macromolecular Bioscience,* 11(6), 748-764.

Kinloch, A. J. (1980). The Science of Adhesion .1. Surface and Interfacial Aspects. *Journal of Materials Science,* 15(9), 2141-2166.

Kleessen, B., Hartmann, L., & Blaut, M. (2003). Fructans in the diet cause alterations of intestinal

mucosal architecture, released mucins and mucosa-associated bifidobacteria in gnotobiotic rats. *British journal of nutrition,* 89(5), 597-606.

Kleiman, S. C., Watson, H. J., Bulik-Sullivan, E. C., Huh, E. Y., Tarantino, L. M., Bulik, C. M., & Carroll, I. M. (2015). The Intestinal Microbiota in Acute Anorexia Nervosa and During Renourishment: Relationship to Depression, Anxiety, and Eating Disorder Psychopathology. *Psychosomatic medicine,* 77(9), 969-981.

Kleinschmidt, D. C., Roberts, B. A., Fuqua, D. L., & Melchion, J. R. (1988). Filling-containing, dough-based products containing cellulosic fibrils and microfibrils. Google Patents.

Lairon, D., Play, B., & Jourdheuil-Rahmani, D. (2007). Digestible and indigestible carbohydrates: interactions with postprandial lipid metabolism. *The Journal of Nutritional Biochemistry,* 18(4), 217-227.

Lee, J. W., Park, J. H., & Robinson, J. R. (2000). Bioadhesive-Based Dosage Forms: The Next Generation. *Journal of Pharmaceutical Sciences,* 89(7), 850-866.

Lee, S.-Y., Chun, S.-J., Kang, I.-A., & Park, J.-Y. (2009). Preparation of cellulose nanofibrils by high-pressure homogenizer and cellulose-based composite films. *Journal of Industrial and Engineering Chemistry,* 15(1), 50-55.

Lee, Y., Deelman, T. E., Chen, K., Lin, D. S. Y., Tavakkoli, A., & Karp, J. M. (2018). Therapeutic luminal coating of the intestine. *Nature Materials,* 17(9), 834-842.

Lehr, C.-M., Bouwstra, J. A., Schacht, E. H., & Junginger, H. E. (1992). In vitro evaluation of mucoadhesive properties of chitosan and some other natural polymers. *International Journal of Pharmaceutics,* 78(1-3), 43-48.

Levine, A. S., & Silvis, S. E. (1980). Absorption of Whole Peanuts, Peanut Oil, and Peanut Butter. *New England Journal of Medicine,* 303(16), 917-918.

Li, H., Limenitakis, J. P., Fuhrer, T., Geuking, M. B., Lawson, M. A., Wyss, M., . . . Macpherson, A. J. (2015). The outer mucus layer hosts a distinct intestinal microbial niche. *Nature communications,* 6, 8292.

Li, J., Wang, Y., Zhang, L., Xu, Z., Dai, H., & Wu, W. (2019). Nanocellulose/Gelatin Composite

Cryogels for Controlled Drug Release. *ACS Sustainable Chemistry & Engineering,* 7(6), 6381-6389.

Lia, A., Andersson, H., Mekki, N., Juhel, C., Senft, M., & Lairon, D. (1997). Postprandial lipemia in relation to sterol and fat excretion in ileostomy subjects given oat-bran and wheat test meals. *The American Journal of Clinical Nutrition,* 66(2), 357-365.

Lin, N., Gèze, A., Wouessidjewe, D., Huang, J., & Dufresne, A. (2016). Biocompatible Double-Membrane Hydrogels from Cationic Cellulose Nanocrystals and Anionic Alginate as Complexing Drugs Codelivery. *ACS Applied Materials & Interfaces,* 8(11), 6880-6889.

Littunen, K., Snoei de Castro, J., Samoylenko, A., Xu, Q., Quaggin, S., Vainio, S., & Seppälä, J. (2016). Synthesis of cationized nanofibrillated cellulose and its antimicrobial properties. *European Polymer Journal,* 75, 116-124.

Liu, L., Kerr, W. L., & Kong, F. (2019). Characterization of lipid emulsions during in vitro digestion in the presence of three types of nanocellulose. *Journal of Colloid and Interface Science*.

Liu, L., Kerr, W. L., Kong, F., Dee, D. R., & Lin, M. (2018). Influence of nano-fibrillated cellulose (NFC) on starch digestion and glucose absorption. *Carbohydrate Polymers,* 196, 146-153.

Liu, L., & Kong, F. (2019a). In vitro investigation of the influence of nano-cellulose on starch and milk digestion and mineral adsorption. *International Journal of Biological Macromolecules,* 137, 1278-1285.

Liu, L., & Kong, F. (2019b). In vitro investigation of the influence of nano-fibrillated cellulose on lipid digestion and absorption. *International Journal of Biological Macromolecules,* 139, 361-366.

Liu, L., & Kong, F. (2019c). Influence of nanocellulose on in vitro digestion of whey protein isolate. *Carbohydrate Polymers,* 210, 399-411.

Lobionda, S., Sittipo, P., Kwon, H. Y., & Lee, Y. K. (2019). The Role of Gut Microbiota in Intestinal Inflammation with Respect to Diet and Extrinsic Stressors. *Microorganisms,* 7(8), 271.

Luo, H., Xiong, G., Hu, D., Ren, K., Yao, F., Zhu, Y., . . . Wan, Y. (2013). Characterization of TEMPO-oxidized bacterial cellulose scaffolds for tissue engineering applications. *Materials Chemistry and Physics,* 143(1), 373-379.

Mackie, A., Gourcy, S., Rigby, N., Moffat, J., Capron, I., & Bajka, B. (2019). The fate of cellulose nanocrystal stabilised emulsions after simulated gastrointestinal digestion and exposure to intestinal mucosa. *Nanoscale,* 11(6), 2991-2998.

Mahmoud, K. A., Mena, J. A., Male, K. B., Hrapovic, S., Kamen, A., & Luong, J. H. (2010). Effect of surface charge on the cellular uptake and cytotoxicity of fluorescent labeled cellulose nanocrystals. *ACS Appl Mater Interfaces,* 2(10), 2924-2932.

Maldonado-Valderrama, J., Wilde, P., Macierzanka, A., & Mackie, A. (2011). The role of bile salts in digestion. *Advances in Colloid and Interface Science,* 165(1), 36-46.

Martens, E. C., Chiang, H. C., & Gordon, J. I. (2008). Mucosal glycan foraging enhances fitness and transmission of a saccharolytic human gut bacterial symbiont. *Cell Host Microbe,* 4(5), 447-457.

Menas, A. L., Yanamala, N., Farcas, M. T., Russo, M., Friend, S., Fournier, P. M., . . . Shvedova, A. A. (2017). Fibrillar vs crystalline nanocellulose pulmonary epithelial cell responses: Cytotoxicity or inflammation? *Chemosphere,* 171, 671-680.

Moon, R. J. (2008). Nanomaterials in the forest products industry. *McGraw-Hill Yearbook of Science and Technology, 2008. New York: McGraw-Hill, c2008: Pages 225-228.*

Moon, R. J., Frihart, C. R., & Wegner, T. (2006). Nanotechnology applications in the forest products industry. *Forest products journal. Vol. 56, no. 5 (May 2006): pages 4-10.*

Moon, R. J., Martini, A., Nairn, J., Simonsen, J., & Youngblood, J. (2011). Cellulose nanomaterials review: structure, properties and nanocomposites. *Chemical Society Reviews,* 40(7), 3941-3994.

Moriceau, S., Besson, C., Levrat, M.-A., Moundras, C., Rémésy, C., Morand, C., & Demigné, C. (2000). Cholesterol-lowering effects of guar gum: Changes in bile acid pools and intestinal reabsorption. *Lipids,* 35(4), 437-444.

Morowitz, M. J., Di Caro, V., Pang, D., Cummings, J., Firek, B., Rogers, M. B., . . . Aneja, R. K. (2017). Dietary Supplementation With Nonfermentable Fiber Alters the Gut Microbiota and Confers Protection in Murine Models of Sepsis. *Critical Care Medicine,* 45(5).

Mudgil, D., & Barak, S. (2013). Composition, properties and health benefits of indigestible carbohydrate polymers as dietary fiber: A review. *International Journal of Biological Macromolecules,* 61, 1-6.

Nagalakshmaiah, M., kissi, N. E., Mortha, G., & Dufresne, A. (2016). Structural investigation of cellulose nanocrystals extracted from chili leftover and their reinforcement in cariflex-IR rubber latex. *Carbohydrate Polymers,* 136, 945-954.

Nicolucci, A. C., Hume, M. P., Martínez, I., Mayengbam, S., Walter, J., & Reimer, R. A. (2017). Prebiotics Reduce Body Fat and Alter Intestinal Microbiota in Children Who Are Overweight or With Obesity. *Gastroenterology,* 153(3), 711-722.

Nsor-Atindana, J., Zhou, Y. X., Saqib, M. N., Chen, M., Douglas Goff, H., Ma, J., & Zhong, F. (2020). Enhancing the prebiotic effect of cellulose biopolymer in the gut by physical structuring via particle size manipulation. *Food Research International,* 131, 108935.

O'Connor, B., Berry, R., & Goguen, R. (2014). *Chapter 10—Commercialization of cellulose nanocrystal (NCC) production: A business case focusing on the importance of proactive ehs management.* In *Nanotechnology Environmental Health and Safety: Risks, Regulation, and Management, 2nd Edition*: Ringgold, Inc.

Ong, K. J., Ede, J. D., Pomeroy-Carter, C. A., Sayes, C. M., Mulenos, M. R., & Shatkin, J. A. (2020). A 90-day dietary study with fibrillated cellulose in Sprague-Dawley rats. *Toxicology Reports,* 7, 174-182.

Park, K., & Robinson, J. R. (1984). Bioadhesive Polymers as Platforms for Oral-Controlled Drug Delivery - Method to Study Bioadhesion. *International Journal of Pharmaceutics,* 19(2), 107-127.

Parker, A., Maclaren, O. J., Fletcher, A. G., Muraro, D., Kreuzaler, P. A., Byrne, H. M., . . . Pin, C. (2017). Cell proliferation within small intestinal crypts is the principal driving force for cell migration on villi. *FASEB journal : official publication of the Federation of American Societies for Experimental Biology,* 31(2), 636-649.

Pasquier, B., Armand, M., Castelain, C., Guillon, F., Borel, P., Lafont, H., & Lairon, D. (1996). Emulsification and lipolysis of triacylglycerols are altered by viscous soluble dietary fibres in acidic gastric medium in vitro. *Biochemical Journal,* 314(1), 269-275.

Pasquier, B., Armand, M., Guillon, F., Castelain, C., Borel, P., Barry, J.-L., . . . Lairon, D. (1996). Viscous soluble dietary fibers alter emulsification and lipolysis of triacylglycerols in duodenal medium in vitro. *The Journal of Nutritional Biochemistry,* 7(5), 293-302.

Patel, J. K., & Patel, M. M. (2007). Stomach specific anti-helicobacter pylori therapy: preparation and evaluation of amoxicillin-loaded chitosan mucoadhesive microspheres. *Current drug delivery,* 4(1), 41-50.

Peng, S., Zheng, Y., Wu, J., Wu, Y., Ma, Y., Song, W., & Xi, T. (2012). Preparation and characterization of degradable oxidized bacterial cellulose reacted with nitrogen dioxide. *Polymer Bulletin,* 68(2), 415-423.

Peng, Y., Gardner, D. J., Han, Y., Kiziltas, A., Cai, Z., & Tshabalala, M. A. (2013). Influence of drying method on the material properties of nanocellulose I: thermostability and crystallinity. *Cellulose,* 20(5), 2379-2392.

Peppas, N. A., & Buri, P. A. (1985). Surface, interfacial and molecular aspects of polymer bioadhesion on soft tissues. *Journal of Controlled Release,* 2, 257-275.

Pickering, S. U. (1907). CXCVI.—Emulsions. *Journal of the Chemical Society, Transactions,* 91(0), 2001-2021.

Pitkanen, M., Kangas, H., Laitinen, O., Sneck, A., Lahtinen, P., Peresin, M. S., & Niinimaki, J. (2014). Characteristics and safety of nano-sized cellulose fibrils. *Cellulose,* 21(6), 3871-3886.

Ponchel, G., Montisci, M. J., Dembri, A., Durrer, C., & Duchêne, D. (1997). Mucoadhesion of colloidal particulate systems in the gastro-intestinal tract. *European Journal of Pharmaceutics and Biopharmaceutics,* 44(1), 25-31.

Postek, M. T., Vladár, A., Dagata, J., Farkas, N., Ming, B., Wagner, R., . . . Beecher, J. (2010). Development of the metrology and imaging of cellulose nanocrystals. *Measurement Science and Technology,* 22(2), 024005.

Pradhan, S. H., Mulenos, M. R., Steele, L. R., Gibb, M., Ede, J. D., Ong, K. J., . . . Sayes, C. M. (2020). Physical, chemical, and toxicological characterization of fibrillated forms of cellulose using an in vitro gastrointestinal digestion and co-culture model. *Toxicology Research,* 9(3), 290-301.

Qi, W., Wu, J., Shu, Y., Wang, H., Rao, W., Xu, H.-N., & Zhang, Z. (2020). Microstructure and physiochemical properties of meat sausages based on nanocellulose-stabilized emulsions. *International Journal of Biological Macromolecules,* 152, 567-575.

Qing, Y., Sabo, R., Zhu, J. Y., Agarwal, U., Cai, Z., & Wu, Y. (2013). A comparative study of cellulose nanofibrils disintegrated via multiple processing approaches. *Carbohydrate Polymers,* 97(1), 226-234.

Rajinipriya, M., Nagalakshmaiah, M., Robert, M., & Elkoun, S. (2018). Importance of Agricultural and Industrial Waste in the Field of Nanocellulose and Recent Industrial Developments of Wood Based Nanocellulose: A Review. *ACS Sustainable Chemistry & Engineering,* 6(3), 2807-2828.

Rajput, G., Majmudar, F., Patel, J., Thakor, R., & Rajgor, N. B. (2010). Stomach-Specific Mucoadhesive Microsphere as a Controlled Drug Delivery System. *Systematic Reviews in Pharmacy,* 1(1), 70-78.

Ranby, B. (1949). Aqueous colloidal solutions of cellulose micelles. (Vol. 3, pp. 649-650): Acta Chemica Scandinavica.

Raschka, L., & Daniel, H. (2005). Mechanisms underlying the effects of inulin-type fructans on calcium absorption in the large intestine of rats. *Bone,* 37(5), 728-735.

Reiner, R. S., & Rudie, A. W. (2017). *Experiences with Scaling-Up Production of TEMPO-Grade Cellulose Nanofibrils*. In *Nanocelluloses: Their Preparation, Properties, and Applications* (pp. 227-245): American Chemical Society

Reinus, J., & Simon, D. (2014). *Gastrointestinal anatomy and physiology : the essentials*: Wiley Blackwell.

Ridlon, J. M., Kang, D. J., Hylemon, P. B., & Bajaj, J. S. (2014). Bile acids and the gut microbiome. *Current Opinion in Gastroenterology,* 30(3), 332-338.

Robertson, M. D., Bickerton, A. S., Dennis, A. L., Vidal, H., & Frayn, K. N. (2005). Insulin-sensitizing effects of dietary resistant starch and effects on skeletal muscle and adipose tissue metabolism. *Am J Clin Nutr,* 82(3), 559-567.

Roediger, W. E. (1980). Role of anaerobic bacteria in the metabolic welfare of the colonic mucosa in man. *Gut,* 21(9), 793-798.

Roman, M. (2015). Toxicity of Cellulose Nanocrystals: A Review. *Industrial Biotechnology,* 11(1), 25-33.

Romo-Araiza, A., Gutiérrez-Salmeán, G., Galván, E. J., Hernández-Frausto, M., Herrera-López, G., Romo-Parra, H., . . . Ibarra, A. (2018). Probiotics and Prebiotics as a Therapeutic Strategy to Improve Memory in a Model of Middle-Aged Rats. *Frontiers in Aging Neuroscience,* 10(416).

Rosa, M. F., Medeiros, E. S., Malmonge, J. A., Gregorski, K. S., Wood, D. F., Mattoso, L. H. C., . . . Imam, S. H. (2010). Cellulose nanowhiskers from coconut husk fibers: Effect of preparation conditions on their thermal and morphological behavior. *Carbohydrate Polymers,* 81(1), 83-92.

Royle, L., Roos, A., Harvey, D. J., Wormald, M. R., Van Gijlswijk-Janssen, D., Redwan, E.-R. M., . . . Rudd, P. M. (2003). Secretory IgA N- and O-Glycans Provide a Link between the Innate and Adaptive Immune Systems. *Journal of Biological Chemistry,* 278(22), 20140-20153.

Ruppin, H., Bar-Meir, S., Soergel, K. H., Wood, C. M., & Schmitt, M. G. (1980). Absorption of Short-Chain Fatty Acids by the Colon. *Gastroenterology,* 78(6), 1500-1507.

Saito, T., Hirota, M., Tamura, N., Kimura, S., Fukuzumi, H., Heux, L., & Isogai, A. (2009). Individualization of nano-sized plant cellulose fibrils by direct surface carboxylation using TEMPO catalyst under neutral conditions. *Biomacromolecules,* 10(7), 1992-1996.

Saito, T., Kimura, S., Nishiyama, Y., & Isogai, A. (2007). Cellulose nanofibers prepared by TEMPO-mediated oxidation of native cellulose. *Biomacromolecules,* 8(8), 2485-2491.

Sakata, T. (1987). Stimulatory effect of short-chain fatty acids on epithelial cell proliferation in the rat intestine: a possible explanation for trophic effects of fermentable fibre, gut microbes and luminal trophic factors. *British journal of nutrition,* 58(1), 95-103.

Salimi, S., Sotudeh-Gharebagh, R., Zarghami, R., Chan, S. Y., & Yuen, K. H. (2019). Production of Nanocellulose and Its Applications in Drug Delivery: A Critical Review. *ACS Sustainable Chemistry & Engineering,* 7(19), 15800-15827.

Salyers, A. A., Whitt, D. D., & Whitt, D. D. (1994). *Bacterial pathogenesis: a molecular approach*: ASM press Washington, DC.

Sanders, M. E., Merenstein, D. J., Reid, G., Gibson, G. R., & Rastall, R. A. (2019). Probiotics and prebiotics in intestinal health and disease: from biology to the clinic. *Nature Reviews Gastroenterology & Hepatology,* 16(10), 605-616.

Saptarshi, S. R., Duschl, A., & Lopata, A. L. (2013). Interaction of nanoparticles with proteins: relation to bio-reactivity of the nanoparticle. *Journal of Nanobiotechnology,* 11(1), 26.

Sarkar, A., Li, H., Cray, D., & Boxall, S. (2018). Composite whey protein–cellulose nanocrystals at oil-water interface: Towards delaying lipid digestion. *Food Hydrocolloids,* 77, 436-444.

Satchithanandam, S., Vargofcak-Apker, M., Calvert, R. J., Leeds, A. R., & Cassidy, M. M. (1990). Alteration of Gastrointestinal Mucin by Fiber Feeding in Rats. *The Journal of Nutrition,* 120(10), 1179-1184.

Scheuble, N., Schaffner, J., Schumacher, M., Windhab, E. J., Liu, D., Parker, H., . . . Fischer, P. (2018). Tailoring Emulsions for Controlled Lipid Release: Establishing in vitro–in Vivo Correlation for Digestion of Lipids. *ACS Applied Materials & Interfaces,* 10(21), 17571-17581.

Schley, P. D., & Field, C. J. (2002). The immune-enhancing effects of dietary fibres and prebiotics. *British journal of nutrition,* 87(S2), S221-S230.

Schoeler, M., & Caesar, R. (2019). Dietary lipids, gut microbiota and lipid metabolism. *Reviews in Endocrine and Metabolic Disorders,* 20(4), 461-472.

Scholz-Ahrens, K. E., & Schrezenmeir, J. (2002). Inulin, oligofructose and mineral metabolism — experimental data and mechanism. *British journal of nutrition,* 87(S2), S179-S186.

Schroeder, B. O., Birchenough, G. M. H., Ståhlman, M., Arike, L., Johansson, M. E. V., Hansson, G. C., & Bäckhed, F. (2018). Bifidobacteria or Fiber Protects against Diet-Induced

Microbiota-Mediated Colonic Mucus Deterioration. *Cell Host & Microbe,* 23(1), 27-40.e27.

Seabra, A. B., Bernardes, J. S., Fávaro, W. J., Paula, A. J., & Durán, N. (2018). Cellulose nanocrystals as carriers in medicine and their toxicities: A review. *Carbohydrate Polymers,* 181, 514-527.

Shahramian, I., Kalvandi, G., Javaherizadeh, H., Khalili, M., Noori, N. M., Delaramnasab, M., & Bazi, A. (2018). The effects of prebiotic supplementation on weight gain, diarrhoea, constipation, fever and respiratory tract infections in the first year of life. *Journal of Paediatrics and Child Health,* 54(8), 875-880.

Shaoul, R., Okada, Y., Cutz, E., & Marcon, M. A. (2004). Colonic Expression of MUC2, MUC5AC, and TFF1 in Inflammatory Bowel Disease in Children. *Journal of Pediatric Gastroenterology and Nutrition,* 38(5), 488-493.

Sharma, R., & Schumacher, U. (1995). The influence of diets and gut microflora on lectin binding patterns of intestinal mucins in rats. *Lab Invest,* 73(4), 558-564.

Sharma, R., & Schumacher, U. (1995). Morphometric analysis of intestinal mucins under different dietary conditions and gut flora in rats. *Digestive Diseases and Sciences,* 40(12), 2532-2539.

Sharma, R., Schumacher, U., Ronaasen, V., & Coates, M. (1995). Rat intestinal mucosal responses to a microbial flora and different diets. *Gut,* 36(2), 209-214.

Shen, J., Obin, M. S., & Zhao, L. (2013). The gut microbiota, obesity and insulin resistance. *Molecular Aspects of Medicine,* 34(1), 39-58.

Shimotoyodome, A., Meguro, S., Hase, T., Tokimitsu, I., & Sakata, T. (2000). Short chain fatty acids but not lactate or succinate stimulate mucus release in the rat colon. *Comp Biochem Physiol A Mol Integr Physiol,* 125(4), 525-531.

Sigleo, S., Jackson, M. J., & Vahouny, G. V. (1984). Effects of dietary fiber constituents on intestinal morphology and nutrient transport. *American Journal of Physiology-Gastrointestinal and Liver Physiology,* 246(1), G34-G39.

Simon, G. L., & Gorbach, S. L. (1986). The human intestinal microflora. *Digestive Diseases and Sciences,* 31(9), 147-162.

Slavin, J. (2013). Fiber and Prebiotics: Mechanisms and Health Benefits. *Nutrients,* 5(4), 1417-1435.

Slavin, J. L., & Marlett, J. A. (1980). Influence of refined cellulose on human bowel function and calcium and magnesium balance. *The American Journal of Clinical Nutrition,* 33(9), 1932-1939.

Smart, J. D. (2005). The basics and underlying mechanisms of mucoadhesion. *Advanced Drug Delivery Reviews,* 57(11), 1556-1568.

Säkkinen, M., Marvola, J., Kanerva, H., Lindevall, K., Lipponen, M., Kekki, T., . . . Marvola, M. (2004). Gamma scintigraphic evaluation of the fate of microcrystalline chitosan granules in human stomach. *European Journal of Pharmaceutics and Biopharmaceutics,* 57(1), 133-143.

Story, J. A. (1986). *Modification of Steroid Excretion in Response to Dietary Fiber*. In G. V. Vahouny & D. Kritchevsky (Eds.), *Dietary Fiber: Basic and Clinical Aspects* (pp. 253-264). Boston, MA: Springer US

Sundaravalli, O. E., Shurpalekar, K. S., & Rao, M. N. (1971). Effects of dietary cellulose supplements on the body composition and cholesterol metabolism of albino rats. *Journal of Agricultural and Food Chemistry,* 19(1), 116-118.

Tanabe, H., Ito, H., Sugiyama, K., Kiriyama, S., & Morita, T. (2006). Dietary Indigestible Components Exert Different Regional Effects on Luminal Mucin Secretion through Their Bulk-Forming Property and Fermentability. *Bioscience, Biotechnology, and Biochemistry,* 70(5), 1188-1194.

Tanabe, H., Sugiyama, K., Matsuda, T., Kiriyama, S., & Morita, T. (2005). Small Intestinal Mucins Are Secreted in Proportion to the Settling Volume in Water of Dietary Indigestible Components in Rats. *The Journal of Nutrition,* 135(10), 2431-2437.

Tang, X. Z., Kumar, P., Alavi, S., & Sandeep, K. P. (2012). Recent Advances in Biopolymers and Biopolymer-Based Nanocomposites for Food Packaging Materials. *Critical Reviews in Food Science and Nutrition,* 52(5), 426-442.

Tasman-Jones, C., Owen, R. L., & Jones, A. L. (1982). Semipurified dietary fiber and small-bowel morphology in rats. *Digestive Diseases and Sciences,* 27(6), 519-524.

Theodoratou, E., Campbell, H., Ventham, N. T., Kolarich, D., Pučić-Baković, M., Zoldoš, V., . . . Lauc, G. (2014). The role of glycosylation in IBD. *Nature Reviews Gastroenterology & Hepatology,* 11(10), 588-600.

Thompson, R. S., Vargas, F., Dorrestein, P. C., Chichlowski, M., Berg, B. M., & Fleshner, M. (2020). Dietary prebiotics alter novel microbial dependent fecal metabolites that improve sleep. *Scientific Reports,* 10(1), 3848.

Tibolla, H., Pelissari, F. M., Martins, J. T., Vicente, A. A., & Menegalli, F. C. (2018). Cellulose nanofibers produced from banana peel by chemical and mechanical treatments: Characterization and cytotoxicity assessment. *Food Hydrocolloids,* 75, 192-201.

Tshikovhi, A., Mishra, S. B., & Mishra, A. K. (2020). Nanocellulose-based composites for the removal of contaminants from wastewater. *International Journal of Biological Macromolecules,* 152, 616-632.

Turbak, A. F., Snyder, F. W., & Sandberg, K. R. (1982). Food products containing microfibrillated cellulose. Google Patents.

Turbak, A. F., Snyder, F. W., & Sandberg, K. R. (1983a). Microfibrillated cellulose, a new cellulose product: properties, uses, and commercial potential. *J. Appl. Polym. Sci.: Appl. Polym. Symp.;(United States)* (Vol. 37): ITT Rayonier Inc., Shelton, WA.

Turbak, A. F., Snyder, F. W., & Sandberg, K. R. (1983b). Suspensions containing microfibrillated cellulose. Google Patents.

Van der Sluis, M., De Koning, B. A. E., De Bruijn, A. C. J. M., Velcich, A., Meijerink, J. P. P., Van Goudoever, J. B., . . . Einerhand, A. W. C. (2006). Muc2-Deficient Mice Spontaneously Develop Colitis, Indicating That MUC2 Is Critical for Colonic Protection. *Gastroenterology,* 131(1), 117-129.

Vartiainen, J., Pöhler, T., Sirola, K., Pylkkänen, L., & Cellulose, A.-H. (2011). Health and environmental safety aspects of friction grinding and spray drying of microfibrillated cellulose. *Cellulose*.

Velcich, A., Yang, W., Heyer, J., Fragale, A., Nicholas, C., Viani, S., . . . Augenlicht, L. (2002). Colorectal Cancer in Mice Genetically Deficient in the Mucin Muc2. *Science,* 295(5560), 1726-1729.

Ventura, C., Pinto, F., Lourenço, A. F., Ferreira, P. J., Louro, H., & Silva, M. J. (2020). On the toxicity of cellulose nanocrystals and nanofibrils in animal and cellular models. *Cellulose*, 1-36.

Vilarinho, F., Sanches Silva, A., Vaz, M. F., & Farinha, J. P. (2018). Nanocellulose in green food packaging. *Critical Reviews in Food Science and Nutrition,* 58(9), 1526-1537.

Ways, T. M. M., Lau, W. M., & Khutoryanskiy, V. V. (2018). Chitosan and Its Derivatives for Application in Mucoadhesive Drug Delivery Systems. *Polymers,* 10(3), 267.

Whisner, C. M., & Castillo, L. F. (2018). Prebiotics, Bone and Mineral Metabolism. *Calcified Tissue International,* 102(4), 443-479.

Willemsen, L. E. M., Koetsier, M. A., van Deventer, S. J. H., & van Tol, E. A. F. (2003). Short chain fatty acids stimulate epithelial mucin 2 expression through differential effects on prostaglandin E(1) and E(2) production by intestinal myofibroblasts. *Gut,* 52(10), 1442-1447.

Winuprasith, T., Khomein, P., Mitbumrung, W., Suphantharika, M., Nitithamyong, A., & McClements, D. J. (2018). Encapsulation of vitamin D3 in pickering emulsions stabilized by nanofibrillated mangosteen cellulose: Impact on in vitro digestion and bioaccessibility. *Food Hydrocolloids,* 83, 153-164.

Winuprasith, T., & Suphantharika, M. (2013). Microfibrillated cellulose from mangosteen (Garcinia mangostana L.) rind: Preparation, characterization, and evaluation as an emulsion stabilizer. *Food Hydrocolloids,* 32(2), 383-394.

Wrzosek, L., Miquel, S., Noordine, M. L., Bouet, S., Joncquel Chevalier-Curt, M., Robert, V., . . . Thomas, M. (2013). Bacteroides thetaiotaomicron and Faecalibacterium prausnitzii influence the production of mucus glycans and the development of goblet cells in the colonic epithelium of a gnotobiotic model rodent. *BMC Biol,* 11, 61.

Xhanari, K., Syverud, K., & Stenius, P. (2011). Emulsions Stabilized by Microfibrillated Cellulose: The Effect of Hydrophobization, Concentration and O/W Ratio. *Journal of Dispersion*

Science and Technology, 32(3), 447-452.

Xia, Y. N., Yang, P. D., Sun, Y. G., Wu, Y. Y., Mayers, B., Gates, B., . . . Yan, Y. Q. (2003). One-dimensional nanostructures: Synthesis, characterization, and applications. *Advanced Materials,* 15(5), 353-389.

Xiao, Y., Liu, Y., Wang, X., Li, M., Lei, H., & Xu, H. (2019). Cellulose nanocrystals prepared from wheat bran: Characterization and cytotoxicity assessment. *International Journal of Biological Macromolecules,* 140, 225-233.

Yu, H.-Y., Qin, Z.-Y., Liu, L., Yang, X.-G., Zhou, Y., & Yao, J.-M. (2013). Comparison of the reinforcing effects for cellulose nanocrystals obtained by sulfuric and hydrochloric acid hydrolysis on the mechanical and thermal properties of bacterial polyester. *Composites Science and Technology,* 87, 22-28.

Yu, H.-Y., Qin, Z.-Y., Liu, Y.-N., Chen, L., Liu, N., & Zhou, Z. (2012). Simultaneous improvement of mechanical properties and thermal stability of bacterial polyester by cellulose nanocrystals. *Carbohydrate Polymers,* 89(3), 971-978.

Zhao, Y., Simonsen, J., Cavender, G., Jung, J., & Fuchigami, L. H. (2019). Nano-cellulose coatings to prevent damage in foodstuffs. Google Patents.

CHAPTER 3.

EVALUATING MUCOADHESION PROPERTIES OF THREE TYPES OF NANOCELLULOSE IN THE GASTROINTESTINAL TRACT *IN VITRO* AND *EX VIVO*[3]

[3] Lin, Y.-J., Shatkin, J. A., & Kong, F. (2019). Evaluating mucoadhesion properties of three types of nanocellulose in the gastrointestinal tract *in vitro* and *ex vivo*. Carbohydrate Polymers, 210, 157-166. Reprinted here and adapted here with permission of publisher. https://doi.org/10.1016/j.carbpol.2019.01.029

Abstract

The mucoadhesive properties of three types of nanocellulose (CNF, CNC, and TEMPO-CNF) was investigated in the digestive condition with ex vivo and in vitro assays. In the ex vivo flow-through method, three nanocellulose materials showed different levels of retention on porcine gastric and intestinal mucosal surfaces. Fluorescence microscopy confirmed that retention of CNF could be due to entanglement with the mucosal layer, while retention of TEMPO-CNF could be due to instantaneous gelling on the mucosal surface. In an in vitro viscometric method, 2% CNC showed the highest viscosity synergism (relative enhancement=11.80 ± 1.14) in the gastric condition, while TEMPO-CNF only displayed synergism under gelling concentrations (0.1%). Evaluation of zeta potential revealed that 0.025–0.1% CNC interacted with mucin particles by changing the surface charge of the mucin-nanocellulose system. These results indicate that nanocellulose shows mucoadhesive properties in digestive tract, where the level of adhesion depends on type of nanocellulose, its concentration and the gastrointestinal section.

Keywords: Mucoadhesion; nanocellulose; flow-through assay; viscometric assay; zeta potential method

3.1 Introduction

Emerging use of nanotechnology greatly increase the chance of human exposure to nanomaterials in daily life. With the great interest in utilizing nanotechnology from the industry sectors in improving nutrient bioavailability, food safety and quality, one would expect to see the arising use of nanomaterials in food applications (Duncan, 2011; Faridi Esfanjani, Assadpour, & Jafari, 2018; Jafari & McClements, 2017; Sozer & Kokini, 2009). Currently, however, knowledge regarding nanomaterial behavior in the gastrointestinal (GI) tract, including understanding of how nanomaterials interact with mucus (the first physical barrier along the GI tract), is limited.

Mucoadhesion describes the behavior in which a substance adsorbs onto the mucosal layer, thus extending the time it remains in certain sections in the body. Mucoadhesion occurs when a foreign substance contacts the mucus layer and forms a bond between the two components that cause attachment (Khutoryanskiy, 2011). Wang et al. (2011) demonstrated that mucoadhesive nanoparticles may alter the microstructure of the mucus gel layer, potentially by increasing the pore size of mucus gel. This phenomenon has possible implications for the safety of nanomaterials that have not been previously discussed, but also suggests applications for enhanced nutrient delivery.

A mucus gel layer covers the internal epithelium along GI tract. The main composition of mucus is mucin, a family of glycoproteins secreted by goblet cells. Mucin is a macromolecule with a protein backbone that forms a gel network via cysteine cross-linking; this cross-linkage is gradually cleaved by gastric acid, proteolytic enzymes such as pepsin, and mucolytic bacteria, thus forming a loose outer layer of mucus gel (Allen & Carroll, 1985; Atuma, Strugala, Allen, & Holm, 2001; Johansson, Larsson, & Hansson, 2011). The mucus gel is a porous adsorbent with an

estimated 1 μm cut-off, meaning that particles smaller than 1 μm may be able to easily diffuse into the mucus layer (Ponchel, Montisci, Dembri, Durrer, & Duchêne, 1997).

Nanocellulose can be generally defined as cellulose-based fibers with at least one dimension lower than 100 nm (Xia et al., 2003). Nanocellulose is generated by applying chemical or mechanical methods to raw cellulosic materials, such as wood or cotton pulp, to break down the fibril-matrix structure (Gómez H et al., 2016; Moon, Martini, Nairn, Simonsen, & Youngblood, 2011). Depending on the structure and origin, plant-based nanocellulose has two main forms: cellulose nanofibers (CNF) and cellulose nanocrystals (CNC). CNF is produced by mechanical shearing and remains fibril-shaped. CNC is produced by sulfuric acid hydrolysis of pulp and has a rod-like shape (Hemmati, Jafari, Kashaninejad, & Barani Motlagh, 2018; Zhou et al., 2013). TEMPO (2,2,6,6-tetramethylpiperidine-1-oxyl)-oxidized CNF is another chemically modified nanocellulose. It is produced by TEMPO oxidation using wood-pulp followed by high-speed homogenization (Uetani & Yano, 2011). This allows the glucose units to carry a carboxylate anion on C6 which leads to interfibrillar repulsion and results in high transparency and viscosity (Saito, Kimura, Nishiyama, & Isogai, 2007).

Recently, it was revealed that nanocellulose could potentially change the digestion process in various aspects (DeLoid et al., 2018; Liu, Kerr, Kong, Dee, & Lin, 2018). Given the nanoscale dimensions of nanocellulose, there is a chance of nanocellulose penetrating or entangling into mucus gel. The interaction between nanocellulose and mucus, however, has yet to be studied.

The present study aimed to investigate the mucoadhesive properties of different types of nanocellulose, specifically in gel or slurry (i.e., hydrated) form. Many proposed food additive applications rely on hydrated forms of nanocellulose, which avoid the structural changes caused by drying in forms such as tablets or film (Peng et al., 2013). Several *in vitro* and *ex vivo*

mucoadhesion tests were conducted to examine the adhesion phenomenon between nanocellulose and the mucus gel layer. The present research explores the mucoadhesion properties of nanocellulose and also emphasizes the importance of future studies on the physiological implications of nanocellulose contact with GI tract mucus (*e.g.*, effects on mucus turnover and nanocellulose penetration across mucus).

3.2 Materials and Methods

3.2.1 Materials

Three types of nanocellulose in slurry or gel form were purchased from the Nanomaterial Pilot Plant at the University of Maine (Figure 3.1). CNF (3% slurry in water) was produced by ultrafine grinding of bleached softwood kraft pulp resulting in fibrils with a width of 50 nm and lengths up to several hundred microns according to the manufacturer's specification. The zeta potential of CNF was analyzed to be −20.74 ± 1.89 mV (0.1% CNF in 1 mM KCl). CNC and TEMPO-CNF were produced by the Nanocellulose Pilot Plant of the Forest Products Laboratory (FPL), USDA United States Forest Service in Madison, Wisconsin. The CNC produced at FPL has been described elsewhere (Reiner & Rudie, 2013). . In brief, wood pulp was hydrolyzed by 64% sulfuric acid, following de-coloring treatment using 4% hypochlorite and then neutralized by 5–8% sodium hydroxide. Finally, salt was removed by diafiltration. This process produces highly crystalline cellulose with negatively charged sulfate group adduction on the surface. CNC used in this study was 12.1% w/w in water containing 0.95% w/w sulfur per gram dry CNC. The dimensions, provided by the manufacturer, are 5–20 nm in width and 150–200 nm in length. The estimated relative size of 1% CNC sample in 1 mM KCl using dynamic light scattering was 98.9

± 2.5 nm assuming a sphere shape, while the zeta potential was -51.84 ± 1.61 mV. TEMPO-CNF production has been described previously by Reiner and Rudie (2017). In short, acid-pretreated Eucalyptus pulp underwent a Tempo/hypochlorite oxidation reaction at pH 10 maintained by a bicarbonate/carbonate buffer system with the addition of sodium bromide. Eventually, the content was collected by filtration and treated with high-pressure homogenization to achieve fibrillation. The size of TEMPO-CNF typically ranges from 5 to 7 nm in diameter and several μm in length (Qing et al., 2013; Saito et al., 2009). TEMPO-CNF used in this study was 0.93 wt% in water and contained 1.3 mM −COONa/g dry TEMPO-CNF, where the degree of substitution of carboxyl groups equals 0.22 according to Lourenço et al. (2017). The zeta potential of TEMPO-CNF when dispersed in 1 mM KCl was -20.74 ± 1.89 mV.

Texas Red C2-Dichlorotriazine was purchased from Thermo Fisher Scientific (Waltham, MA). Acridine Orange was purchased from Cayman Chemical Company (Ann Arbor, MI). Mucin (Type III, sialic acid 0.5–1.5%), porcine bile extract, Fluorescent brightener 28 and other chemicals were purchased from Sigma Aldrich (St. Louis, MO).

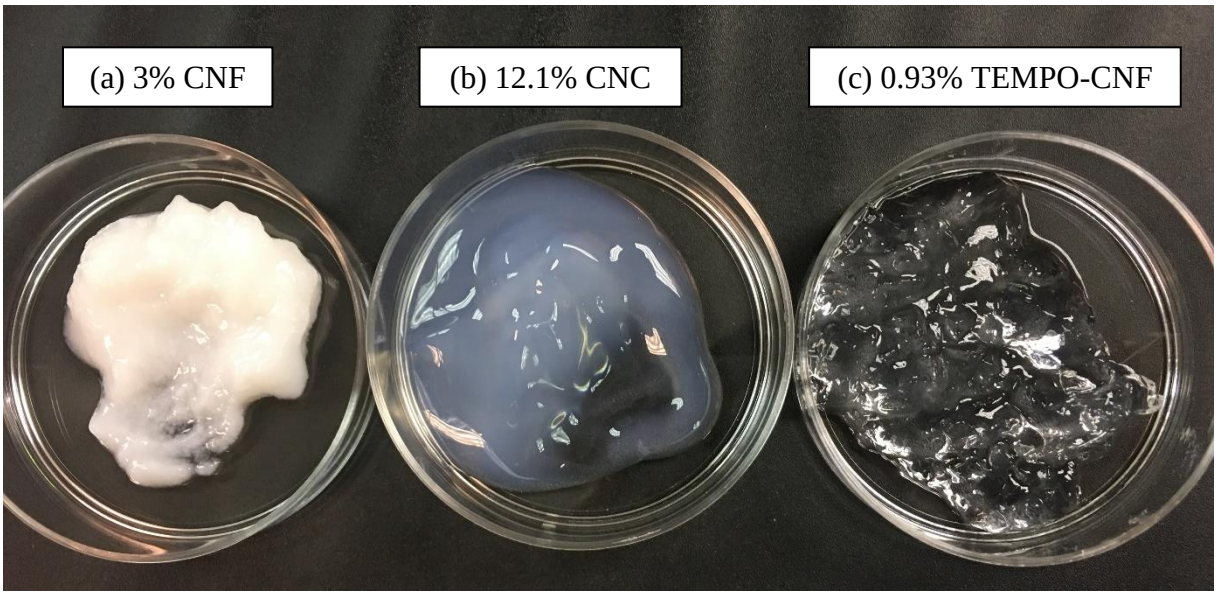

Figure 3.1. Three types of nanocellulose (a) 3% (w/w) CNF in water (b) 12.1% (w/w) CNC in water containing 0.95 % w/w sulfur per gram dry CNC (c) 0.93% (w/w) TEMPO-CNF containing 1.3 mM –COONa/g dry TEMPO-CNF

3.2.2 Preparation of fluorescence-labeled nanocellulose

Nanocellulose was labeled with Texas Red C2-Dichlorotriazine (TR) in a procedure modified from that described by (Zammarano et al., 2011). In brief, the TR-CNF was prepared by soaking CNF in 2 mM Na2CO3 for 30 min and mix with Texas Red for 24 h at room temperature in the dark. and the free dye was removed using repeated centrifugation and resuspension in DI water until neutral. CNC and TEMPO-CNF were labeled using a similar manner as that described above (1 mg TR/g of CNC or TEMPO-CNF). The reaction mixture was dialyzed in 8 kDa cut-off dialysis tubing (Spectra/Por 7, from Spectrum Laboratories, Inc., Waltham, MA) with DI water until no fluorescence was detected in the dialysate by a FLUOstar Omega fluorescence microplate reader (Excitation 584 nm, emission 620 nm, BMG Labtech Inc., Cary, NC). Three types of Texas

Red-labeled nanocellulose (TRNC) were used in the flow-through assay without further purification. The final concentration of TR-CNF, TR-CNC and TR-TEMPO-CNF prepared in this manner was determined by gravimetric analysis to be 1.5% (w/w), 3.7% (w/w) and 0.045% (w/w), respectively.

3.2.3 Preparation of Simulated digestive juice

Simulated gastric fluid (SGF) and simulated intestinal fluid (SIF) with bile without digestive enzymes were prepared following Minekus et al. (2014). Bile concentration was determined using a bile acid assay kit purchased from Sigma Aldrich (St. Louis, MO) where 1 g bile acid equals 2.512 mmol bile acids. The pH was set at 2 for SGF and 7 for SIF.

3.2.4 Preparation of the porcine specimen

Porcine stomach and the small intestine specimen were prepared following a previously published cleaning procedure (Varum, Veiga, Sousa, & Basit, 2010). In brief, porcine stomach and jejunum from three pigs were harvested immediately after slaughtering and kept on ice. The post-harvest cleaning process was conducted in a cold room. Porcine organs were rinsed with 0.9% NaCl to remove food residue, and underlying connective tissue was extracted. Tissue samples were snapfrozen using liquid nitrogen and stored at −80 °C.

3.2.5 Flow-through method ex vivo

The flow-through method was adopted from a previous study with minor modifications (Eshel-Green, Eliyahu, Avidan-Shlomovich, & Bianco-Peled, 2016). The mucoadhesive property of

nanocellulose was tested on porcine specimen ex vivo and on glass slides as a comparison. The specimen was stored on ice; just prior to use, it was defrosted and mounted on glass slides using super glue. One hundred μL of TR-NC was loaded on the test surface and incubated at 37 °C in a humid, dark environment for 10 min. The glass slides were then placed at a 45-degree angle, and a peristaltic pump (Havard Apparatus, Holliston, MA) dripped simulated digestive fluid at 0.5 mL/min for 10 min onto the slide. Fluorescence level in the rinse was scored every 30 s using FLUOstar Omega fluorescence microplate reader (Excitation 584 nm, emission 620 nm) to assess the level of mucoadhesion. The amount of TR-NC in the rinse at every 30 s was calculated as

$$\text{TR-NC amount (\%)} = (F_t\text{-blank})/(F_{100\%}\text{-blank})*100\%$$

where Ft is the fluorescence intensity of the digestive fluid at each 30 seconds, blank is the fluorescence intensity of digestive fluid, and $F_{100\%}$ is a theoretical 100% fluorescence intensity where a mixture of 100 μL TR-NC and 250 μL of digestive fluid was measured, assuming all TR-NC is flushed off at the first 30 seconds. The lower the fluorescence intensity in the rinse indicates the more NC remained on the test surface, hence the stronger mucoadhesive power. Accumulated percentage over 10 minutes was calculated by the sum of each time point.

3.2.6 Confocal microscopy

Nanocellulose was stained with 0.1 mg/mL Fluorescent Brightener 28 (Baur et al., 2005) and pig mucus was stained with 0.1 mg/mL Acridine Orange (Shumilov et al., 2014) in SGF or SIF (without bile salt, as it prevents Acridine Orange dissolution) for at least 10 minutes prior to experiments. Nanocellulose was allowed direct contact with the mucosal surface for 10 min as in the flow-through assay, and, after digestive juice rinsing, the mucosal tissue at the contact area

was scraped off and mounted on glass slides. The morphology and mucoadhesion of nanocellulose were observed using a Zeiss LSM 710 Confocal Microscope (Carl Zeiss AG, Oberkochen, Germany).

3.2.7 Viscometric method

Rheological synergism due to bioadhesion can be assessed using a viscometric method (Hassan & Gallo, 1990; Thirawong, Kennedy, & Sriamornsak, 2008). Ten percent of porcine gastric mucin solution in SGF or SIF was stirred for 2 h at room temperature for complete dispersion. Mucin and nanocellulose solution were prepared separately at twice the final concentration, then mixed in a ratio of 1:1 and incubated for 30 min at 37 °C. The apparent viscosity of 5% mucin, 0.1–1% nanocellulose and a mixture of 5% mucin and nanocellulose was determined using a TA instrument HR-2 Discovery Hybrid Rheometer with a conical Couette geometry (diameter 31.09 mm, length 37.15 mm). The corresponding cup was set at 37 °C and shear rate of 0.1–25 1/s. Viscosity enhancement due to bioadhension ($\eta_{enhancement}$) was calculated by the following equation at a shear rate of 3.98 or 10.00 1/s:

$$\eta_{enhancement} = [\eta_{mixture} - (\eta_{nanocellulose} + \eta_{mucin})]$$

Relative enhancement ($\eta_{relative}$) was calculated as:

$$\eta_{relative} = [\ \eta_{mixture} / (\eta_{nanocellulose} + \eta_{mucin})].$$

3.2.8 Zeta potential method

Changes in zeta potential reflect the changes in the surface properties of particles, which in this case represents the interaction between mucin and the polymers (Takeuchi et al., 2005). The

zeta potential of mucin (0.1% w/w) mixed with different concentration of nanocellulose in the simulated digestive fluid without bile or enzymes was measured by a Brookhaven 90Plus Nanoparticle Size Analyzer with BI-Zeta assembly (Brookhaven Instruments Corporation, NY). Mucin solution was stirred at room temperature for 2 h prior to analysis to achieve complete dispersion. All samples were kept at 37 °C for 30 min to allow interaction.

3.2.9 Statistical analysis

Analysis of variance (ANOVA) followed by Tukey's test or t-test was used to test for significant differences using JMP Pro 13.0.0 (SAS Institute Inc., Cary, NC). At least three replications were conducted for each experiment.

3.3 Results and Discussion

3.3.1 Retention of nanocellulose in *ex vivo* flow-through method

The first set of analyses examined the retention of nanocellulose after consumption using porcine stomach and the small intestine specimen in the ex vivo flow-through model. The accumulated results are presented in Figure 3.2. In Figure 3.2(a) and (b), less than 50% of TR-NC was washed off from the porcine stomach and small intestine, though a gradual release of nanocellulose was observed. Both 1.5% CNF and 3.7% CNC showed mucoadhesion in both gastric and intestinal conditions. The 0.045% TEMPO-CNF, however, was found to have significantly higher adhesion in gastric condition than in intestinal condition (one sample t-test, $p < 0.05$). We suspected that in the flow-through method, the nanocellulose gel itself could be viscous enough to remain on a 45 °-angled surface during rinsing, so the retention of nanocellulose on the glass slides

was investigated further to test the specificity of nanocellulose bioadhesion to the mucosal surface. In Figure 3.2(c) and (d), CNF and CNC was not retained on glass slides, indicating that the adhesion for CNF and CNC was specific to mucus. Interestingly, TEMPO-CNF seemed to resist the flushing even on glass slides in the gastric condition. It was observed that the liquid form of 0.045% TEMPO-CNF turned into a gel as soon as it contacted the acidic digestive buffer, thereby strongly expelling the digestive fluid. Previous studies have reported that gelation of Tempo-CNF is dependent on concentration, ionic strength and pH (Geng et al., 2017; Ma, Burger, Hsiao, & Chu, 2011; Tanaka, Saito, Ishii, & Isogai, 2014). TEMPO-CNF behaves like a Newtonian fluid at a concentration below 0.2%, and the gelation occurs when the system contains more than 100 mM of NaCl for 0.2% TEMPO-CNF at pH < 3 (Ma et al., 2011). In the present study, the gastric fluid and intestinal fluid contained 177.85 mM and 273.23 mM of electrolyte, respectively (Minekus et al., 2014), but gelling in the gastric condition was higher and induced stronger retention than the intestinal condition. This could be due to the carboxylate groups on TEMPO-CNF, which are weak acids and lose some of their surface charges in acidic conditions due to the weak acid equilibrium. Reduced surface charges of polyelectrolytes generally lead to more aggregation (i.e., gelation).

Confocal microscopy was also utilized in the flow-through assay to closely look at the binding mechanisms (Figure 3.3). Interestingly, the three types of nanocellulose performed different mucoadhesion reactions. Although aggregation of CNF was observed, the fibrous structure enabled CNF to entangle in mucus gel. CNC homogenously dispersed in water and spread on the mucus tissue. TEMPO-CNF presented as a non-homogenous gel that remained on mucus after flow-through, but some gel would detach from mucus after the introduction of slight compression during covering with coverslips. To briefly conclude, the flow-through method was used to mimic the first establishment phase in the mucoadhesion phenomenon. The three types of

nanocellulose had different levels of retention on the porcine stomach and small intestine specimen and resisted flushing with digestive juice.

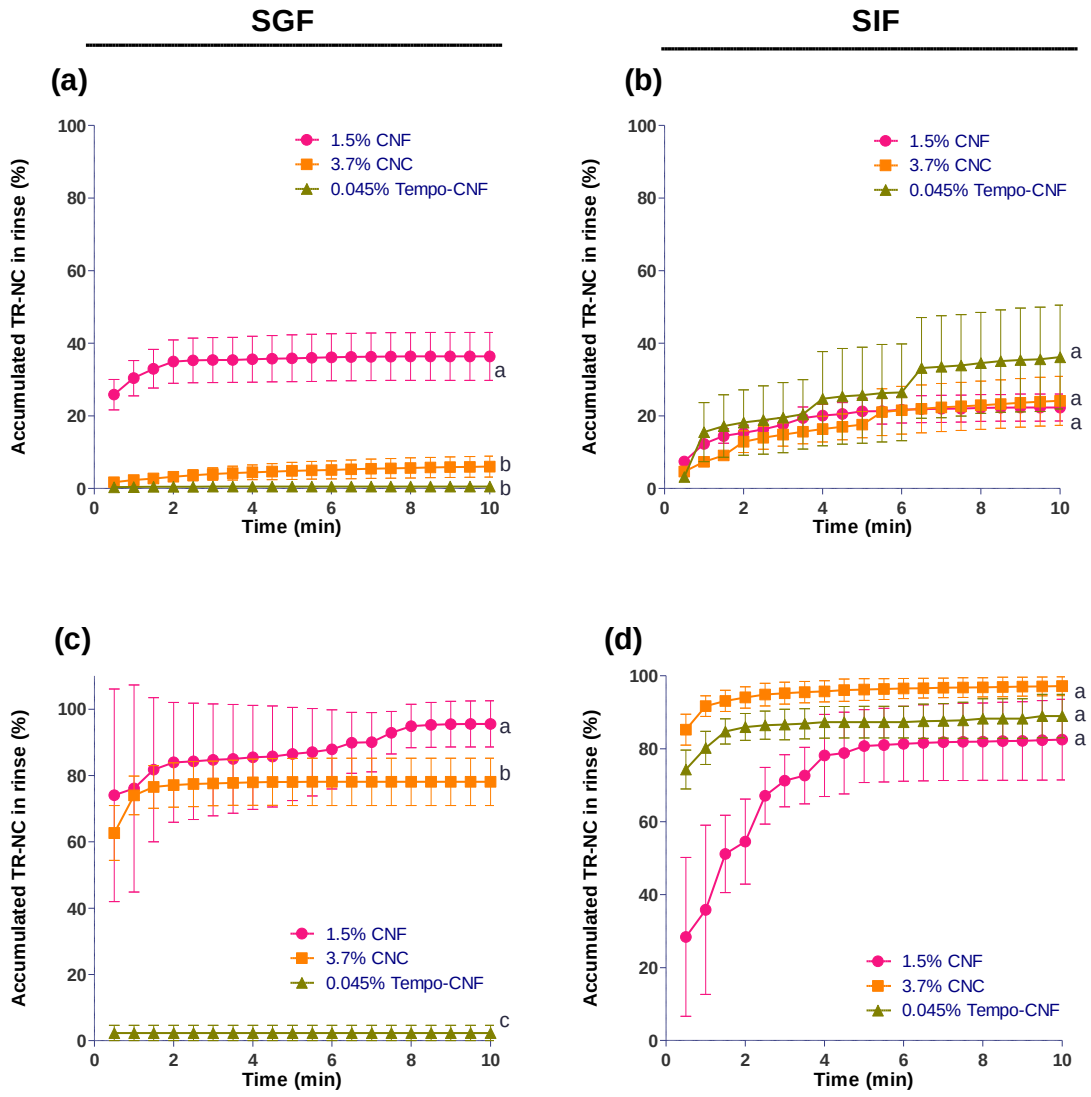

Figure 3.2. Accumulated percentage of Texas Red labeled-nanocellulose (TR-NC) released in the rinse by flow-through method in (a) simulated gastric fluid (SGF) from porcine stomach tissue (b) simulated intestinal fluid (SIF) from porcine jejunum tissue. Mean accumulated TR-NC in rinse ± SEM (n=3, Data from 3 hogs and duplicate for each individual) and in (c) SGF from glass slides (d) SIF from glass slides (Mean accumulated TR-NC in rinse ± SD (n=3) (●) 1.5% CNF, (■)

3.7% CNC, (▲) 0.045% TEMPO-CNF. Statistical analysis was done by testing the accumulated values at the end of 10 minutes. Different letters denote statistical significance by Tukey's test (α=0.05).

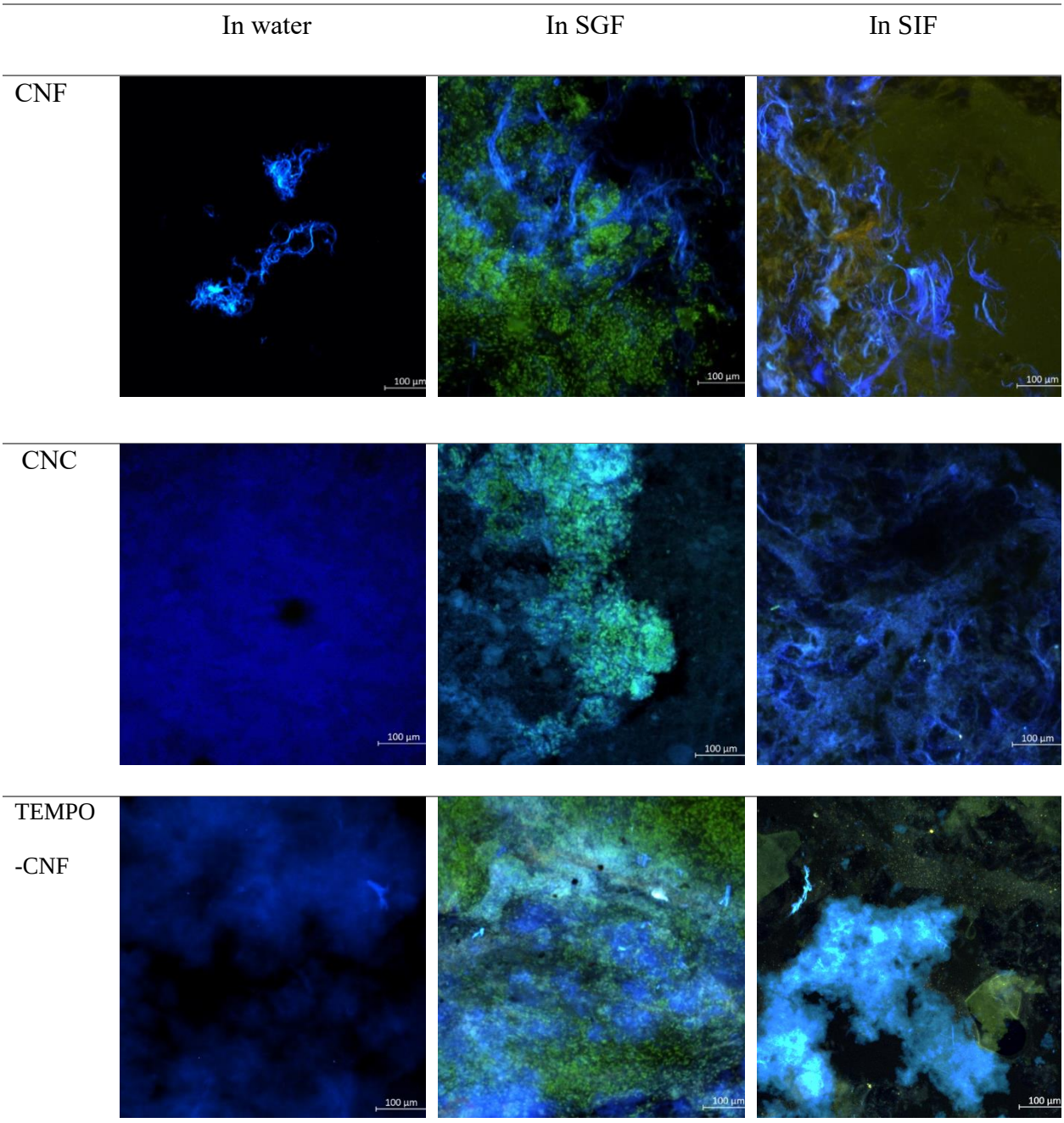

Figure 3.3. Confocal microscopy images of nanocellulose in water and adhered to porcine mucosal layer in simulated gastric fluid (SGF) and simulated intestinal fluid (SIF). Green: Acridine Orange staining of mucus. Blue: Fluorescent Brightener 28 staining of cellulose. Pictures showed in overlapping. Scar Bar shows 100 µm.

3.3.2 Evaluating mucoadhesion effect of nanocellulose by viscometric method

The viscometric method assesses the mucoadhesion properties by viscosity synergism (Hassan & Gallo, 1990). In, Figure 3.4, the viscosity of mucin, nanocellulose at different concentrations, and the mixture of mucin and nanocellulose are shown. All nanocellulose solution showed shear-thinning behavior. The fluid behavior herein reflects comprehensive effects of pH and ionic strength in gastric and intestinal condition. It should be noted that SIF contains a noticeable amount of bile salts (10mM) which may change the surface tension (Mysels, 1984) and reduce free water in the system, and may also interact with nanocellulose, thereby changing the fluid behavior of nanocellulose.

Viscosity synergism of nanocellulose and mucin mixture was observed in all three types of nanocellulose. The degree of bioadhesion depended on several factors including the type of nanocellulose, concentration, shear rate and the digestive system section. The physiological shear rate of digestion is estimated to be within the range of 0.1–10 1/s (de Loubens, Lentle, Love, Hulls, & Janssen, 2013; Hardacre, Lentle, Yap, & Monro, 2016). The shear rate of 3.98 and 10.00 1/s was chosen to compare the rheological synergism, shown in Table 3.1. The relative enhancement, $\eta_{relative}$, is another indicator that normalizes the enhancement based on the viscosity of unmixed solutions. A $\eta_{relative}$ closer to 1 indicates a lack of interaction between the polymer and the mucin, while a higher value indicates a stronger interaction (Hassan & Gallo, 1990; Thirawong et al., 2008).

Generally, $\eta_{enhancement}$ decreases along with increasing shear rate in gastric condition. One reason could be that shearing breaks the internal weak bindings between molecules, as expected for shear-thinning fluid. It could also be that shearing introduces a higher chance of collision and

entanglement between fiber molecules and decreases the level of interaction with mucin. It has been reported that a shear rate of 10.00 1/s maximizes CNF flocculation (Karppinen et al., 2012). In the gastric condition, where higher contraction force is expected, all groups had a $\eta_{relative}$ value significantly higher than 1 at shear rate 10.00 1/s (Table 3.1) (Single tailed T-test, $p<0.05$). This indicates there is synergism for all three types of nanocellulose. Concentration could be an important factor, evidenced by the significantly higher viscosity synergism of 2% CNC as compared to all other groups (two-way ANOVA, $p < 0.05$). However, 0.465% TEMPO-CNF did not show higher synergism than 0.1% TEMPO-CNF. TEMPO-CNF is known to have a critical gelling concentration at 0.2% (Geng et al., 2017; Ma et al., 2011). In the present study, the higher concentration of TEMPO-CNF was found to have the lowest viscosity synergism. Gelling of TEMPO-CNF could introduce a strong intramolecular attraction between fibrils, thus excluding active sites for mucin adhesion. However, lower concentrations of TEMPO-CNF (0.1%) in the viscometric assay still did not show outstanding mucoadhesion as seen in the flow-through assay. This could be explained by the observation that TEMPO-CNF lacks specificity to mucus in gastric condition

When different types of nanocellulose were compared at similar concentrations (~0.5%), CNC was found to be more mucoadhesive than the other two nanocellulose forms. This might be partially explained by the relative surface area of the nanocellulose forms. CNC had the smallest particle size and dimension (5–20 nm wide, 150–200 nm long according to the manufacturer's specification), compared to TEMPO-CNF (5–7 nm wide, several micrometers long) (Qing et al., 2013) and CNF (width 50 nm, lengths up to several hundred microns according to the manufacturer). CNC therefore has more surface area to interact with mucin.

For all three types of nanocellulose, $\eta_{relative}$ was lower in the intestinal condition as compared to the results obtained in the gastric condition. The shear rate effect on $\eta_{relative}$ was also also smaller. The interaction under such condition might be a more persistent interaction that is not affected by shearing. All the groups except 0.465% TEMPO-CNF had $\eta_{relative}$ greater than 1 (single-tailed T-test, $p<0.05$) in both shear rate. No significant differences among the the $\eta_{relative}$ of 1% CNF, 2% CNC and 0.1% TEMPO-CNF were detected at either shear rate in the intestinal condition (two-way ANOVA, $p>0.05$). This finding agrees with the results seen in the flow-through assay.

A similar experiment was conducted in a previous study where mucoadhesion properties of pectin in gastrointestinal condition were determined using the viscometric method (Thirawong et al., 2008). Results from the present study (Table 3.1) could be compared with pectin, Carbomer 934 P, and chitosan, which have been widely studied in mucoadhesion applications. At a similar shear rate (3.96 1/s in the literature), the viscosity enhancement of the three types of nanocellulose in SGF was larger or comparable to 1% pectin or 0.7% chitosan; in SIF, 1% CNF and 2% CNC showed higher enhancement than 0.7% Carbomer934 P.

The viscometric method measures not only the synergism between mucin and the polymers, but also the viscosity, which is a direct indicator of the flow-resistance of the mucin solution (King, 2006). Our results showed that nanocellulose could change the rheology of the mucin solution. A future study focusing on the effects of nanocellulose on mucus gel layer turnover rate is therefore suggested.

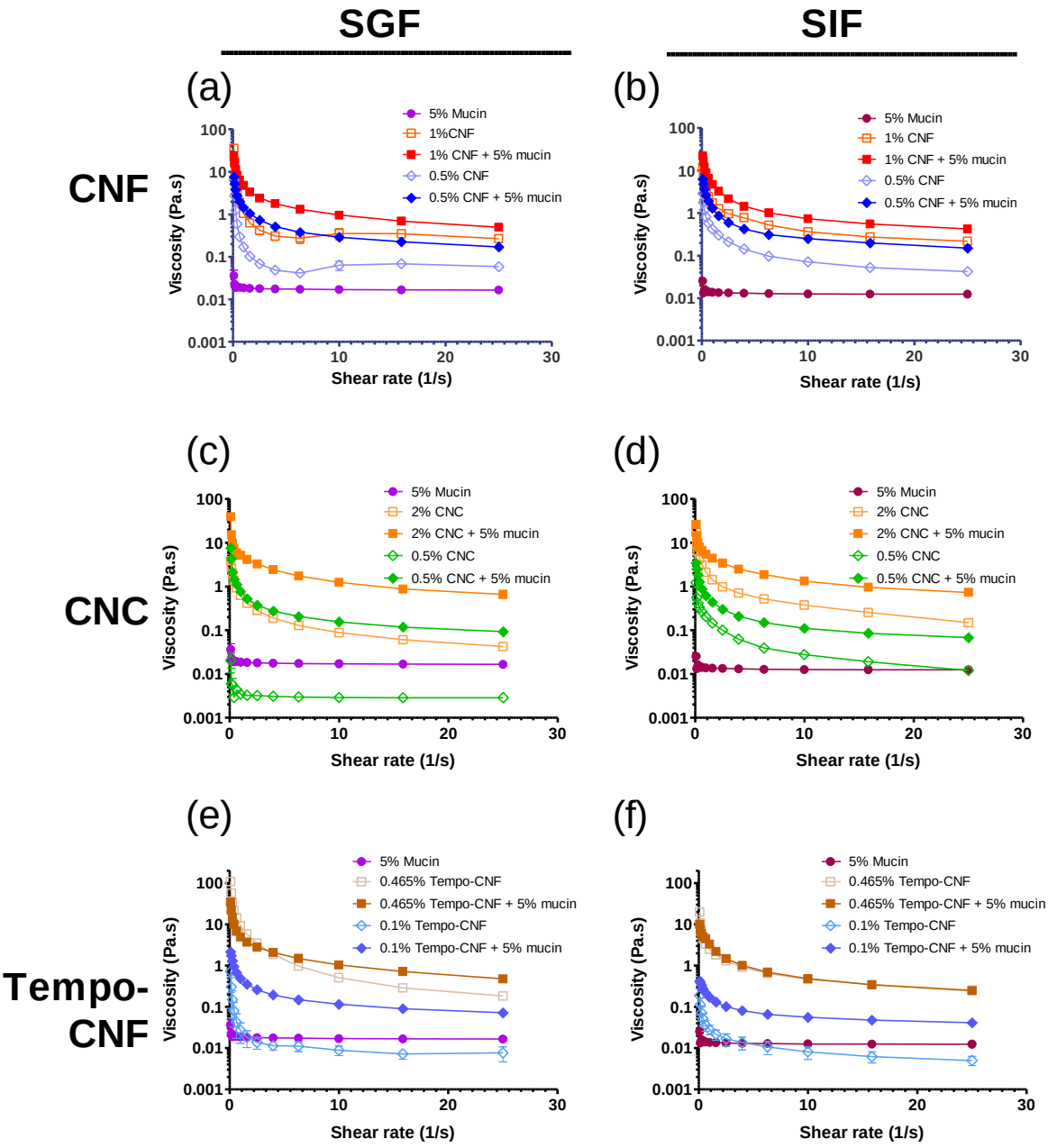

Figure 3.4. Viscosity of various concentration of nanocellulose and the mixture with 5% mucin in simulated gastric fluid (SGF) and simulated intestinal fluid (SIF). Mean apparent viscosity ± SD (n=3)

Table 3.1. Viscosity enhancement, and relative enhancement of nanocellulose in gastric (SGF) and intestinal (SIF) condition at shear rate of 3.98 and 10.00 1/s (n=3).

	In SGF		In SIF	
Shear rate (1/s)	3.98	10.00	3.98	10.00
1% CNF + 5% mucin				
$\eta_{enhancement}$ (mPa s)	1460 ± 167	592 ± 150	656 ± 148	360 ± 45
$\eta_{relative}$	5.98 ± 2.24	3.21 ± 1.96	1.86 ± 0.30	1.98 ± 0.26
0.5% CNF + 5% mucin				
$\eta_{enhancement}$ (mPa s)	449 ± 8	209 ± 15	270 ± 65	166 ± 19
$\eta_{relative}$	7.78 ± 0.61	3.89 ± 1.36	2.86 ± 0.88	2.97 ± 0.16
2% CNC + 5% mucin				
$\eta_{enhancement}$ (mPa s)	2217 ± 41	1132 ± 101	1773 ± 249	943 ± 45
$\eta_{relative}$	11.80 ± 1.14	11.85 ± 1.79	3.50 ± 0.57	3.42 ± 0.25
0.5% CNC+ 5% mucin				
$\eta_{enhancement}$ (mPa s)	254 ± 35	135 ± 8	133 ± 16	71 ± 8
$\eta_{relative}$	13.25 ± 1.46	7.79 ± 0.25	2.77 ± 0.28	2.76 ± 0.21
0.465% TEMPO-CNF + 5% mucin				
$\eta_{enhancement}$ (mPa s)	184 ± 498	514 ± 110	87 ± 360	2 ± 144
$\eta_{relative}$	1.13 ± 0.30	1.99 ± 0.32	1.12 ± 0.41	1.02 ± 0.32
0.1% TEMPO-CNF + 5% mucin				
$\eta_{enhancement}$ (mPa s)	166 ± 8	89 ± 3	54 ± 12	35 ± 4
$\eta_{relative}$	6.82 ± 1.03	4.48 ± 0.66	3.23 ± 1.08	2.75 ± 0.52

$\eta_{enhancement}$: Viscosity enhancement = $[\eta_{mixture} - (\eta_{nanocellulose} + \eta_{mucin})]$

$\eta_{relative}$: Relative enhancement = $[\eta_{mixture} / (\eta_{nanocellulose} + \eta_{mucin})]$.

3.3.3 Zeta potential method

The zeta potential of nanocellulose and the nanocellulose mixture with mucin is shown in Figure 3.5. The zeta potential measurement shows the charge of the particles at the system's slipping plane (Ohshima, 2013) and is suggested to reflect the interaction between different particles (Bogataj et al., 2003; Takeuchi et al., 2005). Mucin charge is close to neutral (0.54 ± 0.21 mV) in SGF (pH 2). This finding agrees with results reported in a previous study (Sogias, Williams, & Khutoryanskiy, 2008). In SIF (pH 7), mucin had a negative charge (−3.98 ± 1.64 mV) which differs from a much lower value of ˜−20 mV reported in the past (Bogataj et al., 2003; Sogias et al., 2008). This could be due to differences in the buffer systems. Previous studies used diluted PBS or deionized water as the neutral test system, but it was also reported that electrophoresis mobility is highly dependent on the salts and buffer system (Cugia, Monduzzi, Ninham, & Salis, 2013). Therefore, to understand the behavior of nanocellulose and mucin particles in digestive juice, digestive buffers that mimic biological ionic strength were used in this study. To minimize systemic solid interference, bile extracts were not added.

CNF does not carry charges in SGF or SIF within the tested concentration range (Figure 3.5 (a),(b)). The lack of strong electrostatic affiliation between CNF and mucin in the digestive juice suggests the moderate mucoadhesivity of CNF seen in the flow-through assay and viscometric assay might largely be due to mechanical entanglement and interpenetration of fibrils with mucus.

TEMPO-CNF carried a low negative charge in SGF and high negative charges in SIF (Figure 3.5 (d) and (e)). In both the gastric and intestinal conditions, adding mucin did not change the charges of TEMPO-CNF, indicating there might not be electrostatic interaction between mucin

and TEMPO-CNF. Because lower concentrations of TEMPO-CNF react with mucin, the carboxylic groups of TEMPO-CNF may play a more important role in forming hydrogen bonding with mucin glycoproteins. In that case, the mechanism might be similar to that observed for Carbomers that carry carboxylic groups (Singla, Chawla, & Singh, 2000).

CNC carried negative charges in both SGF and SIF (Figure 3.5 (c), (d)). Previous studies have reported that CNC presents negative surface charge at around −60 mV and that surface charge exponentially rises to −20 mV in a 10 mM NaCl environment (Boluk, Lahiji, Zhao, & McDermott, 2011; Jiang & Hsieh, 2013). Meanwhile, the impact of pH to zeta potential of CNC in the range of pH 2-12 is known to be relatively minor (Zhong, Fu, Peng, Zhan, & Sun, 2012). In our study, SGF and SIF had a much higher ionic strength than 10mM NaCl and even contained complex cations including K^+, Na^+, Mg^{2+}, and Ca^{2+}. These cations could shield the negatively charged slipping plane of CNC molecules and further raise the zeta potential closer to neutral. The addition of mucin to CNC changed the zeta potential, providing evidence of a higher affinity of CNC to mucin particles. Mucin particles carrying different charges in SGF and SIF could be giving different mechanisms of mucoadhesion. In SGF where the pH is near to the pI of sialic acid (2.6) (Johnson & Rainsford, 1972), it is less likely electrostatic attraction takes place. Nevertheless, it could be hydrogen bonding or hydrophobic attraction driving mucin to adhere to CNC, therefore bringing the zeta potential closer to neutral. The adherence also indicated co-aggregation of particles, which conforms to the greater rheology synergism seen in the viscometric assay. In SIF, mucin is present in an ionized state. Interestingly, after mixing with CNC, which also carries negative charges, the whole mucin-CNC system became more negative. Compared to our results in the flow-through and viscometric methods, where CNC showed medium adhesion with mucus tissue and mucin solution in SIF, this zeta potential result might indicate that CNC also has muco-

penetration properties. Griesser et al. (2018) reported that more negatively charged self-emulsifying drug delivery systems showed enhanced mucus-penetrating ability. In this study, CNC in SIF increased the overall charge of the system, suggesting that CNC may increase repulsion when mixed with mucin particles. Whether this effect directly impacts mucus mesh size remains unknown. However, considering that CNC has the lowest particle size, future research should be undertaken to investigate muco-penetration of CNC and the implications for mucus structure.

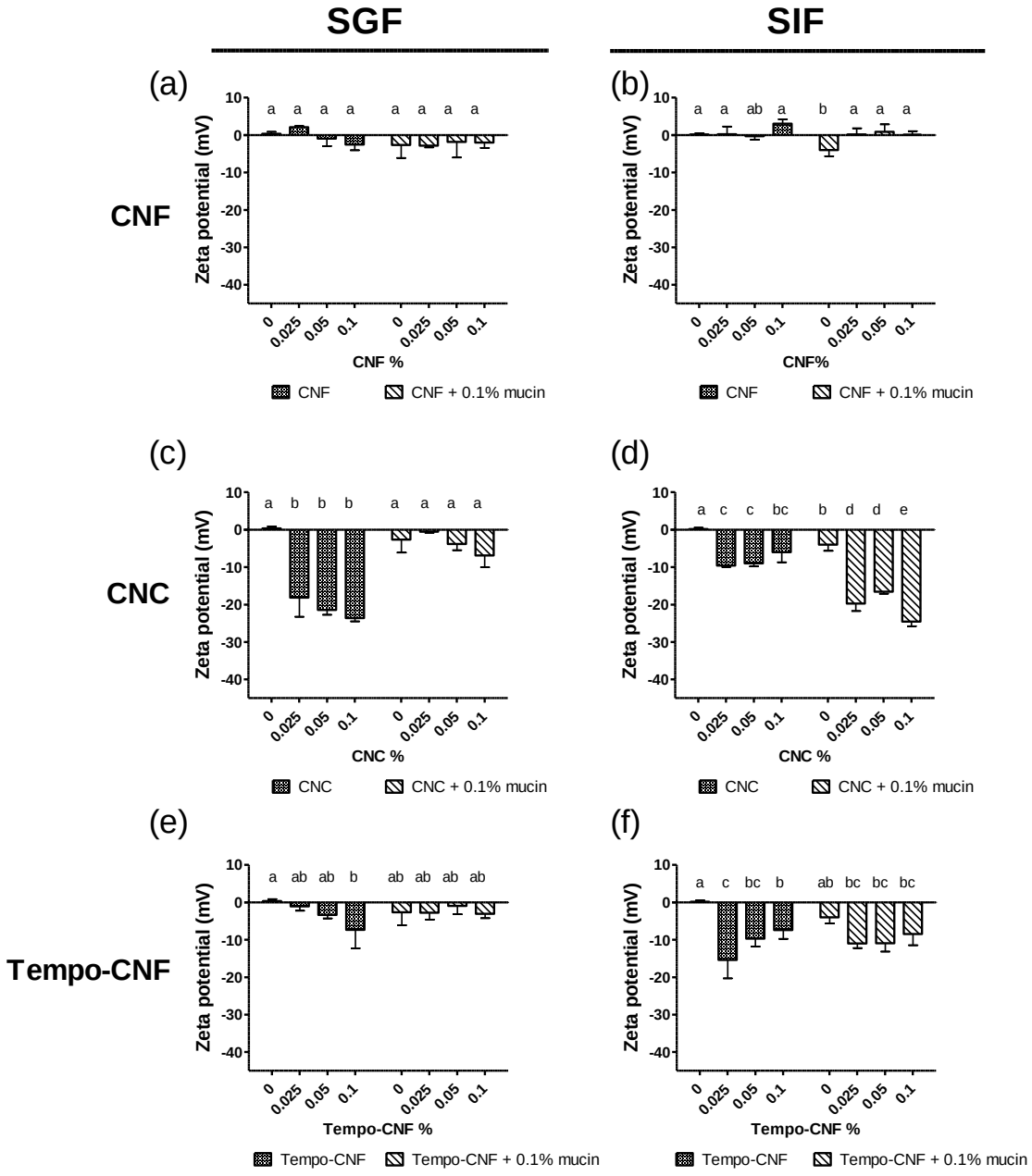

Figure 3.5. Zeta potential analysis of nanocellulose in simulated gastric fluid (SGF) and intestinal fluid (SIF). Mean zeta potential ± SD, n=3. Different alphabets represent statistical significance by Tukey's test (α=0.05).

The present results are significant in at least two major aspects. First, pig specimen was used in the flow-through assay, which is a better model to mimic the human GI tract biology (as compared to other laboratory rodent models) (Kararli, 1995; McConnell, Basit, & Murdan, 2008). Although the limitations of using ex vivo model are inevitable, the results of this study suggest future studies of nanocellulose as a mucoadhesive material are possible. Second, this study demonstrated that the mucoadhesivity of nanocellulose is highly dependent on GI sections, as well as on the concentration and types of nanocellulose. CNF showed mucoadhesion by entanglement with mucus in both the gastric and intestinal conditions. CNC showed adhesion by attraction with mucin particles; this phenomenon is especially strong in the gastric condition. For TEMPO-CNF, however, a concentration lower than the critical gelling concentration would be important to develop mucoadhesion ability.

Current findings suggest nanocellulose could be useful in mucoadhesion applications such as drug delivery as nanocellulose offers more refined control of zeta potential, aggregation, and mucoadhesion. Different types of nanocellulose with different charged groups along the surface could be exploited for specific goals. However, they also provide a different view on the safety aspects of nanocellulose as a mucoadhesive material. Compared to some traditional mucoadhesive materials, such as chitosan or carbomer, where oral exposures may be limited to pharmaceuticals or food coatings (No, Meyers, Prinyawiwatkul, & Xu, 2007; Singla et al., 2000), nanocellulose could be used as a food additive. When used as a thickener or an emulsifier, nanocellulose exposures may occur in higher dosages and over longer periods of time (Gómez H et al., 2016). In this case, the attachment of nanocellulose to the GI wall may extend some of its known effects to digestion, for example by delaying glucose and fat digestion (DeLoid et al., 2018; Liu et al., 2018). Also, because mucoadhesive materials could potentially increase the penetration of some other

particles (Wang et al., 2011), to fully understand the consequence of consuming nanocellulose, it is important to elucidate the long-term effects of nanocellulose on the mucus structure along the GI tract as well as on the in vivo turn-over of mucus. In addition, further work is required to establish the mucoadhesion-concentration profile of each type of nanocellulose. Different product forms, such as film, are also of interest to the food and packaging industries and warrant investigation. Lastly, understanding the effects of nanocellulose on mucus integrity and muco-penetration is still necessary to establish safer ways to use nanocellulose.

3.4 Conclusions

The aim of the present research was to examine the mucoadhesion properties of nanocellulose. Multiple *ex vivo* and *in vitro* analyses revealed that three types of nanocellulose had mucoadhesivity in the gastrointestinal condition depending on concentration and the conditions.

In the flow-through method, nanocellulose showed retention on a porcine mucosal specimen in both gastric and intestinal conditions. The retention of TEMPO-CNF was highest in the gastric condition due to its gelling property, while adhesion of CNF and CNC was moderate but more specific to mucus. Fluorescence microscopy demonstrated that CNF was entangled in the mucus gel layer, while CNC spread on mucus gel, and TEMPO-CNF remained as large gel pieces. In the viscometric method, CNF and CNC showed consistent bioadhesion with mucin. Two percent CNC in the gastric condition had the highest relative enhancement among all the test groups. TEMPO-CNF at 0.465% only showed viscosity in gastric conditions. Using the zeta potential method, CNC showed interaction with mucin particles by changing the surface charge of the mucin-nanocellulose system. Current findings suggest that CNF, CNC and TEMPO-CNF

possess mucoadhesive ability, which will be useful in expanding nanocellulose applications. Meanwhile, the impact of nanocellulose on the mucus gel network will need to be studied in order to validate safety.

Current findings suggest that CNF, CNC and TEMPO-CNF possess mucoadhesive ability, which will be useful in expanding nanocellulose applications. Meanwhile, the impact of nanocellulose on mucus gel network will need to be carried out in order to validate the safety including mucus turnover rate and permeability.

3.5 Acknowledgment

This study was supported by USDA National Institute of Food Agriculture [grant no. 2016-67021-24994/project accession no. 1009090] and in part by P^3 Nano grant E16-39.

The authors also wish to acknowledge Dr. Douglas Fox from American University, Washington, DC for providing TR-CNF, as well as faculty and staffs in University of Georgia, Athens, GA including Mr. Harl R. Crowe for providing hog samples, Dr. Muthugapatti Kandasamy, Dr. William L. Kerr, Dr. Ronald B. Pegg and Dr. Rakesh Singh for equipment and technical support. The imaging data used in this publication was produced in collaboration with the Biomedical Microscopy Core at the University of Georgia.

3.6 References

Allen, A., & Carroll, N. J. H. (1985). Adherent and soluble mucus in the stomach and duodenum. *Digestive Diseases and Sciences,* 30(11 Suppl), 55S-62S.

Atuma, C., Strugala, V., Allen, A., & Holm, L. (2001). The adherent gastrointestinal mucus gel layer: thickness and physical state in vivo. *American Journal of Physiology-Gastrointestinal and Liver Physiology,* 280(5), G922-G929.

Baur, A., Kaufmann, F., Rolli, H., Weise, A., Luethje, R., Berg, B., . . . Gorr, G. (2005). A fast and flexible PEG-mediated transient expression system in plants for high level expression of secreted recombinant proteins. *Journal of Biotechnology,* 119(4), 332-342.

Bogataj, M., Vovk, T., Kerec, M., Dimnik, A., Grabnar, I., & Mrhar, A. (2003). The correlation between zeta potential and mucoadhesion strength on pig vesical mucosa. *Biological and Pharmaceutical Bulletin,* 26(5), 743-746.

Boluk, Y., Lahiji, R., Zhao, L. Y., & McDermott, M. T. (2011). Suspension viscosities and shape parameter of cellulose nanocrystals (CNC). *Colloids and Surfaces a-Physicochemical and Engineering Aspects,* 377(1-3), 297-303.

Cugia, F., Monduzzi, M., Ninham, B. W., & Salis, A. (2013). Interplay of ion specificity, pH and buffers: insights from electrophoretic mobility and pH measurements of lysozyme solutions. *RSC Advances,* 3(17), 5882-5888.

de Loubens, C., Lentle, R. G., Love, R. J., Hulls, C., & Janssen, P. W. M. (2013). Fluid mechanical consequences of pendular activity, segmentation and pyloric outflow in the proximal duodenum of the rat and the guinea pig. *Journal of The Royal Society Interface,* 10(83).

DeLoid, G. M., Sohal, I. S., Lorente, L. R., Molina, R. M., Pyrgiotakis, G., Stevanovic, A., . . . Demokritou, P. (2018). Reducing Intestinal Digestion and Absorption of Fat Using a Nature-Derived Biopolymer: Interference of Triglyceride Hydrolysis by Nanocellulose. *ACS Nano*.

Duncan, T. V. (2011). Applications of nanotechnology in food packaging and food safety: barrier materials, antimicrobials and sensors. *Journal of Colloid and Interface Science,* 363(1), 1-24.

Eshel-Green, T., Eliyahu, S., Avidan-Shlomovich, S., & Bianco-Peled, H. (2016). PEGDA hydrogels as a replacement for animal tissues in mucoadhesion testing. *International journal of pharmaceutics,* 506(1-2), 25-34.

Faridi Esfanjani, A., Assadpour, E., & Jafari, S. M. (2018). Improving the bioavailability of phenolic compounds by loading them within lipid-based nanocarriers. *Trends in Food Science & Technology,* 76, 56-66.

Gómez H, C., Serpa, A., Velásquez-Cock, J., Gañán, P., Castro, C., Vélez, L., & Zuluaga, R. (2016). Vegetable nanocellulose in food science: A review. *Food Hydrocolloids,* 57, 178-186.

Geng, L., Peng, X., Zhan, C., Naderi, A., Sharma, P. R., Mao, Y., & Hsiao, B. S. (2017). Structure characterization of cellulose nanofiber hydrogel as functions of concentration and ionic strength. *Cellulose,* 24(12), 5417-5429.

Griesser, J., Hetényi, G., Kadas, H., Demarne, F., Jannin, V., & Bernkop-Schnürch, A. (2018). Self-emulsifying peptide drug delivery systems: How to make them highly mucus permeating. *International journal of pharmaceutics,* 538(1-2), 159-166.

Hardacre, A. K., Lentle, R. G., Yap, S. Y., & Monro, J. A. (2016). Does viscosity or structure govern the rate at which starch granules are digested? *Carbohydrate Polymers,* 136, 667-675.

Hassan, E. E., & Gallo, J. M. (1990). A simple rheological method for the in vitro assessment of mucin-polymer bioadhesive bond strength. *Pharmaceutical Research,* 7(5), 491-495.

Hemmati, F., Jafari, S. M., Kashaninejad, M., & Barani Motlagh, M. (2018). Synthesis and characterization of cellulose nanocrystals derived from walnut shell agricultural residues. *International Journal of Biological Macromolecules,* 120, 1216-1224.

Jafari, S., & McClements, D. (2017). *Nanotechnology approaches for increasing nutrient bioavailability*. In *Advances in food and nutrition research* (pp. 1-30): Elsevier

Jiang, F., & Hsieh, Y. L. (2013). Chemically and mechanically isolated nanocellulose and their self-assembled structures. *Carbohydrate Polymers,* 95(1), 32-40.

Johansson, M. E. V., Larsson, J. M. H., & Hansson, G. C. (2011). The two mucus layers of colon

are organized by the MUC2 mucin, whereas the outer layer is a legislator of host-microbial interactions. *Proceedings of the National Academy of Sciences,* 108 Suppl 1, 4659-4665.

Johnson, P., & Rainsford, K. (1972). The physical properties of mucus: Preliminary observations on the sedimentation behaviour of porcine gastric mucus. *Biochimica et Biophysica Acta (BBA)-General Subjects,* 286(1), 72-78.

Kararli, T. T. (1995). Comparison of the gastrointestinal anatomy, physiology, and biochemistry of humans and commonly used laboratory animals. *Biopharmaceutics & drug disposition,* 16(5), 351-380.

Karppinen, A., Saarinen, T., Salmela, J., Laukkanen, A., Nuopponen, M., & Seppälä, J. (2012). Flocculation of microfibrillated cellulose in shear flow. *Cellulose,* 19(6), 1807-1819.

Khutoryanskiy, V. V. (2011). Advances in Mucoadhesion and Mucoadhesive Polymers. *Macromolecular Bioscience,* 11(6), 748-764.

King, M. (2006). Physiology of mucus clearance. *Paediatric Respiratory Reviews,* 7, S212-S214.

Liu, L., Kerr, W. L., Kong, F., Dee, D. R., & Lin, M. (2018). Influence of nano-fibrillated cellulose (NFC) on starch digestion and glucose absorption. *Carbohydrate Polymers,* 196, 146-153.

Lourenço, A. F., Gamelas, J. A. F., Nunes, T., Amaral, J., Mutjé, P., & Ferreira, P. J. (2017). Influence of TEMPO-oxidised cellulose nanofibrils on the properties of filler-containing papers. *Cellulose,* 24(1), 349-362.

Ma, H., Burger, C., Hsiao, B. S., & Chu, B. (2011). Ultrafine polysaccharide nanofibrous membranes for water purification. *Biomacromolecules,* 12(4), 970-976.

McConnell, E. L., Basit, A. W., & Murdan, S. (2008). Measurements of rat and mouse gastrointestinal pH, fluid and lymphoid tissue, and implications for in-vivo experiments. *Journal of Pharmacy and Pharmacology,* 60(1), 63-70.

Minekus, M., Alminger, M., Alvito, P., Ballance, S., Bohn, T., Bourlieu, C., . . . Brodkorb, A. (2014). A standardised static in vitro digestion method suitable for food – an international consensus. *Food & Function,* 5(6), 1113-1124.

Moon, R. J., Martini, A., Nairn, J., Simonsen, J., & Youngblood, J. (2011). Cellulose nanomaterials review: structure, properties and nanocomposites. *Chemical Society Reviews,* 40(7), 3941-3994.

Mysels, K. J. (1984). Surface tension studies of bile salt association. *Hepatology,* 4(S2), 80S-84S.

No, H. K., Meyers, S. P., Prinyawiwatkul, W., & Xu, Z. (2007). Applications of Chitosan for Improvement of Quality and Shelf Life of Foods: A Review. *Journal of Food Science,* 72(5), R87-R100.

Ohshima, H. (2013). *Zeta Potential*. In T. Tadros (Ed.), *Encyclopedia of Colloid and Interface Science*. Berlin, Heidelberg: Springer, Berlin, Heidelberg

Peng, Y., Gardner, D. J., Han, Y., Kiziltas, A., Cai, Z., & Tshabalala, M. A. (2013). Influence of drying method on the material properties of nanocellulose I: thermostability and crystallinity. *Cellulose,* 20(5), 2379-2392.

Ponchel, G., Montisci, M. J., Dembri, A., Durrer, C., & Duchêne, D. (1997). Mucoadhesion of colloidal particulate systems in the gastro-intestinal tract. *European Journal of Pharmaceutics and Biopharmaceutics,* 44(1), 25-31.

Qing, Y., Sabo, R., Zhu, J. Y., Agarwal, U., Cai, Z., & Wu, Y. (2013). A comparative study of cellulose nanofibrils disintegrated via multiple processing approaches. *Carbohydrate Polymers,* 97(1), 226-234.

Reiner, R. S., & Rudie, A. W. (2013). *Process Scale-Up of Cellulose Nanocrystal Production to 25 kg per Batch at the Forest Products Laboratory*. In M. T. Postek, R. J. Moon & A. W. Rudie (Eds.), *Production and applications of Cellulose nanomaterials, TAPPI Press* (pp. 21-24): TAPPI

Reiner, R. S., & Rudie, A. W. (2017). *Experiences with Scaling-Up Production of TEMPO-Grade Cellulose Nanofibrils*. In *Nanocelluloses: Their Preparation, Properties, and Applications* (pp. 227-245): American Chemical Society

Saito, T., Hirota, M., Tamura, N., Kimura, S., Fukuzumi, H., Heux, L., & Isogai, A. (2009). Individualization of nano-sized plant cellulose fibrils by direct surface carboxylation using TEMPO catalyst under neutral conditions. *Biomacromolecules,* 10(7), 1992-1996.

Saito, T., Kimura, S., Nishiyama, Y., & Isogai, A. (2007). Cellulose nanofibers prepared by TEMPO-mediated oxidation of native cellulose. *Biomacromolecules,* 8(8), 2485-2491.

Shumilov, D., Popov, A., Fudala, R., Akopova, I., Gryczynski, I., Borejdo, J., . . . Grygorczyk, R. (2014). Real-time imaging of exocytotic mucin release and swelling in Calu-3 cells using acridine orange. *Methods,* 66(2), 312-324.

Singla, A. K., Chawla, M., & Singh, A. (2000). Potential Applications of Carbomer in Oral Mucoadhesive Controlled Drug Delivery System: A Review. *Drug Development and Industrial Pharmacy,* 26(9), 913-924.

Sogias, I. A., Williams, A. C., & Khutoryanskiy, V. V. (2008). Why is chitosan mucoadhesive? *Biomacromolecules,* 9(7), 1837-1842.

Sozer, N., & Kokini, J. L. (2009). Nanotechnology and its applications in the food sector. *Trends in biotechnology,* 27(2), 82-89.

Takeuchi, H., Thongborisute, J., Matsui, Y., Sugihara, H., Yamamoto, H., & Kawashima, Y. (2005). Novel mucoadhesion tests for polymers and polymer-coated particles to design optimal mucoadhesive drug delivery systems. *Advanced Drug Delivery Reviews,* 57(11), 1583-1594.

Tanaka, R., Saito, T., Ishii, D., & Isogai, A. (2014). Determination of nanocellulose fibril length by shear viscosity measurement. *Cellulose,* 21(3), 1581-1589.

Thirawong, N., Kennedy, R. A., & Sriamornsak, P. (2008). Viscometric study of pectin-mucin interaction and its mucoadhesive bond strength. *Carbohydrate Polymers,* 71(2), 170-179.

Uetani, K., & Yano, H. (2011). Nanofibrillation of wood pulp using a high-speed blender. *Biomacromolecules,* 12(2), 348-353.

Varum, F. J. O., Veiga, F., Sousa, J. S., & Basit, A. W. (2010). An investigation into the role of mucus thickness on mucoadhesion in the gastrointestinal tract of pig. *European Journal of Pharmaceutical Sciences,* 40(4), 335-341.

Wang, Y. Y., Lai, S. K., So, C., Schneider, C., Cone, R., & Hanes, J. (2011). Mucoadhesive nanoparticles may disrupt the protective human mucus barrier by altering its microstructure.

PLoS One, 6(6), e21547.

Xia, Y., Yang, P., Sun, Y., Wu, Y., Mayers, B., Gates, B., . . . Yan, H. (2003). One-dimensional nanostructures: Synthesis, characterization, and applications. *Advanced Materials,* 15(5), 353-389.

Zammarano, M., Maupin, P. H., Sung, L.-P., Gilman, J. W., McCarthy, E. D., Kim, Y. S., & Fox, D. M. (2011). Revealing the Interface in Polymer Nanocomposites. *ACS nano,* 5(4), 3391-3399.

Zhong, L., Fu, S., Peng, X., Zhan, H., & Sun, R. (2012). Colloidal stability of negatively charged cellulose nanocrystalline in aqueous systems. *Carbohydrate Polymers,* 90(1), 644-649.

Zhou, Y., Fuentes-Hernandez, C., Khan, T. M., Liu, J. C., Hsu, J., Shim, J. W., . . . Kippelen, B. (2013). Recyclable organic solar cells on cellulose nanocrystal substrates. *Scientific Reports,* 3, 1536.

CHAPTER 4.

SIX WEEKS EFFECT OF DIFFERENT NANOCELLULOSE ON BLOOD LIPID LEVEL AND SMALL INTESTINAL MORPHOLOGY IN MICE [4]

[4]Lin, Y.-J., Chen, Y., Guo, T. L., Kong, F., Short-Term Effect on Blood Lipid Level and Small Intestinal Morphology in Mice Fed with Different Nanocellulose. To be submitted to *Food Hydrocolloids.*

Abstract

Cellulose nanofibrils (CNF), cellulose nanocrystals (CNC), and Tempo (2,2,6,6-tetramethylpiperidine-1-oxyl radical) oxidized CNF (TEMPO-CNF) were compared for the short-term effect on mice fed with a high-fat and high-sugar (Western diet, WD) to investigate their effect when combined with a sub-optimal diet. Thirty C57B/C female mice (10 weeks old; 5-6/group) were given water, cellulose, or three types of nanocellulose once daily in a dose of 30 mg/kg body weight by oral gavage. After six weeks, weight changes, fecal output, glucose homeostasis, and gut permeability showed no significant among groups. Serum analysis including triglycerides, cholesterol and total bile acids and small intestinal morphology including villus length, villus width, crypt depth, goblet cell count and goblet cell density was no difference for all groups. Only the CNC group had higher excretion of bile acids in the feces. These results suggest that three types of nanocellulose showed benign effects on lipid metabolism and small intestinal physiology.

Keywords: Nanocellulose, cellulose nanofibrils (CNF); cellulose nanocrystals (CNC); TEMPO-CNF; Western diet; short-term effect

4.1 Introduction

Nanocellulose can be synthesized by bacteria or artificially derived from plant-based cellulosic materials such as wood or cotton pulp. Plant-based nanocellulose has gathered great interest from both food industries to be used as additives such as stabilizer, emulsifier, and fat replacer. There are two major categories of plant-based nanocellulose: cellulose nanofibrils (CNF) and cellulose nanocrystals (CNC). CNF is mechanically sheared pulps. The mechanical refining produces noodle-like nanofibrils that are 4-20 nm wide and 500-2000 nm long (Moon, Martini, Nairn, Simonsen, & Youngblood, 2011). CNC is made from cellulosic pulp hydrolyzed with acids (e.g., sulfuric acid) followed by decoloring, neutralization and diafiltration to remove the salts. The modification digests the amorphous region of cellulose fibrils, leaving only the crystalline region, meanwhile partially substitutes a sulfuric group on the C6-carbon of glucose unit. As a result, CNC has a rod-like structure with a narrower size distribution compared to CNF, typically the diameter range between 3-5 nm and 50-500 nm in length (Moon et al., 2011; Reiner & Rudie, 2013). (2,2,6,6-tetramethylpiperidine-1-oxyl radical)-oxidized CNF (TEMPO-CNF) is a chemically modified CNF produced by Tempo radical-mediated oxidation using wood-pulp followed by high-speed homogenization (Uetani & Yano, 2011), which typically has a dimension of 5-7nm in width and several μm in length (Qing et al., 2013; Saito et al., 2009). The modification substitutes the C6-carbon with a charged carboxy group, thereby increasing interfibrillar repulsion (Moon et al., 2011). This plant-based nanocellulose, although still yet to be legalized as a food ingredient, may still serve as a fiber source due to its natural composition. Nevertheless, more information on the health impact regarding consuming nanocellulose is needed. Especially, there

is still a lack of research to compare the three aforementioned types of nanocellulose simultaneously in animal studies.

Previously our lab demonstrated how different types of nanocellulose may remain in the gut by adhering to the mucosal layer *in vitro* and *ex vivo* as well as affecting nutrient digestion and absorption (Lin, Shatkin, & Kong, 2019; Liu, Kerr, & Kong, 2019; Liu, Kerr, Kong, Dee, & Lin, 2018; Liu & Kong, 2019a, 2019b, 2019c). CNF show adhesion by coiling into mucus gel, CNC spreads out onto mucus gel and react with mucin molecules due to its small size, while TEMPO-CNF forms instant gelling in the stomach to achieve retention (Lin et al., 2019). CNC at 4% showed a reduction in free amino nitrogen diffusion from whey protein isolate (Liu & Kong, 2019c). CNF and TEMPO-CNF at 0.3% were found to reduce free fatty acids released from milk *in vitro*, while CNC at the same concentration could reduce free amino nitrogen from milk protein (Liu & Kong, 2019a). CNC could also increase the viscosity of lipid emulsion in the gastric phase where the lipid emulsion was made from canola oil and Tween 80, although three types of nanocellulose showed no difference as the final lipolysis level (Liu et al., 2019). Anionic nanocellulose including CNC and TEMPO-CNF show further binding effects compare to non-anionic nanocellulose such as CNF. CNC and TEMPO-CNF bind with whey protein isolate in the gastric phase *in vitro,* causing physiological changes of digesta including viscosity and particle size (Liu & Kong, 2019c). Deloid et al. also conducted screening of CNF and CNC *in vitro* in cream digestion and found CNF had the most significant reduction in hydrolyzed fatty acids from cream compared to CNC (Glen M. DeLoid et al., 2018).

Because different nanocellulose display distinct properties as well as their health benefits *in vitro*, it is expected that they may generate different effects *in vivo*. However, the connection between *in vitro* and *in vivo* studies could be scattered due to the dynamic and complex nature of

biological bodies. The concentration of nanocellulose tested in vivo that reaches the digestive tract may also be very diluted compared to *in vitro* studies. Thus, there is a need in filling the knowledge gap of how different types of nanocellulose affect metabolism *in vivo.*

The current study investigated the short-term effects of daily intake of three types of nanocellulose, CNF, CNC, and TEMPO-CNF and especially focused on lipid metabolism and small intestinal morphology with mice fed with Western diet (WD). Previous researchers have suggested mice fed with a regular diet showed no observable adverse effect for CNF (Andrade et al., 2015; Ong et al., 2020). However, the homeostasis of health may be more vulnerable when taking a suboptimal diet and may be more sensitive to show any adverse effect (Shah, Momcilovic, & McLaughlan, 1980). Western diet (WD) meaning a high-fat and high-sugar diet was chosen in this study to investigate the effect of nanocellulose intake in a suboptimal diet condition, with the idea to reflect any possible adverse effect on people in sub healthy state. Our previous studies showed CNF might reduce nutrient passage due to the non-specific binding of nutrients (Chen, Lin, Nagy, Kong, & Guo, 2020). In this work, the emphasis was put on comparing different types of nanocellulose to further investigate if three types of nanocellulose have different effects on metabolic parameters.

4.2 Materials and Methods

4.2.1 Materials

Three types of nanocellulose were purchased from the following suppliers: CNF was from the Nanomaterial Pilot Plant at the University of Maine and was made by ultrafine grinding of bleached softwood kraft pulp. CNC and TEMPO-CNF were purchased from the Nanocellulose

Pilot Plant of the Forest Products Laboratory (FPL), USDA United States Forest Service in Madison, Wisconsin. All nanocellulose arrived in slurry or hydrogel form. CNF (50 nm in width and several μm in length) was 3 wt% in water; CNC (5-20 nm in width and 150-200 nm in length) was 12.1 wt% in water in sodium form that contained 0.94 wt% sulfur; and TEMPO-CNF was 1.1 wt% and contained 1.3 mM –COONa/g dry TEMPO-CNF in sodium form according to the makers' specifications. CNF and CNC were diluted into 0.3% (w/w). TEMPO-CNF was diluted into 0.15% (w/w) so it is liquified (Ma, Burger, Hsiao, & Chu, 2011) to enable precise oral gavage. The solid content was the same among all-fiber groups.

Heparin was purchased from Sagent Pharmaceuticals, Inc. (Schaumburg, IL). Cellulose (C6288, medium), fluorescein isothiocyanate–dextran (FD4, average molecular weight = 4,000), and other chemicals were purchased from Sigma Aldrich (St. Louis, MO).

4.2.2 Animals

Thirty C57BL/6 female mice (6 weeks old) were purchased from The Jackson Laboratory (Bar Harbor, MA). All animals were housed in Paul D. Coverdell Center for Biomedical & Health Sciences at the University of Georgia. The protocol was approved by the Institutional Animal Care and Use Committee (IACUC) of the University of Georgia (Protocol Number: A2017 09-001-Y1-A0) and all handlings were performed in accordance to "Guide for the Care and Use of Laboratory Animals" (National Research Council, 8th edition, 2011).

Experiments started when the mice reached 10 weeks old and were randomly separated into five groups with 6 mice per group. Western Diet (D12079B, Research Diets, Inc., New Brunswick, NJ.; 17% kcal from protein, 40% kcal from fat, 43% kcal from carbohydrate, and

containing 5%(w/w) Solka Floc, FCC200 as fiber sources) and filtered water were provided *ad libitum*. Mice were fed with cellulose, CNF, CNC, and TEMPO-CNF at a dose of 30 mg/kg body weight and water by oral gavage. Bodyweight gain was calculated in week 6 by the difference comparing to body weight at week 0. Food intake for 24 hours was performed at week 6 by housing each mouse in a single cage with water and food pellet *ad libitum.* Food weight loss and the total number of feces after 24 hours were taken at the same time. Fecal pellets were air-dried overnight to measure the total fecal weight. At the end of the trial, animals were euthanized by carbon dioxide anesthesia followed by cervical dislocation.

4.2.3 Intraperitoneal glucose tolerance test

Glucose homeostasis was evaluated by glucose tolerance tests (Chen, Nagy, & Guo, 2019). Mice were fasted for 16 hours and received 2g/kg body weight of glucose by intraperitoneal administration at week 6. Blood glucose level was measured from venous blood at time 0, 15, 30, 60, 120 min using Prodigy AutoCode® blood glucose meter (Prodigy Diabetes Care, LLC., Charlotte, NC) with a no-coding blood glucose test strip (Prodigy).

4.2.4 Gut permeability test by FD4

The intestinal permeability test was done according to Rahman et al. (2016) with minor modifications. At week 7, mice were fasted for 6 hours with free access to water and were given 500 mg/kg body weight of FD4 by oral gavage. After 3 hours, 100 μL of blood was taken from the tail vein and mixed with 5 units of heparin immediately. The blood samples were spun down at 10000 xg for 5 min at 4°C to collect plasma. The fluorescence intensity was measured after diluted

1:4 with PBS by Synergy HTX Microplate Reader (BioTek Instruments, Inc., Winooski, VT) at Exi485nm/Emi528nm. FD4 concentration was calculated according to an FD4 standard curve.

4.2.5 Serum and fecal analysis

Serum and fecal total bile acids (TBA)

Blood was drawn after anesthesia from the orbital sinus before euthanization and stored at 4°C followed by centrifugation separation the next day. Serum was harvested and stored at -80°C until use. Total bile acid was analyzed by Diazyme Colorimetric Total Bile Acids Assay Kit (NBT Method, Diazyme Laboratories, Poway, CA) following the manufacturer's instruction.

At week 6, fresh feces were collected and combined over 5 days and stored at -80°C. Fecal bile acid was extracted according to literature with minor modifications (Andersson et al., 2013). In brief, 50 mg of lyophilized feces was minced and extracted with 1mL of 75% alcohol at 50°C in a water bath for 2 hours. The supernatant after centrifugation (7000 xg, 5 min) was collected and diluted by 1:9 with water. Samples were then analyzed according to the kit instruction.

Serum total cholesterol

Serum total cholesterol was determined by the o-phthalaldehyde (OPA) method, according to Rudel and Morris (1973). Briefly, 10 μL of serum was mixed with 300 μL of 33% (w/v) KOH and 300 μL of 95% ethanol. A standard curve of cholesterol was prepared in hexane and analyzed parallelly. Samples were heated in a 60°C water bath for 15 min. After the mixture has been cooled, it was mixed with 1 ml of hexane and 300 μL of distilled water and vortexed vigorously. Samples were then held still until phase separation, and 600 μL aliquot of the upper hexane layer was taken into a new tube and evaporated under vacuum at room temperature. Afterward, 400 μL of OPA

reagent (0.5 mg/mL in glacial acetic acid) was added to the tube and vortexed. After 10 min, 200 μL sulfuric acid was added and mixed immediately. The absorbance of the mixture was then taken at 550 nm after 30 min of reaction.

Serum total triglycerides

Serum triglyceride level was analyzed by Triglycerides Colorimetric Assay Kit from Cayman Chemical (Ann Arbor, MI) following the supplier's instruction.

4.2.6 Histological analysis

After euthanization, small intestines were taken out and rinsed in cold PBS. The mesentery was removed, and the intestinal length was then measured. One and a half cm of the beginning, middle, and end sections of the small intestine were taken to represent the duodenum, jejunum, and ileum. Specimen were fixed in Carnoy's solution (absolute alcohol: chloroform: glacial acetic acid = 6:3:1) (Puchtler, Waldrop, Conner, & Terry, 1968) overnight and transferred into cassettes and submerged in absolute alcohol the second day. All samples were then processed on the second day at Histology Laboratory at the College of Veterinary Medicine, the University of Georgia. Samples were dehydrated in a serious concentration of alcohol and cleared in Xylene without formalin, and infiltrated and embedded in parafilm. The parafilm blocks were then sectioned by Microtome and counter-stained with Alcian Blue (pH2.5) and Nuclear Fast Red.

Histological analysis was measured single-blinded under Eclipse 80i microscope (Nikon Instruments Inc., Melville, NY) and analyzed by NIS Elements Imaging Software (ver. 3.22.14). The villus length was measured from the neck to the tip, and the width of the villi was measured in the middle of the villus, all from 6 to 10 complete villi. The crypt depth was measured from the

base to the crypt opening. Goblet cells on each villus were stained in blue with Alcian Blue and were counted under a 20X objective lens. The goblet cell density (goblet cell count per 100 μm villus) was calculated as Goblet cell density = goblet cell count/villus length *100

4.2.7 Statistical analysis

Analysis of variance (ANOVA) followed by Tukey-Kramer HSD test was used to test for significance by JMP Pro 13.0.0 (SAS Institute Inc., Cary, NC).

4.3 Results

4.3.1 Basic physiological parameters and gut permeability

After six weeks of feeding WD with water, cellulose, or nanocellulose (30 mg/kg body weight), basic physiological parameters including body weight change, food intake over 24 hours, the total number of feces count, total fecal weight (dry), average fecal pellet weight (Table 4.1) showed no difference among all groups fed with WD Weight gain was slightly lower in cellulose group and higher in TEMPO-CNF group but both showed no statistical significance towards other groups. These results showed nanocellulose intake at this amount did not change basic physiological parameters after 6 weeks of consumption. Glucose metabolism and intestinal permeability were further assessed by intraperitoneal glucose tolerance test (Figure 4.1 (a)) and FD4 assay (Figure 4.1 (b)), respectively. Results showed no statistical significance among groups, indicating that cellulose or nanocellulose consumption did not improve glucose metabolism and gut permeability compared to the control group.

Table 4.1. Overall weight gain at week 6, and food consumption over 24 hours measured at week 6. Mean ± SEM. (n=5-6) for overall weight gain, food consumption, and total fecal dry weight. (Median, quantile) for feces counts. No significance was detected by ANOVA (α =0.05). The data of water, cellulose, and CNF groups have been published in a previous study (Chen et al., 2020).

	Overall weight gain (g)	Food consumption over 24 hours (g)	Number of feces over 24 hours (granule)	Total fecal dry weight (mg)	Avg fecal pellet weight (mg)
Water	3.18 ± 0.55	2.82 ± 0.21	24.5 ± 7.1	257.7 ± 32.4	10.56 ± 0.61
Cellulose	1.94 ± 0.57	3.30 ± 0.31	23.3 ± 5.2	283.9 ± 36.3	12.36 ± 1.27
CNF	2.54 ± 0.30	2.73 ± 0.19	23.5 ± 3.9	246.7 ± 20.0	10.52 ± 0.60
CNC	3.24 ± 0.61	3.19 ± 0.23	29 ± 4.6	313.5 ± 18.6	10.93 ± 0.71
TEMPO-CNF	3.78 ± 0.93	2.54 ± 0.14	24.6 ± 3.8	256.8 ± 17.1	10.54 ± 0.63

(a)

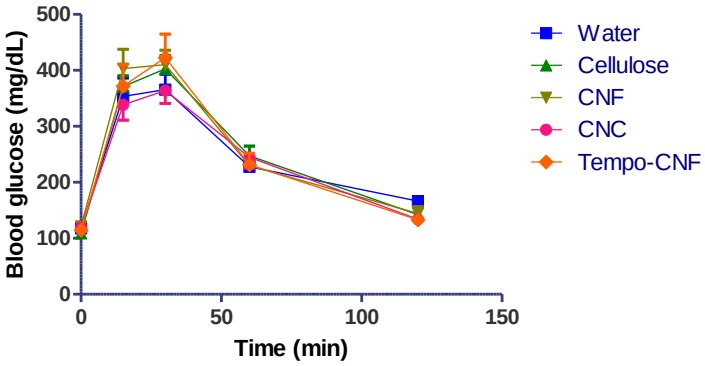

(b)

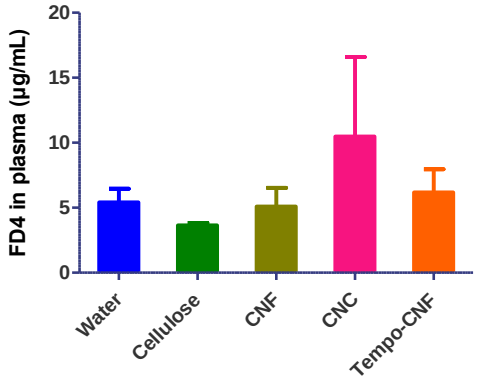

Figure 4.1. (a) Intraperitoneal (i.p.) glucose tolerance test. Mean blood glucose ± SEM. No significance was detected after ANOVA. (n=5-6) The data of water, cellulose, and CNF groups have been published in a previous study (Chen et al., 2020). (b) Gut integrity by plasma FD4 concentration after 3 hrs. Mean FD4 in plasma ± SEM (n=4). No significance was detected by ANOVA (α =0.05).

4.3.2 Serum and fecal analysis

Several lipid metabolic parameters in serum, including triglycerides, cholesterol, and TBA, were analyzed to determine the impact of nanocellulose on lipid metabolism in Figure 4.2. Serum TBA is a sensitive indicator of early-stage liver dysfunction, and increased blood TBA is correlated to a decreased liver function (Korman, Hofmann, & Summerskill, 1974; Luo et al., 2018). In our previous study, CNF was able to protect the formation of fatty liver induced by the Western diet (Chen et al., 2020). Therefore, serum TBA was analyzed as an indicator to detect the liver function changes. After 6 weeks of nanocellulose ingestion combining WD, no significant difference was found on level blood triglycerides, cholesterol, and TBA among all groups. A trend was seen on animals fed with TEMPO-CNF exhibited the lowest serum triglycerides and TBA, although no significance was detected.

Bile acids secreted into the small intestine function as an emulsifier that forms chylomicrons and thus is important in the digestion of fat in the diet. It was estimated that 95% of bile acids were reabsorbed in the ileum while 5% of bile acids enter the large intestine and eventually 1-3% is excreted to feces (Martinez-Augustin & Sanchez de Medina, 2008). A higher level of bile acids in feces could be a result of hindered reabsorption of bile acids in the gut, and it is also one of the mechanisms proposed for the benefit of dietary fibers in lowering blood cholesterol, such as oats (Andersson et al., 2013). Therefore, fecal TBA was analyzed to determine the level of bile acid reabsorption in our model (Figure 4.3). Among all groups, the fecal TBA level in the CNC group was significantly higher than cellulose and CNF, which suggested that CNC decreased bile acid reabsorption.

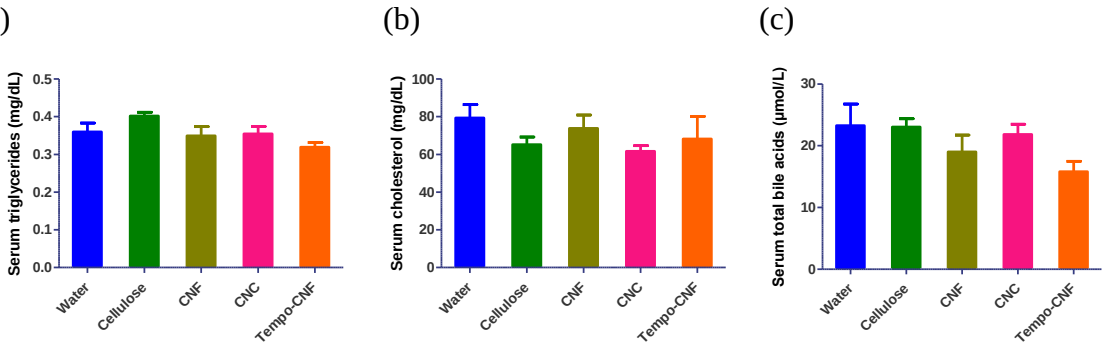

Figure 4.2. (a) Serum triglycerides. The data of water, cellulose, and CNF groups have been published in a previous study (Chen et al., 2020). (b) serum cholesterol, and (c) serum total bile acids. Data was shown in mean ± SEM (n=5-6). No significance was detected by ANOVA (α =0.05).

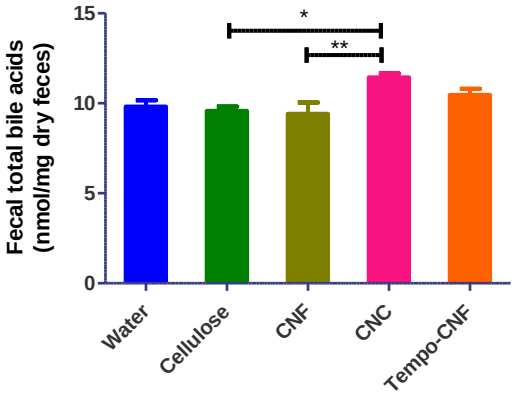

Figure 4.3. Fecal bile acids after 5 weeks of daily nanocellulose consumption with WD. Mean bile acids/mg dry feces ± SEM (n=5-6). (*, $p<0.05$; **, $p<0.01$; ***,$p<0.001$, ANOVA, Tukey's multiple comparison test, α =0.05)

4.3.3 Histological analysis on intestinal morphology

The intestinal morphology may be changed due to dietary fibers. In the small intestine, fibers could increase villus height or width (Chun, Bamba, & Hosoda, 1989; Jin, Reynolds, Redmer, Caton, & Crenshaw, 1994; Sigleo, Jackson, & Vahouny, 1984). In our study, different treatments with WD did not alter the overall length of the small intestine, cecum, and large intestine (Table 4.2). The small intestinal morphology was analyzed and the villus length, villus width, crypt depth, goblet cell count, and goblet cell density of the small intestine showed no significant differences among WD groups (Figure 4.4 and Figure 4.5). Although no significance was detected by ANOVA, there is a trend for the TEMPO-CNF group with the highest goblet cell count per villus in all three sections of the small intestine.

Table 4.2. Intestinal length after euthanization. Mean intestinal length ± SEM (n=5-6). No significance was detected by ANOVA (α =0.05).

	Small intestine (cm)	Cecum (cm)	Colon (cm)
Water	30.97 ± 0.86	1.95 ± 0.10	5.28 ± 0.14
Cellulose	30.77 ± 0.74	1.89 ± 0.09	5.31 ± 0.12
CNF	31.13 ± 0.82	1.89 ± 0.08	4.90 ± 0.22
CNC	30.32 ± 0.39	1.92 ± 0.07	5.12 ± 0.13
TEMPO-CNF	31.05 ± 0.56	2.12 ± 0.14	5.41 ± 0.11

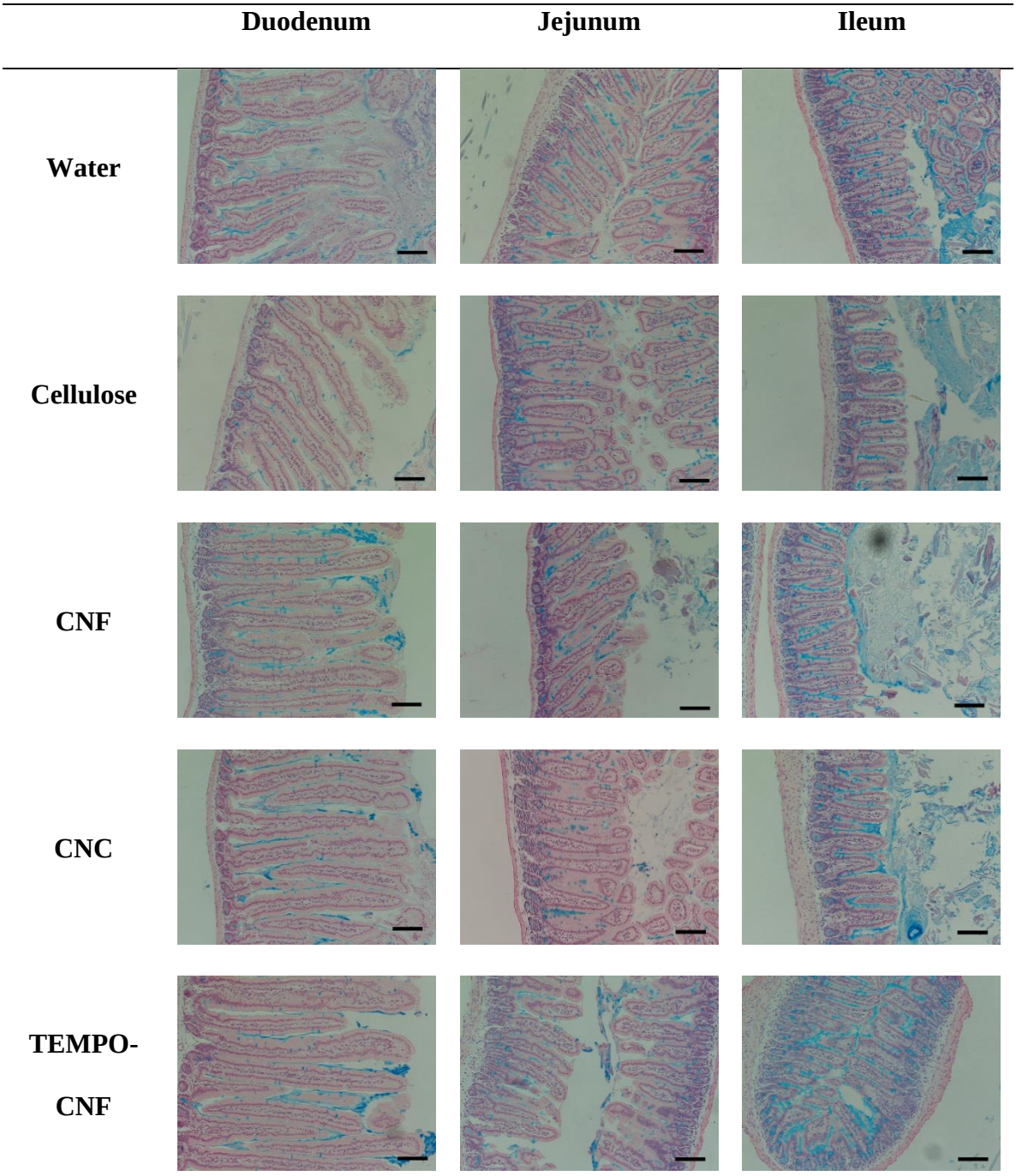

Figure 4.4. Photomicrograph of each section of mice small intestine (scale bar, 100 μm) stained with Alcian blue (pH 2.5) to show mucus in blue and nuclear fast red to show nuclear in pink-red and cytoplasm in pale pink.

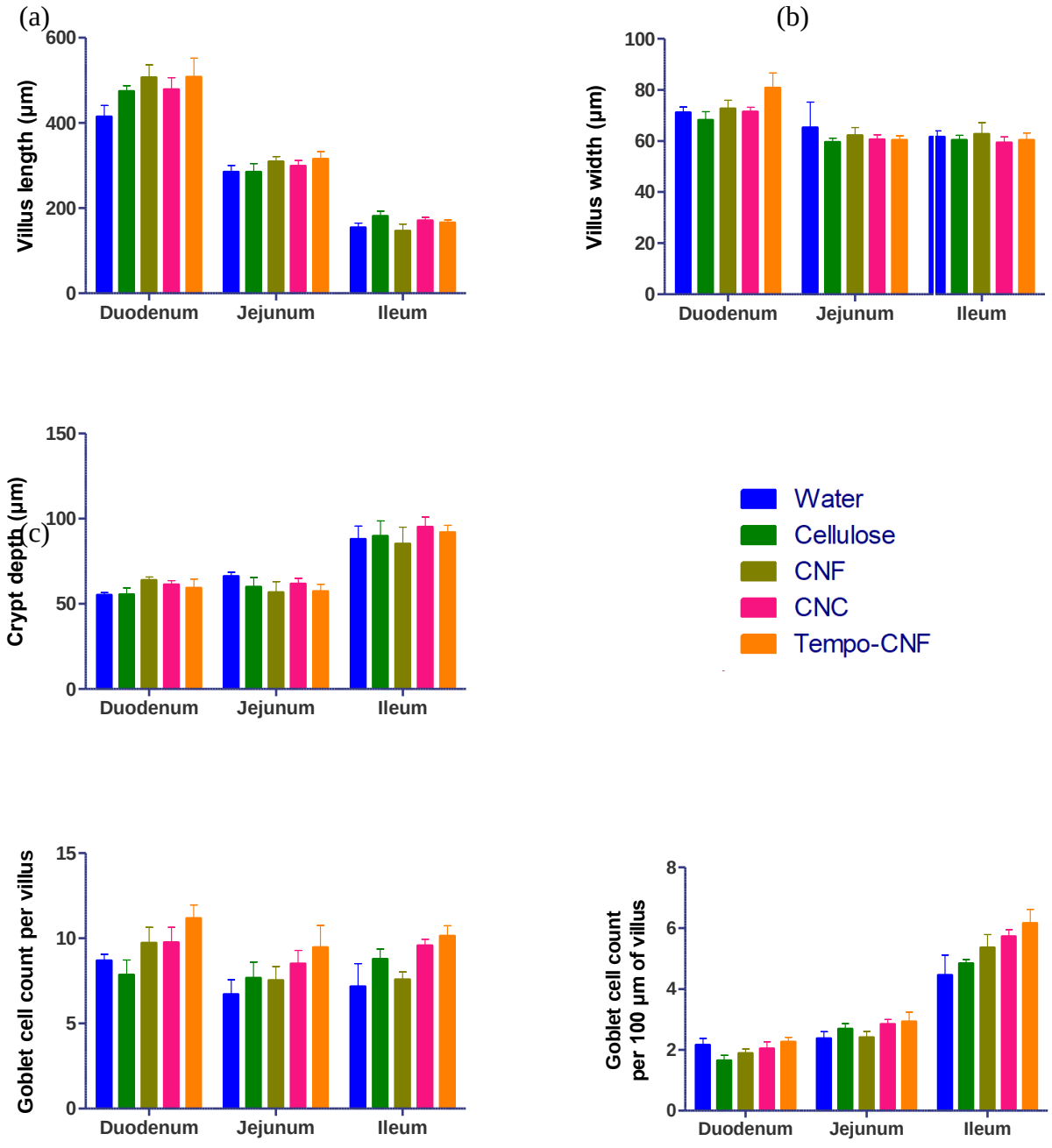

Figure 4.5. (a) Villus length, (b) Villus width, (c) crypt depth, (d) goblet cell count per villus, and (e) goblet cell density (average goblet cell count per 100 µm of the villus) of the small intestine. Seven to ten villi or crypt from each mouse was measured and averaged. Data was shown in mean ± SEM (n= 5-6). No significance was detected by ANOVA (α =0.05).

4.4 Discussion

The current study examined the effect of 30 mg/kg body weight of daily nanocellulose consumption and how they differed from cellulose in an animal model under the condition of high fat and high sugar diet. The design may be correlated to a group of adults (75kg) eating WD while taking a bolus of 2.25 gram (dry basis) of nanocellulose to increase the daily fiber intake or as a food additive in some foods. Our study used a daily dosage of nanocellulose but with a suboptimal diet that potentially could induce obesity and increase metabolic stress. WD represents a more extreme dietary condition and has been related to increased health risk including Crohn's disease, dyslipidemia, metabolic syndrome in both human and animal studies (Kaser, Zeissig, & Blumberg, 2010; Lutsey, Steffen, & Stevens, 2008; Soh, Iqbal, Queiroz, Fernandez-Hernando, & Hussain, 2013). It is hence expected that effects from nanocellulose might be different under such circumstances compared to the literature where a regular diet was used (Andrade et al., 2015; Glen M DeLoid et al., 2018; Ong et al., 2020).

Results showed no significant difference in all the tested parameters in cellulose and CNF when compared to the water group. Cellulose is a non-digestible fiber, and it is also water-insoluble, so the effect of cellulose on digesta viscosity could be very limited, even with up to 2% concentration in the digesta (Liu et al., 2018). It is thus expected to see the results that cellulose does not have significant impacts on all the physiological parameters tested in this study. Likewise, CNF below 0.5% (w/w) also did not increase the viscosity of digesta drastically (Liu et al., 2018) as well as lipid emulsion particle size or viscosity during digestion *in vitro* (Liu et al., 2019). Although a temporary effect of CNF to retard fat absorption after ingestion of CNF is possible as seen in Glen M. DeLoid et al. (2018), our results suggested one dose daily for 30 mg/body weight

to decrease fat absorption might not be enough to have significant long term impacts. DeLoid et al. (2019) also tested CNF in an acute gavage animal model by feeding the rats with 1% CNF mixed with cream, twice a week for five weeks. It was found that no impact occurred on hematology, serum markers, or histology. A previous study (Chen et al., 2020) using WD *in vivo* shows CNF could potentially bind with nutrients to decrease absorption. Note that the use of student's t-test to detect significance may greatly increase the risk of type I error for the biological effect of CNF. Our conclusion on CNF was similar to Andrade et al. (2015) that no significant changes in lipid profile including serum triglycerides and total cholesterol, where they tested male rats with regular control diet (AIN-93) mixed with 7-21% CNF suspension for up to 30 days. Recent study of mice fed with 4% CNF in Standard Diet D11112219N Rodent Diet for 90 days also showed no observable adverse effects (Ong et al., 2020). Our result of the addition of 30 mg/kg body weight of CNF with WD for 6 weeks once again supports the conclusion that CNF had little effect in some major serum lipid parameters and small intestinal morphology compared to the water or cellulose group in the tested concentration.

CNC was found to increase fecal TBA output in this study, which is similar to the effect that was reported for many dietary fibers in the literature (Andersson et al., 2013; Ebihara & Schneeman, 1989; Ellegård & Andersson, 2007; Illman & Topping, 1985). The effect of CNC on serum cholesterol was not significant but a lower value was seen. Proposed mechanisms include direct binding of cholesterol and bile acids (Zhang, Huang, & Ou, 2011), altering bile acids metabolism through molecular pathway such as changing mRNA expression of hepatic enzyme CYP7A1 and CYP8B1 as well as LDL receptor (Andersson et al., 2013), and changes in microbiota and increasing SCFA production, which suppresses hepatic cholesterol synthesis (Hara, Haga, Aoyama, & Kiriyama, 1999). In our study, CNC was able to increase bile acid output in

feces compared to cellulose and CNF groups. The consumption of CNC may decrease serum cholesterol, although the current dosage did not induce a significant reduction. Previous literature has also reported that CNC increased fecal TBA and lowered total serum cholesterol while no significant changes in serum triglycerides compared to cellulose in ovariectomized rats (Lu, Gui, Guo, Wang, & Liu, 2015). It is possible in our study that healthy female mice with regular estrogen production had a stronger ability to maintain lipid homeostasis (Boldarine et al., 2020). CNC was found to be less effective to prevent hydrolyzation of free fatty acids than CNF in an *in vitro* titration assay (Glen M. DeLoid et al., 2018), which might explain why CNC did not affect serum triglyceride level in the present study. Therefore, it was suggested that CNC may adsorb bile acids in the lumen to prevent reabsorption while does not decrease the digestion of triglycerides. Taken together, future studies on the adsorption of bile acids by CNC could better explain the mechanisms.

The current study found TEMPO-CNF in the current dosage did not significantly change the physiological parameters tested in this study. A lowered serum triglyceride level and serum TBA level, as well as elevated goblet cell density in the ileum was seen although not significant. Serum TBA level is a sensitive early-stage liver function indicator. Generally, serum TBA level is elevated when liver function has defected and thus unable to extract bile acids from the blood (Korman et al., 1974; Luo et al., 2018). Fiber intake, especially prebiotics, is correlated to improved liver function of metabolic disorders such as non-alcoholic fatty liver disease. Prebiotics stimulate probiotics growth, and their metabolites, SCFA, reduce the bacteria-derived hepatotoxins, including ethanol, acetaldehyde, and volatile organic compound, therefore lower the risk of liver damage (Parnell, Raman, Rioux, & Reimer, 2012). Given the low concentration of TEMPO-CNF, the gelling during digestion, and the changes in the viscosity of digesta could be the highest among all four types of cellulose in this study. It was of interest to investigate if the

effect of TEMPO-CNF would have the same health benefit *in vivo* as previously suggested to delay free fatty acid release *in vitro* (Liu & Kong, 2019a) and to form gels and interact with mucin in the small intestine *in vitro* and *ex vivo* (Lin et al., 2019). These characteristics could potentially contribute to prolonging the effect of interfering fat absorption in the small intestine. Our result suggests TEMPO-CNF was unable to induce a significant difference in lowering overall lipid metabolisms, although it may worth a future investigation using a higher dose for its effect on lowering serum triglyceride level and serum TBA level. The slight increase in goblet cell density by TEMPO-CNF may also be another mechanism in modulation fat absorption if the product of goblet cell, i.e. mucin, also increases. Mucins absorb water in the lumen and form a viscous mucus layer with an unstirring water layer along the wall of the lumen which acts as a barrier for nutrient absorption (Smithson, Millar, Jacobs, & Gray, 1981). Fibers that thicken the unstirring water layer, such as pectin, may decrease fat and glucose absorption (Fuse, Bamba, & Hosoda, 1989). Again, our result was unable to support this hypothesis, but more studies, for example, mucus thickness in both small intestine and large intestine and more liver function tests are suggested in the future to examine if TEMPO-CNF alleviates liver damage.

Increasing fiber intake in the diet has several health benefits in fighting obesity by improving lipid homeostasis. Fibers have the health benefits to lower blood triglyceride and cholesterol (Lia et al., 1997), increase fecal bile acid excretion (Ellegård & Andersson, 2007; Moriceau et al., 2000). There is also a correlation of fiber intervention causes changes in the small intestinal morphology such as longer or wider villi and deeper crypt due to increased cell proliferation and migration (Chun et al., 1989; Hino et al., 2012; Jacobs, 1983; Jin et al., 1994). Although nanocellulose has not yet been approved as a food additive in the US, nanocellulose may enter the human diet. It has great potential to be used as food additives such as fat replacers or

emulsifiers in ice cream, cream, and sausage, etc or be utilized in food packaging (Gómez H et al., 2016; Marchetti, Muzzio, Cerrutti, Andrés, & Califano, 2017; Sun, Chen, Liu, Li, & Yu, 2015; Velásquez-Cock et al., 2019; Wang et al., 2018). Our results suggested consuming three types of nanocellulose in the dose of 30 mg/kg body weight for 6 weeks with a high-fat and high-sugar diet did not have a detrimental effect nor a substantial health benefit of fiber consumption. We also acknowledged that in this study only female mice were used and is insufficient to demonstrate gender bias. Future studies on both genders, using a higher dose of nanocellulose or for a longer period of treatment time would reveal the long-term effect of consuming nanocellulose.

4.5 Conclusions

In conclusions, after fed with WD (high fat and high sugar) and different nanocellulose in a daily dose of 30 mg/kg body weight for six weeks, body weight gain, food intake and fecal output over 24 hours, blood glucose homeostasis, and gut integrity were not different among all groups. Serum analysis on triglycerides, cholesterol, and total bile acids also showed no significant difference. The fecal analysis showed higher bile acids in the CNC group than cellulose and CNF groups. Nanocellulose and cellulose consumption also did not alter small intestinal morphology, including villus length, villus width, crypt depth, goblet cell count, and goblet cell density. Overall, nanocellulose and cellulose did not show substantial health benefits nor detrimental effects in the test dose when combined with WD. The mechanism of increased fecal bile acid output by CNC needs further studies. A slight decrease of TEMPO-CNF and CNC on serum triglycerides, cholesterol, and bile acids, as well as a slight increase in goblet cell density, were seen although not significant, therefore a higher dose of nanocellulose may be recommended to investigate their

impacts on fat absorption. The results suggest three types of nanocellulose all showed benign effects on lipid metabolisms and small intestinal morphology.

4.6 Acknowledgment

This study was supported by the USDA National Institute of Food Agriculture [grant no. 2016-67021-24994/project accession no. 1009090].

4.7 References

Andersson, K. E., Axling, U., Xu, J., Swärd, K., Ahrné, S., Molin, G., . . . Hellstrand, P. (2013). Diverse effects of oats on cholesterol metabolism in C57BL/6 mice correlate with expression of hepatic bile acid-producing enzymes. *European Journal of Nutrition,* 52(7), 1755-1769.

Andrade, D. R. M., Mendonça, M. H., Helm, C. V., Magalhães, W. L. E., de Muniz, G. I. B., & Kestur, S. G. (2015). Assessment of Nano Cellulose from Peach Palm Residue as Potential Food Additive: Part II: Preliminary Studies. *Journal of Food Science and Technology,* 52(9), 5641-5650.

Boldarine, V. T., Pedroso, A. P., Brandão-Teles, C., LoTurco, E. G., Nascimento, C. M. O., Oyama, L. M., . . . Ribeiro, E. B. (2020). Ovariectomy modifies lipid metabolism of retroperitoneal white fat in rats: a proteomic approach. *American Journal of Physiology-Endocrinology and Metabolism,* 319(2), E427-E437.

Chen, Y., Lin, Y.-J., Nagy, T., Kong, F., & Guo, T. L. (2020). Subchronic exposure to cellulose nanofibrils induces nutritional risk by non-specifically reducing the intestinal absorption. *Carbohydrate Polymers,* 229, 115536.

Chen, Y., Nagy, T., & Guo, T. L. (2019). Glycated whey proteins protect NOD mice against type 1 diabetes by increasing anti-inflammatory responses and decreasing autoreactivity to self-antigens. *Journal of Functional Foods,* 56, 171-181.

Chun, W., Bamba, T., & Hosoda, S. (1989). Effect of Pectin, a Soluble Dietary Fiber, on Functional and Morphological Parameters of the Small Intestine in Rats. *Digestion,* 42(1), 22-29.

DeLoid, G., Cao, X., Molina, R. M., Silva, D. I., Bhattacharya, K., Ng, K. W., . . . Demokritou, P. (2019). Toxicological effects of ingested nanocellulose in in vitro intestinal epithelium and in vivo rat models. *Environmental Science: Nano*.

DeLoid, G. M., Sohal, I. S., Lorente, L. R., Molina, R. M., Pyrgiotakis, G., Stevanovic, A., . . . Bousfield, D. W. (2018). Reducing intestinal digestion and absorption of fat using a nature-derived biopolymer: Interference of triglyceride hydrolysis by nanocellulose. *ACS nano,* 12(7), 6469-6479.

DeLoid, G. M., Sohal, I. S., Lorente, L. R., Molina, R. M., Pyrgiotakis, G., Stevanovic, A., . . .

Demokritou, P. (2018). Reducing Intestinal Digestion and Absorption of Fat Using a Nature-Derived Biopolymer: Interference of Triglyceride Hydrolysis by Nanocellulose. *ACS nano,* 12(7), 6469-6479.

Ebihara, K., & Schneeman, B. O. (1989). Interaction of bile acids, phospholipids, cholesterol and triglyceride with dietary fibers in the small intestine of rats. *The Journal of Nutrition,* 119(8), 1100-1106.

Ellegård, L., & Andersson, H. (2007). Oat bran rapidly increases bile acid excretion and bile acid synthesis: an ileostomy study. *European Journal of Clinical Nutrition,* 61(8), 938-945.

Fuse, K., Bamba, T., & Hosoda, S. (1989). Effects of pectin on fatty acid and glucose absorption and on thickness of unstirred water layer in rat and human intestine. *Digestive Diseases and Sciences,* 34(7), 1109-1116.

Gómez H, C., Serpa, A., Velásquez-Cock, J., Gañán, P., Castro, C., Vélez, L., & Zuluaga, R. (2016). Vegetable nanocellulose in food science: A review. *Food Hydrocolloids,* 57, 178-186.

Hara, H., Haga, S., Aoyama, Y., & Kiriyama, S. (1999). Short-chain fatty acids suppress cholesterol synthesis in rat liver and intestine. *The Journal of Nutrition,* 129(5), 942-948.

Hino, S., Takemura, N., Sonoyama, K., Morita, A., Kawagishi, H., Aoe, S., & Morita, T. (2012). Small Intestinal Goblet Cell Proliferation Induced by Ingestion of Soluble and Insoluble Dietary Fiber Is Characterized by An Increase in Sialylated Mucins in Rats. *The Journal of Nutrition,* 142(8), 1429-1436.

Illman, R. J., & Topping, D. L. (1985). Effects of dietary oat bran on faecal steroid excretion, plasma volatile fatty acids and lipid synthesis in rats. *Nutrition Research,* 5(8), 839-846.

Jacobs, L. R. (1983). Effects of dietary fiber on mucosal growth and cell proliferation in the small intestine of the rat: a comparison of oat bran, pectin, and guar with total fiber deprivation. *The American Journal of Clinical Nutrition,* 37(6), 954-960.

Jin, L., Reynolds, L. P., Redmer, D. A., Caton, J. S., & Crenshaw, J. D. (1994). Effects of dietary fiber on intestinal growth, cell proliferation, and morphology in growing pigs2. *Journal of Animal Science,* 72(9), 2270-2278.

Kaser, A., Zeissig, S., & Blumberg, R. S. (2010). Inflammatory bowel disease. *Annual review of immunology,* 28, 573-621.

Korman, M. G., Hofmann, A. F., & Summerskill, W. H. J. (1974). Assessment of activity in chronic active liver disease: Serum bile acids compared with conventional tests and histology. *New England Journal of Medicine,* 290(25), 1399-1402.

Lia, A., Andersson, H., Mekki, N., Juhel, C., Senft, M., & Lairon, D. (1997). Postprandial lipemia in relation to sterol and fat excretion in ileostomy subjects given oat-bran and wheat test meals. *The American Journal of Clinical Nutrition,* 66(2), 357-365.

Lin, Y.-J., Shatkin, J. A., & Kong, F. (2019). Evaluating mucoadhesion properties of three types of nanocellulose in the gastrointestinal tract in vitro and ex vivo. *Carbohydrate Polymers,* 210, 157-166.

Liu, L., Kerr, W. L., & Kong, F. (2019). Characterization of lipid emulsions during in vitro digestion in the presence of three types of nanocellulose. *Journal of Colloid and Interface Science,* 545, 317-329.

Liu, L., Kerr, W. L., Kong, F., Dee, D. R., & Lin, M. (2018). Influence of nano-fibrillated cellulose (NFC) on starch digestion and glucose absorption. *Carbohydrate Polymers,* 196, 146-153.

Liu, L., & Kong, F. (2019a). In vitro investigation of the influence of nano-cellulose on starch and milk digestion and mineral adsorption. *International Journal of Biological Macromolecules,* 137, 1278-1285.

Liu, L., & Kong, F. (2019b). In vitro investigation of the influence of nano-fibrillated cellulose on lipid digestion and absorption. *International Journal of Biological Macromolecules,* 139, 361-366.

Liu, L., & Kong, F. (2019c). Influence of nanocellulose on in vitro digestion of whey protein isolate. *Carbohydrate Polymers,* 210, 399-411.

Lu, H., Gui, Y., Guo, T., Wang, Q., & Liu, X. (2015). Effect of the particle size of cellulose from sweet potato residues on lipid metabolism and cecal conditions in ovariectomized rats. *Food & Function,* 6(4), 1185-1193.

Luo, L., Aubrecht, J., Li, D., Warner, R. L., Johnson, K. J., Kenny, J., & Colangelo, J. L. (2018). Assessment of serum bile acid profiles as biomarkers of liver injury and liver disease in humans. *PLoS One,* 13(3), e0193824-e0193824.

Lutsey, P. L., Steffen, L. M., & Stevens, J. (2008). Dietary intake and the development of the metabolic syndrome: the Atherosclerosis Risk in Communities study. *Circulation,* 117(6), 754-761.

Ma, H., Burger, C., Hsiao, B. S., & Chu, B. (2011). Ultrafine polysaccharide nanofibrous membranes for water purification. *Biomacromolecules,* 12(4), 970-976.

Marchetti, L., Muzzio, B., Cerrutti, P., Andrés, S. C., & Califano, A. N. (2017). Bacterial nanocellulose as novel additive in low-lipid low-sodium meat sausages. Effect on quality and stability. *Food Structure,* 14, 52-59.

Martinez-Augustin, O., & Sanchez de Medina, F. (2008). Intestinal bile acid physiology and pathophysiology. *World journal of gastroenterology,* 14(37), 5630-5640.

Moon, R. J., Martini, A., Nairn, J., Simonsen, J., & Youngblood, J. (2011). Cellulose nanomaterials review: structure, properties and nanocomposites. *Chemical Society Reviews,* 40(7), 3941-3994.

Moriceau, S., Besson, C., Levrat, M.-A., Moundras, C., Rémésy, C., Morand, C., & Demigné, C. (2000). Cholesterol-lowering effects of guar gum: Changes in bile acid pools and intestinal reabsorption. *Lipids,* 35(4), 437-444.

Ong, K. J., Ede, J. D., Pomeroy-Carter, C. A., Sayes, C. M., Mulenos, M. R., & Shatkin, J. A. (2020). A 90-day dietary study with fibrillated cellulose in Sprague-Dawley rats. *Toxicology Reports,* 7, 174-182.

Parnell, J. A., Raman, M., Rioux, K. P., & Reimer, R. A. (2012). The potential role of prebiotic fibre for treatment and management of non-alcoholic fatty liver disease and associated obesity and insulin resistance. *Liver International,* 32(5), 701-711.

Puchtler, H., Waldrop, F. S., Conner, H., & Terry, M. S. (1968). Carnoy fixation: practical and theoretical considerations. *Histochemie,* 16(4), 361-371.

Qing, Y., Sabo, R., Zhu, J. Y., Agarwal, U., Cai, Z., & Wu, Y. (2013). A comparative study of cellulose nanofibrils disintegrated via multiple processing approaches. *Carbohydrate Polymers,* 97(1), 226-234.

Rahman, K., Desai, C., Iyer, S. S., Thorn, N. E., Kumar, P., Liu, Y., . . . Anania, F. A. (2016). Loss of Junctional Adhesion Molecule A Promotes Severe Steatohepatitis in Mice on a Diet High in Saturated Fat, Fructose, and Cholesterol. *Gastroenterology,* 151(4), 733-746.e712.

Reiner, R. S., & Rudie, A. W. (2013). *Process Scale-Up of Cellulose Nanocrystal Production to 25 kg per Batch at the Forest Products Laboratory*. In M. T. Postek, R. J. Moon & A. W. Rudie (Eds.), *Production and applications of Cellulose nanomaterials, TAPPI Press* (pp. 21-24): TAPPI

Rudel, L. L., & Morris, M. (1973). Determination of cholesterol using o-phthalaldehyde. *Journal of Lipid Research,* 14(3), 364-366.

Saito, T., Hirota, M., Tamura, N., Kimura, S., Fukuzumi, H., Heux, L., & Isogai, A. (2009). Individualization of nano-sized plant cellulose fibrils by direct surface carboxylation using TEMPO catalyst under neutral conditions. *Biomacromolecules,* 10(7), 1992-1996.

Shah, B., Momcilovic, B., & McLaughlan, J. (1980). Increased retention of lead in young rats fed suboptimal protein and minerals. *Nutrition Reports International (USA)*.

Sigleo, S., Jackson, M. J., & Vahouny, G. V. (1984). Effects of dietary fiber constituents on intestinal morphology and nutrient transport. *American Journal of Physiology-Gastrointestinal and Liver Physiology,* 246(1), G34-G39.

Smithson, K. W., Millar, D. B., Jacobs, L. R., & Gray, G. M. (1981). Intestinal diffusion barrier: unstirred water layer or membrane surface mucous coat? *Science,* 214(4526), 1241-1244.

Soh, J., Iqbal, J., Queiroz, J., Fernandez-Hernando, C., & Hussain, M. M. (2013). MicroRNA-30c reduces hyperlipidemia and atherosclerosis in mice by decreasing lipid synthesis and lipoprotein secretion. *Nature Medicine,* 19(7), 892-900.

Sun, L., Chen, W., Liu, Y., Li, J., & Yu, H. (2015). Soy protein isolate/cellulose nanofiber complex gels as fat substitutes: rheological and textural properties and extent of cream imitation. *Cellulose,* 22(4), 2619-2627.

Uetani, K., & Yano, H. (2011). Nanofibrillation of wood pulp using a high-speed blender. *Biomacromolecules,* 12(2), 348-353.

Velásquez-Cock, J., Serpa, A., Vélez, L., Gañán, P., Hoyos, C. G., Castro, C., . . . Zuluaga, R. (2019). Influence of cellulose nanofibrils on the structural elements of ice cream. *Food Hydrocolloids,* 87, 204-213.

Wang, Y., Wang, W., Jia, H., Gao, G., Wang, X., Zhang, X., & Wang, Y. (2018). Using cellulose nanofibers and its palm oil pickering emulsion as fat substitutes in emulsified sausage. *Journal of Food Science,* 83(6), 1740-1747.

Zhang, N., Huang, C., & Ou, S. (2011). In vitro binding capacities of three dietary fibers and their mixture for four toxic elements, cholesterol, and bile acid. *Journal of Hazardous Materials,* 186(1), 236-239.

CHAPTER 5.

INFLUENCE OF CELLULOSE NANOCRYSTALS (CNC) ON PERMEATION THROUGH AN INTESTINAL MONOLAYER AND AN MUCUS MODEL *IN VITRO* [5]

[5] Lin, Y.-J., Paton C. M., Fox, D. M, Kong F., Influence of cellulose nanocrystals (CNC) on permeation through an intestinal monolayer and an mucus model *in vitro*. Submitted to *Carbohydrate Polymers*, 8/20/2020

Abstract

Cellulose nanocrystals (CNC) as a novel ingredient in foods and pharmaceuticals still lack the safety and functionality information. We aimed to assess the absorption of CNC in the small intestine and the effect on cell viability. In the second part, the impact of CNC on substance permeation through the mucus layer, including the potential functionality in improving lipid metabolism, was tested. No noticeable amount of CNC was found to penetrate through differentiated Caco-2 monolayer and *ex vivo* mucus layer, and CNC had low toxicity on Caco-2 cell viability up to 10 mg/mL. CNC at 2% (w/w) may affect the permeability of the mucus layer and larger molecules are more easily influenced. CNC may also alleviate hypercholesteremia by increasing viscosity of digesta, adsorbing of cholesterol, and decreasing bile acids permeation. The results suggest CNC may not penetrate the small intestinal lining and may be used as a functional supplement.

Keywords: Nanocellulose; cellulose nanocrystals; permeability; *in vitro* mucus model; bile acids; cholesterol

5.1 Introduction

Nanocellulose (NC) as one type of nanomaterials has drawn attention to the food and pharmaceutical industry for years in applications such as emulsifiers, coating, and encapsulation agents, thickeners, and packaging materials (Azeredo, Rosa, & Mattoso, 2017; Gómez H et al., 2016; Plackett, Letchford, Jackson, & Burt, 2014). Currently, the U.S. Food and Drug Administration has not yet officially legalized NC as food additives due to limited understanding of its behavior in the human GI tract and the safety risks. And more investigation on the health impacts of NC upon entering the body is still needed. There are three major types of nanocellulose: Cellulose nanofibrils (CNF), cellulose nanocrystals (CNC), and bacterial cellulose (BC). Generally, nanocellulose is defined as polysaccharides composed of repetitive D-anhydroglucopyranose units connected by β-(1→4)-glycosidic bonds, forming fibrous and linear structures with a diameter lower than 100 nm (Xia et al., 2003). Three different categories of nanocellulose vary in size, viscosity, gelling properties, physical and chemical properties, and the characterization can be referred to in a recent in-depth review article (Foster et al., 2018). In this study, we focus primarily on CNC based on the consideration that the size is the smallest among different types of nanocellulose.

CNC can also be referred to as whiskers, needles, or nanocrystalline cellulose (NCC). It can be obtained from acid hydrolysis of the starting materials, for example, wood pulp, cotton linters, and microcrystalline cellulose (Habibi, Lucia, & Rojas, 2010). The acid hydrolysis cleaves the disordered region of the fibrils, leaving the amorphous region of cellulose in a rod-like shape. The most common acid used for producing CNC at the industrial level is sulfuric acid, which also partially substitute the C6 with sulfate half ester surface groups (Foster et al., 2018). Several *in*

vitro researches have been done to investigate the toxicity of CNC on different cell models and found low or no toxicity at low concentration, and significant cytotoxicity was only seen at above 1000 μg/mL (Foster et al., 2018; Hanif, Ahmed, Shin, Kim, & Um, 2014; Xiao et al., 2019). Studies have also been done to investigate the cellular uptake of CNC and found that CNC could be an uptake *in vitro* by both non-phagocytic cells and macrophage, although many considered the internalization was in a limited amount (Hosseinidoust, Alam, Sim, Tufenkji, & van de Ven, 2015; Mahmoud et al., 2010; Menas et al., 2017; Roman, Dong, Hirani, & Lee, 2009; Samulin Erdem et al., 2019). However, there are still lack of studies in investigating the translocation of CNC across the mucosal layer, which is directly related to the retention of nanoparticles in the body.

For most particles to be absorbed in the small intestine after oral administration, it can be roughly divided into three major steps in translocation across the small intestinal mucosal barrier into the systemic circulation. The first is diffusion through mucus to contact the enterocyte surface, the second is cellular trafficking of the epithelial layer, and the third is exocytosis into systemic dissemination (Hussain, Jaitley, & Florence, 2001). In other words, particles must navigate through both the mucus gel layer and the epithelial cell layer to successfully enter the body. The mucus layer is a layer of viscous gel secreted by Goblet cells that covers along the lumen throughout the intestine. It serves as the first-line barrier in the lumen for the defensive purpose and is closely related to one's health status (Dharmani, Srivastava, Kissoon-Singh, & Chadee, 2009; Liévin-Le Moal & Servin, 2006). Nutrients, similarly, will need to diffuse through this layer to contact the epithelium to be absorbed. It was reported that porcine mucus has a net-like structure and the pore size was estimated to be 211 ± 7 nm (Bajka, Rigby, Cross, Macierzanka, & Mackie, 2015). Hence it is suspected that CNC, typically with a size range from 3 to 5 nm in diameter and 50 to 500 nm in length (Moon, Martini, Nairn, & Simonsen, 2011), could presumably permeate through the

mucus gel layer and reach the epithelial cell layer. In the current study, both the permeation of CNC across the mucus gel layer and the epithelial layer were tested. An *in vitro* mucus gel layer model was built to study the permeation of CNC across small intestinal mucus gel layer. Further, the effect of CNC on cell viability was evaluated and the permeation of CNC through *in vitro* Caco-2 cell monolayer model was examined with fluorescently-labeled CNC.

Another aspect that nanocellulose may affect health is that nanocellulose may hinder the diffusion of substances or bind with minerals as previously shown in our lab (Liu, Kerr, Kong, Dee, & Lin, 2018; Liu & Kong, 2019a, 2019c). While the use of dialysis tubing provides a stable and homogenous environment for testing diffusivity, we have also shown that nanocellulose has the potential to increase the viscosity of mucus gel (Lin, Shatkin, & Kong, 2019), which may not be shown using the aforementioned method. The impacts of a mucoadhesive material on the mucus gel layer, the first layer of intestinal defensive lining, however, should not be excluded in the model. Phenol red and fluorescein isothiocyanate–dextran 4kDa were chosen as markers to study how nanocellulose might decrease the permeation across the *ex vivo* mucus gel layer model. Moreover, dietary fibers are known to have functional properties to alleviate hyperlipidemia and hypercholesteremia by decreasing bile acids and cholesterol reabsorption (Kaczmarczyk, Miller, & Freund, 2012). Such an effect of CNC, however, has not yet been evaluated. Hence, the impact of CNC on the permeation of cholesterol and bile acids across the mucus gel layer was also investigated.

In the current study, we hypothesize nanocellulose can translocate across the mucosal layer including small intestine epithelium lining and mucus gel layer and may affect the permeation of substances. The first section of this paper will examine whether CNC penetrates *in vitro* the Caco-2 monolayer and a novel *in vitro* mucus gel layer model, as well as the impact of CNC on cell

viability with the Caco-2 cell model. Secondly, the effect of CNC on mucus permeability was evaluated. The potential of CNC to improve hypercholesteremia and the possible mechanisms were also investigated.

5.2 Material and methods

5.2.1 Materials

CNC was purchased from The Process Development Center at the University of Maine. The specification of CNC was 12.1 wt% in water in sodium form that contained 0.94 wt% sulfur and in 5-20nm length and 150-200 nm width. The estimated relative size of CNC was 98.9 ± 2.5 nm assuming a sphere shape (1% CNC in 1mM KCl using dynamic light scattering). Characterization of CNC from this source has been described by Reiner and Rudie (2013). Cellulose was used as a reference and purchased from Sigma Aldrich (product catalog #C6288) (St. Louis, MO). The RAMAN FT-IR spectrum showed two major peaks between 100-1500 and 2800-3000 wavenumbers, according to the manufacturer's specification. The size was determined in our lab as 63.82 ± 43.34 μm using LS13 320 Laser Particle Size Analyzer (Beckman Coulter Life Sciences, Indianapolis, IN) assuming a sphere shape which was deemed appropriate for comparison purpose (Foster et al., 2018).

Dulbecco's Modified Eagle Medium (DMEM, high glucose, pyruvate, no glutamine), L-glutamine (200mM), MEM (Minimum Essential Medium) Non-Essential Amino Acids Solution (NEAA, 100X), and 2.5% trypsin were purchased from Thermo Fisher Scientific (Waltham, MA). 3-(4,5-dimethylthiazol-2-yl)-2,5-diphenyl tetrazolium bromide (MTT) was purchased from Research Products International (Mt. Prospect, IL). Texas Red™ C2-Dichlorotriazine (TR) was

purchased from ThermoFisher Scientific (Waltham, MA). Other chemicals were purchased from Sigma Aldrich (St. Louis, MO).

The labeling of Texas Red-CNC was described in previous literature (Lin et al., 2019) and is additionally credited to Dr. Douglas M. Fox from American University. Briefly, CNC was mixed with 2 mM of NaOH for 1 hour. TR was added (1 mg TR/g of CNC) and the mixture was stirred for 24 hours at room temperature in the dark. Then, the mixture was put in an 8 kDa cut-off dialysis tubing (Spectra/Por 7, Spectrum Laboratories, Inc., Waltham, MA) and washed towards DI water until no fluorescence was detected in the water (excitation 584 nm/emission 620 nm) (FLUOstar Omega fluorescence microplate reader, BMG Labtech Inc., Cary, NC). The final TR-CNC concentration was 3.7% by gravimetric analysis.

5.2.2 Preparation of mucus

Porcine intestinal mucus from two pigs was collected as suggested in the literature with minor modifications (Pereira de Sousa et al., 2015). Porcine duodenum and the first 1 meter of jejunum were taken immediately after slaughter and kept on ice and were processed within one hour. The small intestine sections were first washed with ice-cold 0.1M sodium chloride to remove large debris. Mucus was then scraped off from the tissue with a spatula. The mucus was then mixed with 5 times volume of 0.1M sodium chloride, stirred for 1 hour, and centrifuged at 10,500 xg for 2 hours. All of the above handlings were done in a 4°C cold room and the centrifuge was set at 4°C. The supernatant liquid and large debris at the bottom were discarded and the mucus was collected. Mucus from two pigs was collected separately and eventually pooled together and made

into aliquots and stored at -20°C. The characterization of the collected mucus was shown in Figure S5.7.

5.2.3 *In vitro* mucus layer model

The mucus model was inspired by Franz diffusion cells but with a simplified setting with equipment available in most laboratories (Figure 5.1(a) and (b)). The model was composed of a 3 mL BD plastic syringe (diameter 8.66 mm), with an insert of grade GF/A filter (pore size 1.6 μm) cut by a hole punch (diameter 7.14 mm), a glass tube (inner diameter 14 mm and 10 cm in length) and a mini stir bar (length 12 mm) to mix the sample in the basal compartment at the end of the experiment. GF/A filter was chosen considering its pore size is larger than the reported pore size of mucus gel (211 ± 7 nm) (Bajka et al., 2015) so it could be a supportive base without affecting permeation.

First, pig mucus was defrosted and loaded (35 μL) on both sides of the GF/A filter paper to allow adhesion for 15 min. The system was then set up and 4.2 mL of receptor solution was loaded to the barrel and let flow into the test tube to ensure no bubbles remain in the syringe tip. Then the mucus-loaded filter paper was carefully picked up with a spatula and slowly pushed onto the bottom of the 3 mL syringe barrel with a rod, e.g. a plunger from a 1 mL syringe. The mucus-coated filter paper must be ensured to lay flat in the center of the barrel, completely covering the tip opening. The test solution (1.5 mL) was then loaded on top of the coated filter paper. The water static pressure would then start the permeation.

Simulated intestinal fluid (SIF) (Minekus et al., 2014) with or without bile (SIFB or SIF, respectively) was used depending on if bile salts would interfere with the reading of tested markers.

(a) (b)

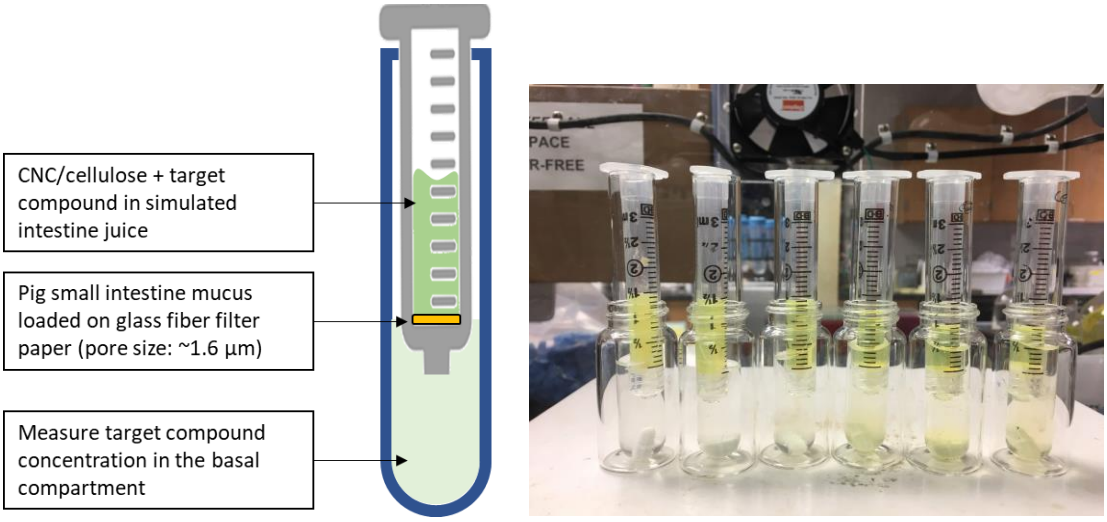

Figure 5.1. (a) Schematics of the mucus diffusion model (b) Set-up picture of the model

5.2.4 Permeation of TR-CNC through the mucus layer

Using the above *ex vivo* mucus model, 5 and 10 mg/mL TR-CNC in SIF was loaded on the apical side followed by 2 hours of incubation to allow permeation. Samples from the basal were collected and analyzed by a fluorescence spectrophotometer. A negative control group without TR-CNC was conducted in parallel as the background result and was used to calculate the detection limit by the fluorescent intensity of mean background plus 3.3 times of standard deviation of the background. The cofactor (3.3) was chosen according to the U.S. Food and Drug Administration (FDA) guideline (ICH, 1996).

5.2.5 Caco-2 cell culture

The human colon carcinoma Caco-2 cell line was obtained from ATCC (Manassas, VA, USA). Cells were grown in DMEM supplemented with 4 mM glutamine, 100 U/mL penicillin, 100 U/mL streptomycin, 1% non-essential amino acids (NEEA), and 10% heat-inactivated fetal bovine serum (Natoli, Leoni, D'Agnano, Zucco, & Felsani, 2012). Cells were maintained at 37°C in 95% air and 5% CO_2 incubator. The culture medium was changed every two days. Plates reaching 80% confluency were subcultured by trypsinization with 0.25% trypsin, 10 mM EDTA in 1X PBS and passaged in a 1:4 ratio.

5.2.6 Permeation of CNC through Caco-2 monolayer

Caco-2 cell monolayer was grown on a 24-well Transwell plate with transparent PET membranes with a pore diameter of 1 μm (Greiner Bio-one, Monroe, NC) by seeding $8.74x10^4$ cells per well ($2.6x10^5$ cells cm^{-2}) and changing culture medium every two days for 21 days to allow monolayer differentiation (Hubatsch, Ragnarsson, & Artursson, 2007). For the pore size of the transwells, 1 μm was selected to prevent cells from passing while allowing the largest pore size for the passage of nanoparticles according to the manufacturer's information. On day 22, 500 μM phenol red in HBSS with 25mM HEPES was loaded on the apical side for 2 hours in a 37°C, 150 rpm shaking incubator to detect any leakage of the monolayer (García-Casal, Leets, & Layrisse, 2000). Two hundred μL of aliquot was taken from the basal side and mixed with 10 μL of 0.1N NaOH to enhance the color intensity by alkalization (Garrick, Mulvihill, Buack, Maeda-Hagiwara, & Tache, 1988). The concentration of phenol red was read at 560 nm and calculated with a standard curve.

Fluorescently labeled CNC (TR-CNC) in 0.5%(w/w) was tested for permeation through the differentiated Caco-2 cell monolayer. TR-CNC was diluted in HBSS and loaded on the apical side of the transwells and allowed to permeate for 2 hours. Fluorescence intensity from the basal side was measured with an Agilent Cary Eclipse Fluorescence Spectrophotometer (Santa Clara, CA). The detection limit of TR-CNC was based on the 3.3 times of standard deviation of the blank according to the U.S. Food and Drug Administration (U.S. FDA) guidelines (ICH, 1996). The detection limit was 0.419 a.u. with HBSS as the blank. The results of the validation assay using known concentrations of TR-CNC in HBSS is shown in the supplementary material.

5.2.7 Cell viability

The effect of CNC on cell viability was tested with 3-[4, 5-dimethylthiazol-2-yl]-2, 5 diphenyl tetrazolium bromide (MTT) assay (Gerlier & Thomasset, 1986; van de Loosdrecht, Beelen, Ossenkoppele, Broekhoven, & Langenhuijsen, 1994). Cells were trypsinized and $5*10^4$ cells/well were seeded in 96 well plates (Corning, Corning, NY) and let grow for two days. Wells without cells were run in parallel as background to assess the interference of CNC to the assay. CNC was made into exact concentration with complete medium. Cell medium was discarded by suctioning and 200 µL of CNC in cell medium was gently pipetted into the wells and incubated for 24 hours. Afterward, each well was gently washed with PBS twice. Cells were then incubated with 110 µL of complete medium containing 0.5 mg/mL of MTT for 3 hours at 37°C and then emptied. Two hundred µL of DMSO was added into each well to dissolve formazan crystals. Absorbance was taken at 570 nm. Cell viability was calculated as:

$$Cell\ viability\ (\%) = \frac{A - A_0}{A_c - A_0} \times 100\% \quad (1)$$

Where A is the absorbance of sample wells treated with NC, A_0 is the absorbance of blank wells containing medium only, and A_c is the untreated control cells.

5.2.8 Mucus permeability affected by CNC

The effect on mucus permeability with CNC in the digesta was tested by two markers with different molecular sizes. Phenol red (Molecular weight=354.38) and fluorescein isothiocyanate–dextran 4kDa (FD4, molecular weight=~4000) were used as markers as small and large molecules, respectively. Either 1.5 mL of 2 mM Phenol red in SIFB or 1.5 mL of 250 μM FD4 in SIF mixed with various CNC concentration was put in the apical side and allowed for permeation for 1 hour. Phenol red and FD4 concentration in the bottom side was measured with spectrophotometer and fluorescence spectrophotometer, respectively.

5.2.9 *In vitro* permeation of cholesterol affected by CNC after *in vitro* digestion

Egg yolk was used as a sample food to investigate the effect of CNC on cholesterol diffusion across the mucus gel layer after *in vitro* digestion. The *in vitro* digestion process as well as the preparation of simulated salivary juice (SSF) and simulated gastric fluid (SGF) were conducted following the literature with minor modifications (Minekus et al., 2014). In brief, 0.5 gram of egg yolk was whipped and mixed with 0.5 gram of 4%, 1%, 0.25%, 0.0625% of CNC or 4% cellulose to achieve 2%, 0.5%, 0.125%, 0.031% concentration of CNC in the sample food. The samples were then mixed with 1 mL of SSF (1:1). The mixture was vortexed to ensure full mixing and incubated at 37°C in a shaking water bath (100 rpm) for 5 min as the salivary phase. Then 2 mL of SGF was added into the mixture and vortexed, followed by a 2-hour incubation in 37°C

shaking water bath. Four mL of SIFB was then added and vortexed with the digesta, and 1.5 mL of aliquot was immediately transferred into the mucus diffusion *ex vivo* model to allow diffusion for 2 hours. At the end of the trials, samples were taken from the test tube for analysis of the concentration of cholesterol. The digesta samples in the syringe were collected and subjected to rheological analysis.

O-phthalaldehyde (OPA) method was used to quantify cholesterol in the samples according to the literature (Liu & Kong, 2019b; Rudel & Morris, 1973) with minor modifications. Samples were centrifuged (3000 xg, 10 min) and 500 μL of the supernatant was vigorously mixed with 200 μL of 50% (w/v) potassium hydroxide and 300 μL of 95% ethanol followed by heating in an 85°C heating block for 15 min. When the samples were cooled, 500 μL of n-hexane was forcefully added into the tube and well mixed, and then 300 μL of deionized water was added and the tube was vortexed for at least 1 min. The mixtures were then set still for 5 min to allow phase separation and 600 μL of the upper hexane layer aliquots were then taken to new tubes and allowed to dry under vacuum. Four hundred μL of 0.5 mg/mL OPA in glacial acetic acid was later added to each tube and vortexed. After 10 min, 200 μL of concentrated sulfuric acid was carefully added into the samples and mixed well by vortexing. Samples were allowed to react for 10 min (and not exceed 90 min) and then measured absorbance at 550 nm. A standard curve of samples was prepared in parallel.

5.2.10 Cholesterol binding capacity

The capacity of CNC to adsorb cholesterol was tested without the interference of digestive juice or enzymes. The assay was modified from Zhang, Huang, and Ou (2011). First, egg yolk was

mixed with 9 times the volume of DI water to achieve 10 times dilution. And then 25 mL of the egg yolk solution was mixed with 1g cellulose or 1g, 0.25g, 0.125g, 0.031g (dry basis) of CNC from 12.1%(w/w) CNC stock. The solution was vortex and shaken at 37°C for 2 hours. Aliquots were taken to centrifuge at 4000 xg for 20 min followed by the analysis of the cholesterol concentration in the supernatant. Data were shown as the remaining cholesterol in the yolk solution. Cholesterol adsorption percentage was calculated as the following:

$$\text{Cholesterol adsorption percentage} = (C_{yolk} - C_{fiber})/C_{yolk} \times 100\% \quad (2)$$

and adsorption capacity was calculated as:

$$\text{adsorption capacity} = (C_{yolk} - C_{fiber}) \times V/w \quad (3)$$

where C_{yolk} is the cholesterol concentration remaining in the supernatant of the yolk mixture without fibers (control) and C_{fiber} is the cholesterol concentration remaining in the supernatant of yolk mixture with CNC or cellulose. V is the solution volume and w is the dry weight of the fiber.

5.2.11 Rheological analysis

Samples in the apical compartment after permeation were collected right after the experiment and analyzed for the viscosity using a TA instrument HR-2 Discovery Hybrid Rheometer with a parallel plate geometry (diameter 20 mm). The temperature was set at 37°C and a shear rate of 0.1 to 100 1/s.

5.2.12 Bile acids (BA) permeation affected by CNC through *in vitro* mucus model

Bile salts solution (8% w/w) was mixed with SIF, incubated at 37°C for 30 min, and vortex frequently until dissolved. Then the bile salt solution was mixed 1:1 to 2X concentrated CNC solution prepared in SIF to achieve the final concentration of 2%, 0.5%, 0.125%, 0.0313% (w/w) of CNC or 0% as control. Using the *ex vivo* mucus model, 1.5 mL of the CNC-BA-SIF solution was loaded in the apical side of the syringe on top of the mucus-coated filter and let permeate for 1 hour. Total bile acid content of aliquots from the basal side was analyzed by Diazyme Colorimetric Total Bile Acids Assay Kit (NBT Method, Diazyme Laboratories, Poway, CA).

5.2.13 Statistical analysis

Analysis of variance (ANOVA) followed by Tukey HSD test was used to test for significant differences using JMP Pro 13.0.0 (SAS Institute Inc., Cary, NC). At least three replications were conducted for each experiment.

5.3 Results and discussion

5.3.1 Permeation of CNC through *in vitro* mucus layer

The pore size of the mucus gel layer was reported to be 20 to 200 nm (Round et al., 2012). CNC has a size of 5-20 nm in width and 150-200 nm in length, which makes it susceptible to diffusing across the mucus gel layer. Here, the permeation of 5 and 10 mg/mL of TR-CNC across the mucus gel layer was examined with a novel *ex vivo* mucus layer model and allowed to permeate for two hours (Figure 5.2(a)). Both concentrations of TR-CNC were under the detection limit compared to the background and therefore there was no evidence that CNC would penetrate the mucus gel layer. This result suggests that the major effect of CNC on digestion would remain in

the lumen because no significant amount of CNC was found to permeate across the porcine mucus layer. Mucus as the first major defensive lining of the intestinal tract might be effective in blocking CNC from further touching the intestinal cell lining. In our previous study, CNC was found to have synergism in increasing viscosity of mucin solution and had a high affinity to mucin particles (Lin et al., 2019). It is possible that given the small size of CNC, the attachment to mucus was high so CNC sticks to the mucus layer and prevents the transport of CNC. Our result suggests a similar conclusion to a previous study using an *ex vivo* rodent model (Mackie et al., 2019) that CNC might be stuck in the mucus layer.

5.3.2 Permeation of CNC through Caco-2 monolayer

Fluorescently labeled CNC (TR-CNC) was also used to test if CNC could permeate Caco-2 differentiated monolayer. The detected fluorescence intensity was lower than the qualification limit, therefore there was no evidence that CNC would permeate the Caco-2 monolayer (Figure 5.2(b), and a more detailed result can be found in Figure S5.8). Our results indicate there was no detectable CNC penetrating the Caco-2 monolayer. A note of caution is due here since the Caco-2 monolayer model is considered to be less permeable than *in vivo* due to higher tight junction expression (Le Ferrec et al., 2001; Sun, Chow, Liu, Du, & Pang, 2008). Despite the limitation of the Caco-2 single-cell *in vitro* model, it can be concluded that there is no evidence to support that CNC may cross the enterocyte lining. DeLoid et al. (2019) also tested CNC with an average diameter of 25 nm (CNC-25) and found the transepithelial electrical resistance (TEER) of CNC-25 group was not different from the control group after 24 hrs of incubation in a triculture cell model (Caco-2, HT29-MTX, and Raji B cells). Based on our studies that CNC was not found to

penetrate both the mucus gel layer and enterocyte lining, it may be less likely that CNC would enter the metabolic circulation in the body through the intestinal route.

(a) (b)

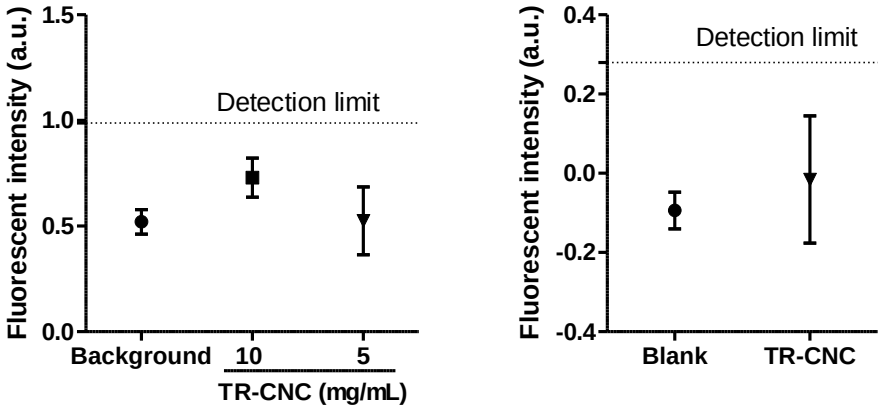

Figure 5.2. (a) Qualitative result of TR-CNC in the basal side of the intestinal *ex vivo* mucus layer model after 2 hours of incubation when 5 and 10 mg/mL of CNC was loaded in the upper compartment of *ex vivo* mucus layer model. The gridline shows the detection limit based on the standard deviation of the background (SIF) and. Mean fluorescent intensity ± SD (n=4) (b) Qualitative result of TR-CNC in the basal compartment of Caco-2 monolayer after 2 hours of incubation with 5 mg/mL of TR-CNC in the apical compartment. Gridline shows the detection limit based on the standard deviation of the blank (HBSS). Mean fluorescent intensity ± SD (n=3)

5.3.3 Cell viability (MTT assay)

CNC was also tested to investigate whether it could affect the enterocyte viability. When Caco-2 cells were treated with CNC for 24 hours, no significant difference in the viability was

detected with up to 10 mg/mL of CNC by MTT assay (Figure 5.3) and the background value was obtained in parallel without cells to ensure there was no interference from nanoparticles (data not shown). CNC has been tested for cytotoxicity with several human cell lines, with most studies concluded that CNC has no cytotoxicity, while some studies have seen dose-dependent cytotoxicity (Roman, 2015). CNC-25 with small intestinal digesta was tested with an *in vitro* triculture model (Caco-2, HT29-MTX, and Raji B cells) by DeLoid et al. (2019) for cytotoxicity and reactive oxygen species (ROS) production, and results showed CNC-25 at 0.75% (w/w) showed no significant increase while increased toxicity was seen at 1.5% (w/w) CNC-25. Our results also showed that up to 1% (=10 mg/mL) of CNC, there was no observable on cell viability. A recent study of CNC made from wheat bran, also using the Caco-2 model and MTT assay, showed increased cytotoxicity for CNC at 5 mg/mL (Xiao et al., 2019). The source of raw material may cause discrepancy although the CNF results suggest this possibility is low (Pradhan et al., 2020). It could also be due to the lack of a washing step before adding MTT reagent and the potential interference of nanoparticles (Rocha et al., 2017). Despite the different results in CNC toxicity among studies, our result and previous literature suggest that CNC has a relatively low impact on intestinal cell viability *in vitro*.

On the other hand, it is acknowledged that even though CNC was found not to permeate the *ex vivo* mucus gel or *in vitro* Caco-2 monolayer, it could still be affecting the permeation of other nutrients. To examine this possibility, the effect of CNC on mucus permeability was tested.

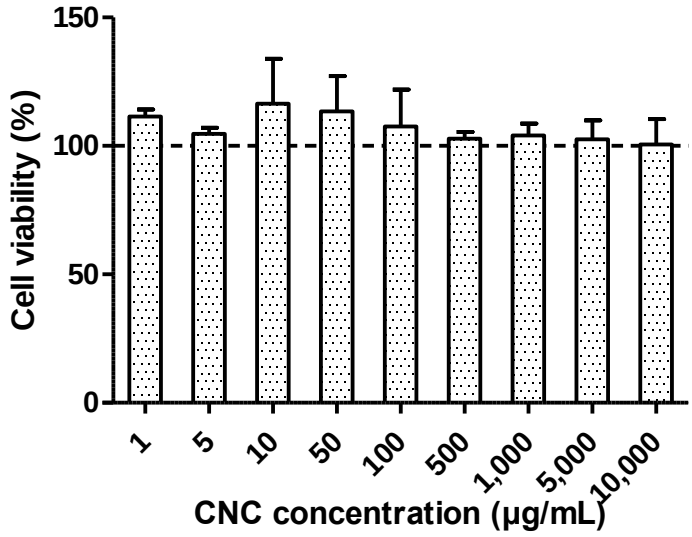

Figure 5.3. Caco-2 cell viability after 24 hours of incubation with CNC by MTT assay. Mean cell viability ± SD (n=3). No statistical significance was detected by ANOVA (α=0.05).

5.3.4 Mucus permeability affected by CNC

To assess whether and how CNC affect the permeation of molecules across the small intestinal mucus layer, two compounds, phenol red (molecules weight = 354.38) and FD4 (average molecular weight = 4,000), were used to represent small and large hydrophilic molecules were mixed with various concentration of CNC and were loaded in the top compartment in the *in vitro* mucus layer model. Results (Figure 5.4) showed CNC affected mucus layer permeability in a concentration-dependent manner for both small molecules (phenol red) and large molecules (FD4). For phenol red, only 2% of CNC(w/w) showed a significant decrease of phenol red across the *in vitro* mucus layer compared to the control group (0% CNC) while 2%, 0.5%, and 0.125% of CNC significantly decreased the permeation of FD4. On the contrary, 2% cellulose did not decrease the permeation of phenol red or FD4 compared to the control group. This result suggests that high

CNC content in the lumen may raise the concern of the absorption problem. The reason could be due to the increase in viscosity above 2% CNC in the digesta as seen by Liu and Kong (2019a) and could also be CNC blocking the mucus pore due to its mucoadhesive properties (Lin et al., 2019). The larger effect seen with FD4 may be due to its larger size or may be due to its similar structure to cellulose, with strong intermolecular forces between glucose units.

(a) (b)

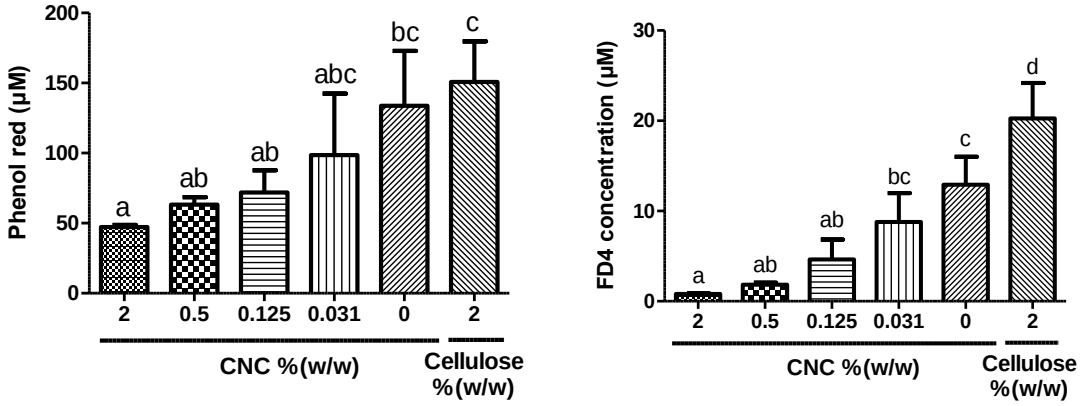

Figure 5.4. CNC decreased the permeation of (a) phenol red and (b) FD4 across the *in vitro* small intestinal mucus gel layer. Mean phenol red or FD4 concentration ± SD (n=3). Different letters denote statistical significance by ANOVA followed by Tukey's test (α=0.05).

5.3.5 Cholesterol permeation through mucus layer affected by CNC

The egg yolk was used as a model food for cholesterol to test the effect of CNC on cholesterol permeation in *in vitro* digestion. Four different concentration of CNC, 0.031% to 2%, was mixed with egg yolk and run through *in vitro* digestion process with digestive enzymes. At the end of digestion, all samples were diluted to one-eighth of its original concentration. For

example, 2% CNC was diluted with 7 portions of digestive juice (including salivary juice, gastric juice, and intestinal juice), which made the CNC final concentration to 0.25% CNC in the intestinal phase. It was found that 2% of CNC when mixing with egg yolk before digestion significantly decreased cholesterol permeation (Figure 5.5 (a)) despite no noticeable change in the intestinal phase viscosity compared to other groups (Figure 5.5 (b)). Lower concentrations of CNC did not significantly affect cholesterol permeation, while a dose-dependent effect was seen.

CNC as a mucoadhesive material may react with mucus and decreases the permeability of the mucus gel layer as seen previously in the FD4 assay. Especially as cholesterol in yolk exists as larger emulsion particles, the effect of decreased permeability could be particularly evident. Another possible mechanism could be that CNC adsorbs cholesterol and prevent permeation through the mucus layer, therefore the cholesterol adsorption ability of CNC was further tested.

CNC was mixed with diluted egg yolk to investigate its ability in cholesterol adsorption (Figure 5.5 (c)). CNC in a relatively low amount (0.0156 g) showed a similar effect compared to cellulose at 1 g. To analyze the adsorption capacity, only the group of 0.0156 g of CNC was calculated (Table 5.1) because the amount of cholesterol in the system was higher than the capacity, and those higher concentrations of CNC groups had the adsorption percentage nearly 100%. The results indicated per gram of CNC absorbed 122.5 ± 39.1 mg of cholesterol, making CNC a very outstanding fiber to adsorb cholesterol compared to that per gram of cellulose adsorbed 1.9 ± 0.6 mg of cholesterol. These results also showed CNC adsorbs more cholesterol than other fibers such as wheat bran, soybean hull and apple peel which range from 3.48 to 11.34 mg/g of fiber (Zhang et al., 2011), chitosan (63.48 mg/g of fiber) (Jin, Yu, Wang, Li, & Li, 2017). CNC also showed higher cholesterol adsorbing capacity than CNF (8.5 ± 0.7 mg/g of fiber) (Liu & Kong, 2019b). The high adsorption capacity of CNC could be a result of its high surface area, 150 m^2/g for CNC

(Terech, Chazeau, & Cavaille, 1999) as compared to 1-3 m^2/g for cellulosic fibers (Scott, 1996). The cholesterol adsorption ability of CNC may have also contributed to slowing the cholesterol permeation in the permeation of cholesterol in the *in vitro* mucus permeation assay.

(a)

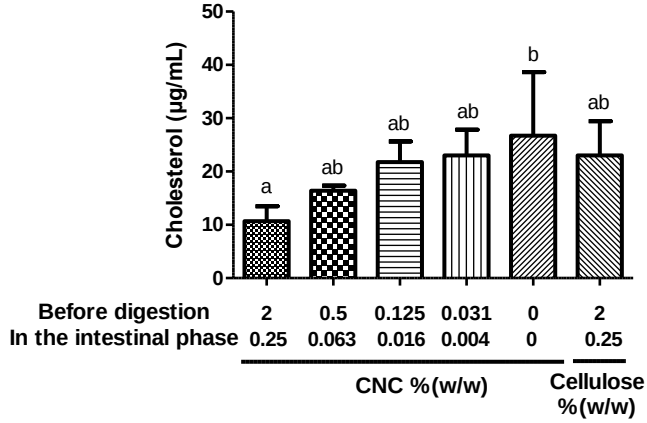

(b)

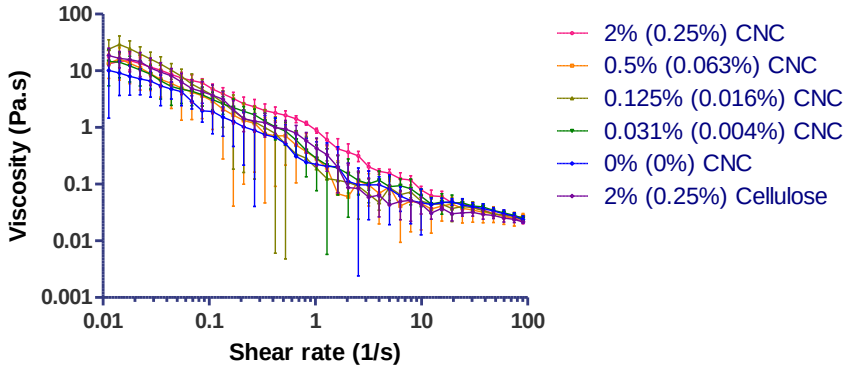

(c)

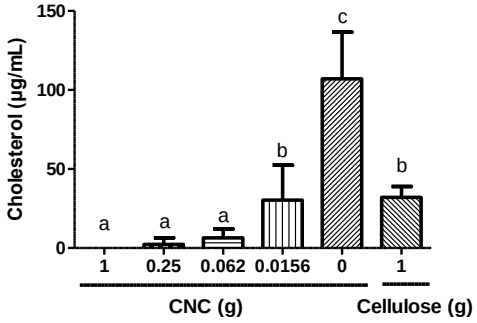

Figure 5.5. (a) Permeation of cholesterol in yolk mixed with CNC or cellulose after *in vitro* digestion. Mean cholesterol concentration ± SD (n=3). (b) the viscosity of the CNC or cellulose

and egg yolk mixture in the intestinal phase. Mean viscosity ± SD (n=3). The brackets show the concentration of CNC or cellulose in the final intestinal digestion stage. (c) Remaining free cholesterol after mixing with CNC or cellulose in water. Mean cholesterol concentration ± SD (n=3). Different letters denote statistical significance by ANOVA followed by Tukey's test (α=0.05)

Table 5.1. Cholesterol adsorption % and capacity of CNC and cellulose. Mean adsorption % or adsorption capacity ± SD (n=3).

	Adsorption (%)	Adsorption capacity (mg cholesterol/g fiber)
0.0156 g CNC	72.2 ± 15.2	122.5 ± 39.1[a]
1 g cellulose	69.2 ± 6.1	1.9 ± 0.6[b]

5.3.6 Bile acids permeation affected by CNC in *in vitro* mucus layer model

One of the benefits of dietary fibers is to alleviate hypercholesterolemia by regulating bile salts homeostasis. The mechanisms include binding of cholesterol or bile acids or increasing viscosity to decrease the reabsorption of bile acids from the small intestine. Because cholesterol is the key material of bile acids, when less cholesterol is entering the body while the same amount of bile acids are made, the cholesterol pool within the body would be transformed into bile acids, thereby lowering blood cholesterol level (Brown, Rosner, Willett, & Sacks, 1999).

Here the effect of CNC in attenuating bile acids permeation through the mucus layer was examined (Figure 5.6(a)). After allowing bile acids and CNC mixture to permeate for one hour, lower bile acid concentration in the basal side was found with increasing CNC concentration. Unlike previous phenol red and FD4 permeation assay that showed dose-dependent results, in this

assay, a drastic decrease of permeation was seen between 0.5% and 0.125% CNC groups. Viscosity was suspected to be the main mechanism and was investigated (Figure 5.6(b)). The 2% CNC mixture had a higher viscosity than other groups, which explained the mechanism for retarding bile acids permeation. On the contrary, the viscosity of 0.5% CNC mixture and 0.125% CNC mixture were similar. This suggests that the retarded permeation of bile salts for CNC could be due to mechanisms other than just the viscosity effect. Previous literature has also reported decreased absorption of bile acids in the ileum section when mixing with CNC stabilized emulsion (Mackie et al., 2019). Our results again emphasized the ability of CNC to reduce bile acid permeation through mucus and also suggested both the viscosity effect and the bile acid-binding effect of CNC. The mechanisms of bile acid-binding, however, will need further studies. Three hypotheses of bile acids-binding mechanisms of dietary fibers have been proposed, including an increase of the unstirred water layer in the lumen, molecular association of dietary fibers and bile acids, and structural formation of dietary fibers to entrap bile acids (Gunness & Gidley, 2010). In summary, it can, therefore, be assumed that CNC may have similar properties to dietary fibers in fighting obesity by improving cholesterol metabolism by decreasing reabsorption of cholesterol in food and bile acids.

(a)

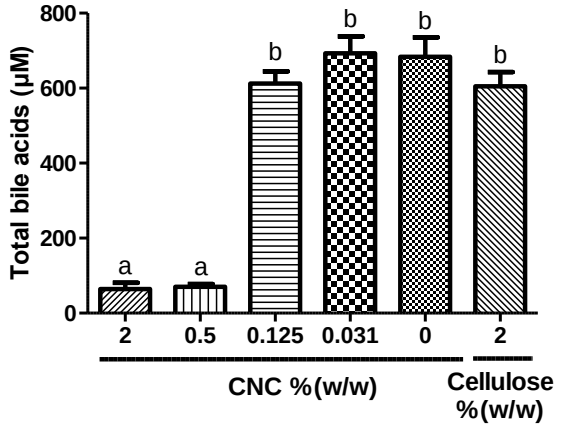

(b)

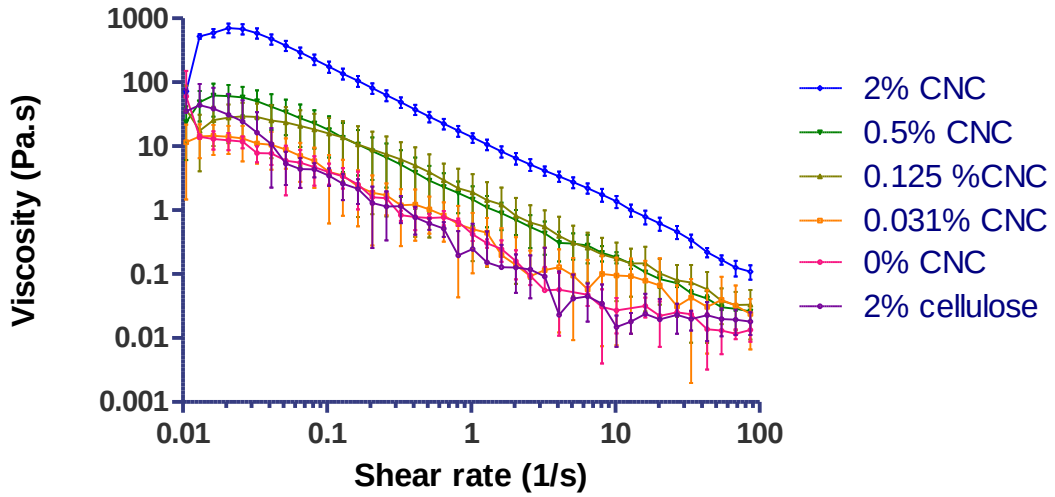

Figure 5.6. (a) Bile acid content in the basal side of the *in vitro* small intestinal mucus gel layer model affected by different CNC concentration in the apical side. Mean bile acids concentration ± SD (n=3). Different letters denote statistical significance by ANOVA followed by Tukey's test (α=0.05). (b) The viscosity of various concentrations of CNC in SIF mixed with 8% bile salts. Mean viscosity ± SD (n=3)

5.4 Conclusion

This study aimed to answer two questions. First, whether CNC could be taken up via the intestinal route, and second, how does it affect substances to permeate through the mucus layer. The present *in vitro* results found no evidence of CNC permeation through mucus layer or enterocyte cell lining and does not affect enterocyte cell viability. Our study provides similar conclusions as to the literature that CNCs might not reach the epithelium and has little impact on the intestinal epithelium viability, therefore there may be less chance to see a direct impact on the epithelium or uptake of CNC via the small intestine. Further work using animal models or a more complex cell model may be required to determine the safety and translocation of CNC.

It is also found that a high concentration of CNC may affect the permeation of large substances or carbohydrates across the intestinal mucus layer. CNC may also generate a hypercholesteremic effect due to hindering the reabsorption of cholesterol and bile acids and binding of cholesterol. This information provides a promising future of CNC as a functional additive in foods in alleviating obesity. More studies, however, are required to determine the extent of this effect and proper usage.

5.5 Acknowledgment

This study was supported by the USDA National Institute of Food Agriculture [grant no. 2019-67021-29859/project accession no. 1019017].

The authors also wish to acknowledge faculty and staff at the University of Georgia, Athens, GA including Dr. William L. Kerr and Dr. George Cavender for equipment and technical support, Dr. Alexander M Stelzleni and Mr. Harl R. Crowe for providing hog samples.

5.6 Supplementary materials

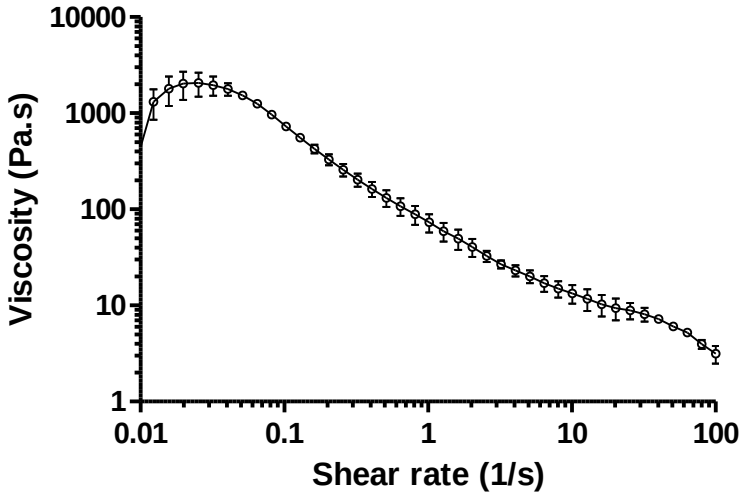

Figure S5.7. The viscosity of collected porcine intestinal mucus. The mucus was a shear-thinning fluid with yield stress at a low shear rate. The sample was analyzed using a TA instrument HR-2 Discovery Hybrid Rheometer with a parallel plate geometry with a diameter of 20 mm at 37°C and a shear rate of 0.01 to 100 s^{-1}. The collected mucus has a water content of 86.57±0.10% (n=3), which is in agreement with reported by Groo et al. (2013).

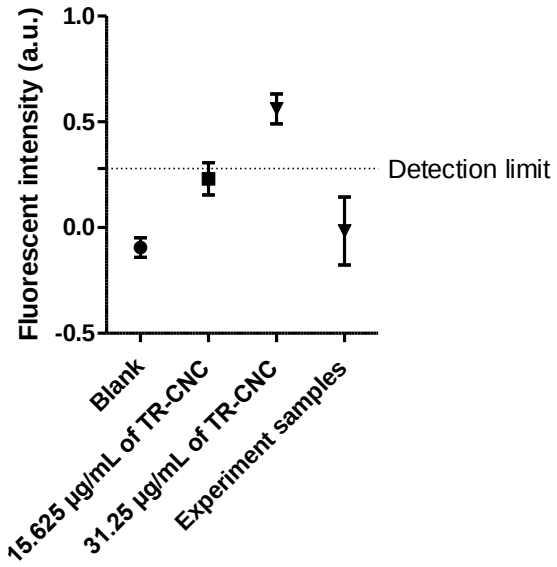

Figure S5.8. Blank, a known concentration of TR-CNC in HBSS (15.625 µg/mL and 31.25 µg/mL), and experiment samples collected from the basal side when 5 mg/mL TR-CNC was loaded in the *in vitro* Caco-2 model after 2 hours of permeation. Mean fluorescent intensity ± SD (n=3)

5.7 References

Azeredo, H. M. C., Rosa, M. F., & Mattoso, L. H. C. (2017). Nanocellulose in bio-based food packaging applications. *Industrial Crops and Products,* 97, 664-671.

Bajka, B. H., Rigby, N. M., Cross, K. L., Macierzanka, A., & Mackie, A. R. (2015). The influence of small intestinal mucus structure on particle transport ex vivo. *Colloids and Surfaces B: Biointerfaces,* 135, 73-80.

Brown, L., Rosner, B., Willett, W. W., & Sacks, F. M. (1999). Cholesterol-lowering effects of dietary fiber: a meta-analysis. *The American Journal of Clinical Nutrition,* 69(1), 30-42.

DeLoid, G., Cao, X., Molina, R. M., Silva, D. I., Bhattacharya, K., Ng, K. W., . . . Demokritou, P. (2019). Toxicological effects of ingested nanocellulose in in vitro intestinal epithelium and in vivo rat models. *Environmental Science: Nano*.

Dharmani, P., Srivastava, V., Kissoon-Singh, V., & Chadee, K. (2009). Role of Intestinal Mucins in Innate Host Defense Mechanisms against Pathogens. *Journal of Innate Immunity,* 1(2), 123-135.

Foster, E. J., Moon, R. J., Agarwal, U. P., Bortner, M. J., Bras, J., Camarero-Espinosa, S., . . . Youngblood, J. (2018). Current characterization methods for cellulose nanomaterials. *Chemical Society Reviews,* 47(8), 2609-2679.

Gómez H, C., Serpa, A., Velásquez-Cock, J., Gañán, P., Castro, C., Vélez, L., & Zuluaga, R. (2016). Vegetable nanocellulose in food science: A review. *Food Hydrocolloids,* 57, 178-186.

García-Casal, M. N., Leets, I., & Layrisse, M. (2000). β-Carotene and Inhibitors of Iron Absorption Modify Iron Uptake by Caco-2 Cells. *The Journal of Nutrition,* 130(1), 5-9.

Garrick, T., Mulvihill, S., Buack, S., Maeda-Hagiwara, M., & Tache, Y. (1988). Intracerebroventricular pressure inhibits gastric antral and duodenal contractility but not acid secretion in conscious rabbits. *Gastroenterology,* 95(1), 26-31.

Gerlier, D., & Thomasset, N. (1986). Use of MTT colorimetric assay to measure cell activation. *Journal of Immunological Methods,* 94(1), 57-63.

Groo, A.-C., Saulnier, P., Gimel, J.-C., Gravier, J., Ailhas, C., Benoit, J.-P., & Lagarce, F. (2013). Fate of paclitaxel lipid nanocapsules in intestinal mucus in view of their oral delivery. *International journal of nanomedicine,* 8, 4291.

Gunness, P., & Gidley, M. J. (2010). Mechanisms underlying the cholesterol-lowering properties of soluble dietary fibre polysaccharides. *Food & Function,* 1(2), 149-155.

Habibi, Y., Lucia, L. A., & Rojas, O. J. (2010). Cellulose Nanocrystals: Chemistry, Self-Assembly, and Applications. *Chemical Reviews,* 110(6), 3479-3500.

Hanif, Z., Ahmed, F. R., Shin, S. W., Kim, Y.-K., & Um, S. H. (2014). Size- and dose-dependent toxicity of cellulose nanocrystals (CNC) on human fibroblasts and colon adenocarcinoma. *Colloids and Surfaces B: Biointerfaces,* 119, 162-165.

Hosseinidoust, Z., Alam, M. N., Sim, G., Tufenkji, N., & van de Ven, T. G. M. (2015). Cellulose nanocrystals with tunable surface charge for nanomedicine. *Nanoscale,* 7(40), 16647-16657.

Hubatsch, I., Ragnarsson, E. G., & Artursson, P. (2007). Determination of drug permeability and prediction of drug absorption in Caco-2 monolayers. *Nat Protoc,* 2(9), 2111-2119.

Hussain, N., Jaitley, V., & Florence, A. T. (2001). Recent advances in the understanding of uptake of microparticulates across the gastrointestinal lymphatics. *Advanced Drug Delivery Reviews,* 50(1-2), 107-142.

ICH. (1996). *Guidance for industry: Q2B validation of analytical procedures: Methodology*. In *Federal Register* Food and Drug Administration, Centre for Drug Evaluation and Research, Centre for Biologics Evaluation and Research

Jin, Q., Yu, H., Wang, X., Li, K., & Li, P. (2017). Effect of the molecular weight of water-soluble chitosan on its fat-/cholesterol-binding capacities and inhibitory activities to pancreatic lipase. *PeerJ,* 5, e3279.

Kaczmarczyk, M. M., Miller, M. J., & Freund, G. G. (2012). The health benefits of dietary fiber: Beyond the usual suspects of type 2 diabetes mellitus, cardiovascular disease and colon cancer. *Metabolism,* 61(8), 1058-1066.

Le Ferrec, E., Chesne, C., Artusson, P., Brayden, D., Fabre, G., Gires, P., . . . Scarino, M.-L. (2001). In Vitro Models of the Intestinal Barrier:The Report and Recommendations of ECVAM Workshop 461,2. *Alternatives to Laboratory Animals,* 29(6), 649-668.

Liévin-Le Moal, V., & Servin, A. L. (2006). The Front Line of Enteric Host Defense against Unwelcome Intrusion of Harmful Microorganisms: Mucins, Antimicrobial Peptides, and Microbiota. *Clinical Microbiology Reviews,* 19(2), 315-337.

Lin, Y.-J., Shatkin, J. A., & Kong, F. (2019). Evaluating mucoadhesion properties of three types of nanocellulose in the gastrointestinal tract in vitro and ex vivo. *Carbohydrate Polymers,* 210, 157-166.

Liu, L., Kerr, W. L., Kong, F., Dee, D. R., & Lin, M. (2018). Influence of nano-fibrillated cellulose (NFC) on starch digestion and glucose absorption. *Carbohydrate Polymers,* 196, 146-153.

Liu, L., & Kong, F. (2019a). In vitro investigation of the influence of nano-cellulose on starch and milk digestion and mineral adsorption. *International Journal of Biological Macromolecules,* 137, 1278-1285.

Liu, L., & Kong, F. (2019b). In vitro investigation of the influence of nano-fibrillated cellulose on lipid digestion and absorption. *International Journal of Biological Macromolecules,* 139, 361-366.

Liu, L., & Kong, F. (2019c). Influence of nanocellulose on in vitro digestion of whey protein isolate. *Carbohydrate Polymers,* 210, 399-411.

Mackie, A., Gourcy, S., Rigby, N., Moffat, J., Capron, I., & Bajka, B. (2019). The fate of cellulose nanocrystal stabilised emulsions after simulated gastrointestinal digestion and exposure to intestinal mucosa. *Nanoscale,* 11(6), 2991-2998.

Mahmoud, K. A., Mena, J. A., Male, K. B., Hrapovic, S., Kamen, A., & Luong, J. H. (2010). Effect of surface charge on the cellular uptake and cytotoxicity of fluorescent labeled cellulose nanocrystals. *ACS Appl Mater Interfaces,* 2(10), 2924-2932.

Menas, A. L., Yanamala, N., Farcas, M. T., Russo, M., Friend, S., Fournier, P. M., . . . Shvedova, A. A. (2017). Fibrillar vs crystalline nanocellulose pulmonary epithelial cell responses: Cytotoxicity or inflammation? *Chemosphere,* 171, 671-680.

Minekus, M., Alminger, M., Alvito, P., Ballance, S., Bohn, T., Bourlieu, C., . . . Brodkorb, A. (2014). A standardised static in vitro digestion method suitable for food – an international consensus. *Food & Function,* 5(6), 1113-1124.

Moon, R. J., Martini, A., Nairn, J., & Simonsen, J. (2011). Cellulose nanomaterials review: structure, properties and nanocomposites.

Natoli, M., Leoni, B. D., D'Agnano, I., Zucco, F., & Felsani, A. (2012). Good Caco-2 cell culture practices. *Toxicology In Vitro,* 26(8), 1243-1246.

Pereira de Sousa, I., Cattoz, B., Wilcox, M. D., Griffiths, P. C., Dalgliesh, R., Rogers, S., & Bernkop-Schnürch, A. (2015). Nanoparticles decorated with proteolytic enzymes, a promising strategy to overcome the mucus barrier. *European Journal of Pharmaceutics and Biopharmaceutics,* 97, 257-264.

Plackett, D., Letchford, K., Jackson, J., & Burt, H. (2014). A review of nanocellulose as a novel vehicle for drug delivery. 29(1), 105.

Pradhan, S. H., Mulenos, M. R., Steele, L. R., Gibb, M., Ede, J. D., Ong, K. J., . . . Sayes, C. M. (2020). Physical, chemical, and toxicological characterization of fibrillated forms of cellulose using an in vitro gastrointestinal digestion and co-culture model. *Toxicology Research,* 9(3), 290-301.

Reiner, R. S., & Rudie, A. W. (2013). *Process Scale-Up of Cellulose Nanocrystal Production to 25 kg per Batch at the Forest Products Laboratory*. In M. T. Postek, R. J. Moon & A. W. Rudie (Eds.), *Production and applications of Cellulose nanomaterials, TAPPI Press* (pp. 21-24): TAPPI

Rocha, V., Marques, C., Figueiredo, J. L., Gaio, A. R., Costa, P. C., Sousa Lobo, J. M., & Almeida, I. F. (2017). In vitro cytotoxicity evaluation of resveratrol-loaded nanoparticles: Focus on the challenges of in vitro methodologies. *Food and Chemical Toxicology,* 103, 214-222.

Roman, M. (2015). Toxicity of Cellulose Nanocrystals: A Review. *Industrial Biotechnology,* 11(1), 25-33.

Roman, M., Dong, S., Hirani, A., & Lee, Y. W. (2009). *Cellulose Nanocrystals for Drug Delivery*. In *Polysaccharide Materials: Performance by Design* (pp. 81-91): American Chemical Society

Round, A. N., Rigby, N. M., Garcia de la Torre, A., Macierzanka, A., Mills, E. N. C., & Mackie, A. R. (2012). Lamellar Structures of MUC2-Rich Mucin: A Potential Role in Governing the Barrier and Lubricating Functions of Intestinal Mucus. *Biomacromolecules,* 13(10), 3253-3261.

Rudel, L. L., & Morris, M. (1973). Determination of cholesterol using o-phthalaldehyde. *Journal of Lipid Research,* 14(3), 364-366.

Samulin Erdem, J., Alswady-Hoff, M., Ervik, T. K., Skare, Ø., Ellingsen, D. G., & Zienolddiny, S. (2019). Cellulose nanocrystals modulate alveolar macrophage phenotype and phagocytic function. *Biomaterials,* 203, 31-42.

Scott, W. E. (1996). Principles of Wet End Chemistry TAPPI PRESS. Atlanta.

Sun, H., Chow, E. C. Y., Liu, S., Du, Y., & Pang, K. S. (2008). The Caco-2 cell monolayer: usefulness and limitations. *Expert Opinion on Drug Metabolism & Toxicology,* 4(4), 395-411.

Terech, P., Chazeau, L., & Cavaille, J. Y. (1999). A Small-Angle Scattering Study of Cellulose Whiskers in Aqueous Suspensions. *Macromolecules,* 32(6), 1872-1875.

van de Loosdrecht, A. A., Beelen, R. H. J., Ossenkoppele, G. J., Broekhoven, M. G., & Langenhuijsen, M. M. A. C. (1994). A tetrazolium-based colorimetric MTT assay to quantitate human monocyte mediated cytotoxicity against leukemic cells from cell lines and patients with acute myeloid leukemia. *Journal of Immunological Methods,* 174(1), 311-320.

Xia, Y. N., Yang, P. D., Sun, Y. G., Wu, Y. Y., Mayers, B., Gates, B., . . . Yan, Y. Q. (2003). One-dimensional nanostructures: Synthesis, characterization, and applications. *Advanced Materials,* 15(5), 353-389.

Xiao, Y., Liu, Y., Wang, X., Li, M., Lei, H., & Xu, H. (2019). Cellulose nanocrystals prepared from wheat bran: Characterization and cytotoxicity assessment. *International Journal of Biological Macromolecules,* 140, 225-233.

Zhang, N., Huang, C., & Ou, S. (2011). In vitro binding capacities of three dietary fibers and their mixture for four toxic elements, cholesterol, and bile acid. *Journal of Hazardous Materials,* 186(1), 236-239.

CHAPTER 6. SUMMARY AND RECOMMENDATIONS

6.1 Summary

Nanocellulose has different physical and chemical properties that are easily dispersed and suspended in water due to the smaller size and/or surface charge, which is different from unmodified cellulose. Meanwhile, nanocellulose still has relatively low toxicity, high biocompatibility, and is environmentally friendly. Nanocellulose as novel nanomaterials has gathered great interest in food applications such that there are already many patents and research focusing on applying nanocellulose in foods and food-related uses. Nowadays we have gained more and more knowledge on the safety of nanocellulose, and yet more questions need to be answered for the impacts on health after consumption. Industrial companies and academic labs are teaming up to conduct safety studies in determining such as NOAEL to legalize nanocellulose as a food additive. With the growing public awareness of green and sustainability, nanocellulose is expected to be the next generation of renewable products to replace petroleum products. But of course, enough investigation should be devoted before nanocellulose enters the environment and our mouths.

The present understanding of nanocellulose to gut health remains insufficient. On the other hand, there is interest in understanding if nanocellulose serves as dietary fibers and improves gut health. This project aims to highlight the importance of studying the behavior of nanocellulose and its interaction with GI mucus and intestinal epithelium. Because of the uniqueness of the environment of the stomach and small intestinal, the changes of nanocellulose under different

conditions are of particular interest and need in-depth investigation. Our results provide important information in understanding the behavior and interaction of nanocellulose with the GI mucosa and mucus layer.

Three types of nanocellulose have a different level of mucoadhesion properties. They generated mucoadhesion through different mechanisms. In the stomach, CNF is entangled with the mucus gel network, CNC homogenously distributed on the mucus gel surface and TEMPO-CNF formed aggregates that are non-specifically retained on the gastric mucus surface *ex vivo*. In the intestinal condition, a more moderate retention was seen on all three types of nanocellulose. It was confirmed using the viscometric method by looking at the viscosity enhancement with mucins by nanocellulose. Also, the zeta potential method suggested CNC may interact with mucin particles by changing the surface charge of the mucin-nanocellulose mixture.

In our *in vivo* study, mice were fed with a Western diet and given one dose of 30mg/kg bodyweight of CNF, CNC, and TEMPO-CNF daily for 6 weeks. Results showed no significant differences in weight gain, fecal output, food intake, blood glucose homeostasis, and gut integrity. Serum analysis on triglyceride, cholesterol, and total bile acids did not indicate any difference among groups, either. The fecal analysis showed that CNC increased fecal bile acid output. One possible mechanism was the binding of bile acids by CNC to prevent reabsorption, although the effect on lowering serum cholesterol was seen but insufficient to show statistical significance. The small intestinal morphology analysis on villus, crypt, and goblet cells was statistically insignificant. CNF and TEMPO-CNF did not show a significant difference among the tested assays compared to the control group, which indicated no observable harmful or beneficial effects with the amount of consumption. The mechanisms and the details of CNC on changing bile acid excretion could be further tested.

CNC was further studied for its impacts on intestinal mucus permeability and the translocation across the Caco-2 monolayer. Although it is possible nanocellulose remains in the lumen track for longer time due to mucoadhesion, it did not permeate differentiated Caco-2 cell monolayer *in vitro*, and had minimal effect on Caco-2 cell viability. CNC did not translocate the *in vitro* mucus layer freely, either. But 2% w/w CNC may decrease cholesterol absorption. Proposed mechanisms include decreased mucus permeability, resulting in reduced absorption of cholesterol, decreased bile acid reabsorption by binding, or increased viscosity.

To conclude, we found nanocellulose may retain in the GI tract longer after consumption due to mucoadhesion and only a high concentration of CNC may change the permeability of the mucus gel layer and the bioaccessibility of nutrients and bile acids *in vitro*. *In vivo* short-term daily consumption of nanocellulose did not have detrimental effects nor did they benefit lipid metabolisms or change intestinal morphology. Overall, our findings illustrate the behavior of nanocellulose in the GI tract, but the biological health benefits of using nanocellulose as a fiber supplement may be low at the tested concentration.

6.2 Recommendations

Based on what was known and the limitations of the current studies, several future investigations are recommended. For the mucoadhesion properties of nanocellulose, the peristalsis of the GI tract was not introduced in the test system, while the shear force in the GI tract is important to the detachment of mucoadhesive materials and the turnover of mucus. Hence future *in vitro* mucoadhesion tests under dynamic digestion with peristalsis would better mimic the actual

condition. Using radio-labeled nanocellulose to test the mucoadhesion effect in animals could also be more biologically related.

For the *in vivo* studies, more studies on colon morphology and mucus properties as well as changes on microbiota and intestinal SCFAs profile could more precisely determine if nanocellulose has the functionalities of a prebiotic. Analysis of mucin profile and mucin gene expression may further provide important information on the homeostasis of mucus production. Blood tests and pathological examination for the mouse organs are needed to give a thorough report on the health impacts of nanocellulose. Trials using male mice are also suggested to understand gender bias. Female mice tend to be affected with estrogen production. Using male mice would be able to eliminate this effect.

More studies on TEMPO-CNF is necessary before its applications in food-related uses. The aggregation of TEMPO-CNF in the acidic environment in the stomach is also an interesting feature that could be further tested for the encapsulation of functional ingredients.

Lastly, comparisons of nanocellulose to other cellulosic food additives such as carboxymethylcellulose and hydroxypropyl cellulose would be important to distinguish the market value of nanocellulose from the current legal cellulosic food additives and facilitate future research.

APPENDIX.

PERMEATION OF CNF AND TEMPO-CNF THROUGH IN VITRO CACO-2 MONOLAYER AND EFFECT ON CACO-2 CELL VIABILITY

A.1 Objective

To study the permeation of CNF and TEMPO-CNF through *in vitro* Caco-2 monolayer model to understand if they would be taken up by enterocytes and enter systemic circulation. And the effect on Caco-2 cell viability was also assessed.

A.2 Materials and methods

A.2.1 Materials

The labeling of Texas Red (TR)-CNF and TR-TEMPO-CNF have been described in Chapter 3.2.2.

A.2.2 Permeation of CNC through *in vitro* Caco-2 monolayer

Same procedure of permeation assay through Caco-2 monolayer model was used as described in Chapter 5.2.6. In brief, Caco-2 was allowed to differentiate for 21 days and monolayer integrity was first confirmed by phenol red. Afterwards, 5 mg/mL TR-CNF and 0.15 mg/mL TR-TEMPO-CNF was loaded on the apical side followed by 2-hour incubation on a 37°C shaking incubator.

A.2.3 Cell viability (MTT assay)

Same procedure of MTT assay was used as described in Chapter 5.2.7.

A.2.4 Statistical analysis

Analysis of variance (ANOVA) followed used to test for significant differences using JMP Pro 13.0.0 (SAS Institute Inc., Cary, NC). Three replications were conducted for each experiment.

A.3 Results and discussion

The result of CNF and TEMPO-CNF on their permeation across differentiated Caco-2 monolayer was shown in Figure A.2. Fluorescent intensity of samples collected from the basal side of TR-CNF and TR-TEMPO-CNF and was below detection limit by fluorescence spectrophotometer. Hence it is concluded that there was no observable permeation of CNF and TEMPO-CNF through differentiated Caco-2 monolayer model. Our CNF result also supported the previous observation that CNF did not increase the trans-epithelial electrical resistance (TEER) value of Caco-2, HT29-MTX and Raji B tri-culture model (DeLoid et al., 2019), which means CNF did not increase the permeability of *in vitro* intestinal monolayer.

Further, CNF and TEMPO-CNF and cellulose were tested for their effect on Caco-2 cell viability shown in Figure A.3. TEMPO-CNF and cellulose did not show dose-dependent on cell viability at the tested dose, while there was a decrease on the cell viability of CNF when the dose reached above 1000 μg/mL. This result was similar with previous literature (Chen, Lin, Nagy, Kong, & Guo, 2020). However, the concentration that could generate toxicity is a relatively high dose and in reality, the small intestine of human may never reach such high concentration considering the applicable dosage of nanocellulose. On top of that, above 70% is generally considered non-toxic for cell culture assays by ISO standard 10993-5 (Roman, 2015). Our results do not provide enough evidence to conclude that CNF has cytotoxicity.

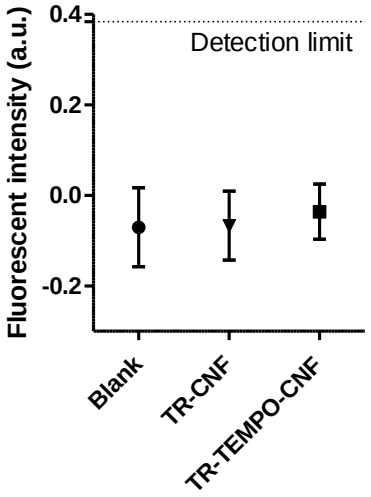

Figure A.2. Qualitative result of TR-CNC in the basal compartment of Caco-2 monolayer after 2 hours of incubation with 5 mg/mL of TR-CNF and 0.15 mg/mL of TR-TEMPO-CNF in the apical compartment. Gridline shows the detection limit based on the standard deviation of the blank (HBSS). Mean fluorescent intensity ± SD (n=3)

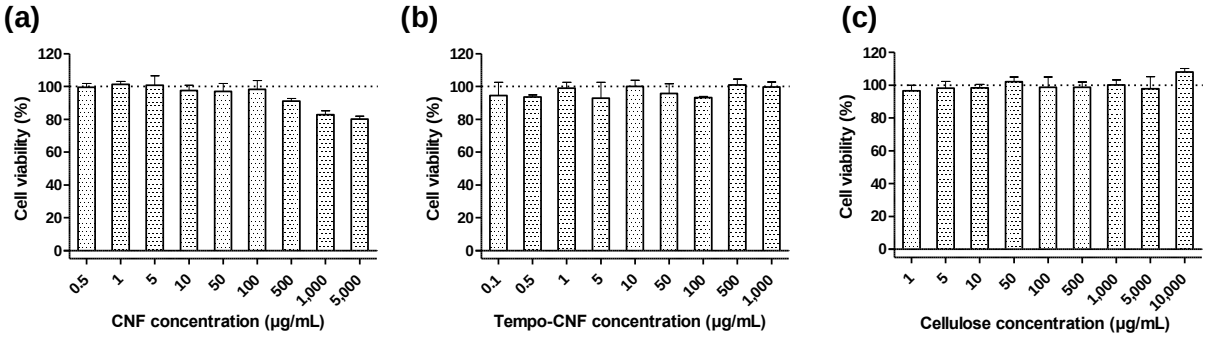

Figure A.3. Caco-2 cell viability after 24 hours of incubation with CNF, TEMPO-CNF and cellulose by MTT assay. Mean cell viability ± SD (n=3). No statistical significance was detected by ANOVA (α=0.05)

A.4 Conclusions

CNF, TEMPO-CNF were tested if they would permeate enterocyte lining *in vitro* and their cytotoxicity *in vitro*. Our result showed there was no detectable penetration of CNF and TEMPO-CNF through Caco-2 cell monolayer, and both nanocellulose also showed generally low toxicity on cell viability.

A.5 References

Chen, Y., Lin, Y.-J., Nagy, T., Kong, F., & Guo, T. L. (2020). Subchronic exposure to cellulose nanofibrils induces nutritional risk by non-specifically reducing the intestinal absorption. *Carbohydrate Polymers,* 229, 115536.

DeLoid, G., Cao, X., Molina, R. M., Silva, D. I., Bhattacharya, K., Ng, K. W., . . . Demokritou, P. (2019). Toxicological effects of ingested nanocellulose in in vitro intestinal epithelium and in vivo rat models. *Environmental Science: Nano*.

Roman, M. (2015). Toxicity of Cellulose Nanocrystals: A Review. *Industrial Biotechnology,* 11(1), 25-33.